SEMICONTINUOUS SEPARATION OF DIMETHYL ETHER FROM BIOMASS

SEMICONTINUOUS SEPARATION OF DIMETHYL ETHER FROM BIOMASS

By ALICIA PASCALL, B.Sc.

A Thesis Submitted to the School of Graduate Studies

in Partial Fulfilment of the Requirements

for the Degree

Masters of Applied Science

McMaster University

MASTER OF APPLIED SCIENCE (2013) McMaster University

(Chemical Engineering) Hamilton, Ontario, Canada

TITLE: Semicontinuous Separation of Dimethyl Ether from Biomass

AUTHOR: Alicia Pascall, B.Sc. (University of the West Indies)

SUPERVISOR: Dr. Thomas Adams II

NUMBER OF PAGES: xvii, 114

ABSTRACT

Environmental concerns about greenhouse gas emissions and energy security are the main drivers for the production of alternative fuels from bio-based feedstock. Dimethyl ether has attracted interest of many researches and is touted as "A fuel for the 21st century" due to its versatility. However, the production of DME from biomass is dependent on the overall economics of its production.

This thesis considers the application of semicontinuous distillation to improve the economics of the separation section in a biomass-to-DME facility. Semicontinuous distillation systems operate in a forced cycle to effect multiple separations using a single distillation column integrated with a middle vessel. The control system plays an integral role in the driving the forced cycle behaviour of the process in which no steady state exists.

The separation section consists of a series of flash drums followed by a distillation train consisting of three (3) columns. In the first phase of this work, a semicontinuous system was developed to achieve the separation of the second and third distillation columns in the separation section. Rigorous models were used to simulate the semicontinuous system in which several control configurations were evaluated. The final control structure based on classic PI control was shown to achieve the specification objectives of the system and handle disturbances while avoiding weeping and flooding conditions. Optimization followed by an economic analysis showed that the semicontinuous system was economically preferable to the traditional continuous process for a range of DME production rates.

Next, a semicontinuous system was developed to achieve the separation of the first and second distillation columns in the separation section. In this phase the application of semicontinuous distillation was extended to partial condenser configurations and the separation of biphasic mixtures. The control structure developed was effective in handling disturbance, attaining specification objectives while remaining with operational limits. An economic analysis, however, showed the traditional continuous configuration to be more economical for all DME production rates. Findings show that the operating cost is highly depending on the middle vessel

purity so while uneconomical for this process it could result in favourable economics for less stringent purity specifications.

ACKNOWLEDGEMENTS

I wish to take this opportunity to express my thanks to my superb support network, which consist of a group of magnificent individuals, each of whom played an integral but unique role in assisting me towards the completion of this programme.

Firstly, I wish to express my gratitude to my advisor Dr. Thomas Adams II for providing me the opportunity to partake in this programme, for his patience, invaluable suggestions and guidance which directed me throughout the course of this work. I could not have imagined a better advisor for my Masters study.

Also, I would like to thank my family: my parents Anthony and Carol, my brother Anthony Jr. and my cousin Tessa for their continuous support, their love and encouragement. I would also like to say thanks to my penthouse friends, Jaffer, Jake, Yasser, Brandon, Dominik, Chris and Chinedu for the stimulating discussions, moral support and for all the fun times throughout this study.

To my friends back home in Trinidad, thank you so much for keeping me sane and grounded throughout this whole experience. Thanks to Lynn Falkiner, Cathie Roberts for their assistance in administrative matters and to Dan Wright for technical support.

Finally, but by no means lastly, I thank God for giving me the strength to complete this work. Thank you God for your grace, your mercy and your guidance

Once again thank you everyone.

TABLE OF CONTENTS

LIST OF FIGURES

Chapter 1

Chapter 2

Chapter 3

Chapter 4

LIST OF TABLES

Chapter 2

Chapter 3

Chapter 4

LIST OF ABBREVIATIONS AND SYMBOLS

B	Bottoms rate (kmol/hr)
c_1	Personal influence constant
c_2	Social influence constant
d_H	Tray hole diameter (m)
D	Distillate rate (kmol/hr)
$e_{S,EL}$	Error – ethyl lactate in side stream
F	Feed rate (kmol/hr)
F_{in}	Total vapor-liquid feed rate to the reflux drum (kmol/hr)
$F_{in,liq}$	Liquid flowrate in feed stream to reflux drum (kmol/hr)
F_{liq}	Liquid feed flowrate to column (kmol/hr)
F_{min}	Minimum gas load ($Pa^{0.5}$)
F_{vap}	Vapour feed flowrate to column (kmol/hr)
g	Acceleration due to gravity (m/s^2)
K_c	Controller gain (%/%)
L	Reflux rate (kmol/hr)
L_i	Lower bound for dimension i
L/D	Reflux ratio
L_R/D_R	Length to diameter ratio for reflux drum
M_L	Liquid holdup in reflux drum (kmol)
M_v	Vapour holdup in reflux drum (kmol)
N	Total number of stages
N_p	Number of particles
P_j	Particle's position vector
$P_{j,best}$	Particle's best position vector
P_{global}	Position vector of best particle in the population
Q_B	Reboiler heat duty (GJ/hr)
Q_c	Condenser heat duty (GJ/hr)
S	Side stream rate (kmol/hr)

S/F	Side stream/Feed ratio
TAC	Total annualized cost ($/yr)
u_{min}	Minimum vapour velocity (m/s)
U_i	Upper bound for dimension *i*
v_j	Velocity vector for particle *j*
$v_{j,i}$	Velocity of dimension *i* (tuning parameters) for particle j
$v_{max,i}$	Maximum velocity for dimension *i*
V	Boil-up rate (kmol/hr)
V/B	Reboil ratio
x_B	Bottoms composition
$x_{B,DME}$	DME composition in bottoms
$x_{B,MeOH}$	Methanol composition in bottoms
x_D	Distillate composition
$x_{D,DME}$	DME composition in distillate
$x_{D,MeOH}$	Methanol composition in distillate
$x_{F,DME}$	DME composition in feed
$x_{F,MeOH}$	Methanol composition in feed
$x_{F,EL}$	Ethyl lactate composition in feed
$x_{S,DME}$	DME composition in side stream
$x_{S,MeOH}$	Methanol composition in side stream
ΔT	Temperature difference (K)
ΔH_v	Latent heat of vaporization (kJ/kg)

Greek Letters

$\mathbb{N}_i$	Interfacial mass transfer rate (kmol/hr)
ρ_L	Liquid density (kg/m^3)
ρ_V	Gas density (kg/m^3)
τ_I	Controller integral time (min)
φ	Relative free area
χ	Constriction factor

Abbreviations

CSTR	Continuous stirred tank reactor
DOF	Degree of freedom
DME	Dimethyl ether
ISE	Integral squared error
LPG	Liquefied petroleum gas
MV	Middle vessel
P	Proportional control
PI	Proportional integral control
PRWS-UNIFAC	Peng Robinson Wong Sandler UNIFAC
PSO	Particle swarm optimization
R_{boil}	Reboil ratio
R_{ref}	Reflux ratio
VBA	Visual basic application
VLE	Vapour liquid equilibrium

Chapter 1

INTRODUCTION

1.1. Motivation

In Canada, the transportation and petroleum sectors are the major greenhouse gases (GHG) contributors, accounting for 46% of the nation's total GHG emissions in 2010 (Environment Canada, 2012). Environmental concerns about climate change have stimulated interest in alternative fuels, especially those produced from biomass, as they present both a solution to mitigating climate change and reducing dependency on fossil fuels. Dimethyl ether (DME) is one such alternative fuel which has attracted interest of researchers due to its environmentally benign characteristics.

DME, the simplest of ethers, is mainly used as an aerosol propellant (Ogawa, Inoue, Shikada, & Ohno, 2003) but shows great promise as a petroleum-based fuel additive or substitute. As an alternative to diesel fuel, DME exhibits a high cetane rating (55-60), high thermal efficiency and low auto-ignition temperature with lower NO_x, CO, and SO_x emissions (Arcoumanis, Bae, Crookes, & Kinoshita, 2008; Semelsberger, Borup, & Greene, 2006). Additionally, the absence of carbon-carbon bonds and high oxygen content (35 wt%) results in smoke-free combustion (Arcoumanis et al., 2008). Moreover, the physical and chemical properties of DME make it a highly suitable fuel for various applications. For example, DME can be used as:

i. Substitute to liquefied petroleum gas (LPG) in residential heating and cooking as it has physical properties similar to that of LPG requiring minimal infrastructure modifications (Semelsberger et al., 2006).

ii. Natural gas replacement in power generation as it shows equivalent operational performance when compared to natural gas (Cocco, Tola, & Cau, 2006).
iii. Chemical feedstock for olefins production replacing methanol due to higher olefin selectivity (Liu, Sun, Wang, Wang, & Cai, 2000).
iv. Feedstock for fuel cells since it possesses a high H/C ratio and can be reformed at low temperature to produce a hydrogen rich feed (Semelsberger et al., 2006).

Despite the versatility of DME and its environmental benefits, especially when produced from biomass synthesis gas, its production pathway must be economically competitive to achieve widespread adoption. Unlike natural gas-to-DME and coal-to-DME production processes, in which production cost decreases with increasing plant size due to economy of scale benefit (Jenkins, 1997), the production cost of DME from biomass is sensitive to plant capacity. As biomass is distributed in nature and has a low energy density, the feedstock collection area increases with increasing plant size (Floudas, Elia, & Baliban, 2012; Searcy, Flynn, Ghafoori, & Kumar, 2007). This leads to large transportation costs which offsets the economy of scale benefit such that the optimal capacity of the biomass facility is at intermediate production rates (Jenkins, 1997; Wright, Brown, & August, 2007).

DME can be manufactured from synthesis gas by the traditional indirect method or the newly developed direct process. In the indirect method, methanol is first formed from synthesis gas followed by dehydration to DME (Moradi, Ahmadpour, Yaripour, & Wang, 2011; Ogawa et al., 2003). However, in the direct method methanol synthesis and dehydration reactions are performed in a single reactor over bi-functional catalysts leading to improved economics. The simultaneous production of methanol and DME lessens the thermodynamic limitation of methanol synthesis due to the lower concentration of methanol in the reactor resulting in higher conversion efficiency in addition to lower investment costs (Ju et al., 2009). In spite of the economic improvement in the DME synthesis step, the downstream separation section is more complex and costly than the indirect process due to the presence of CO_2 (Peng, Wang, Toseland, & Tijm, 1999).

The above considerations have motivated the application of a process intensification technique in the separation section which is cost effective at intermediate production rates to improve the profitability of the biomass-to-DME facility. Semicontinuous distillation is one type of process intensification strategy which often has the advantage of lower lifetime costs compared to conventional continuous and batch processes at intermediate production rates (Adams & Pascall, 2012).

The semicontinuous distillation system will be integrated in a bio-DME facility consisting of the main steps as shown in Figure 1.1.

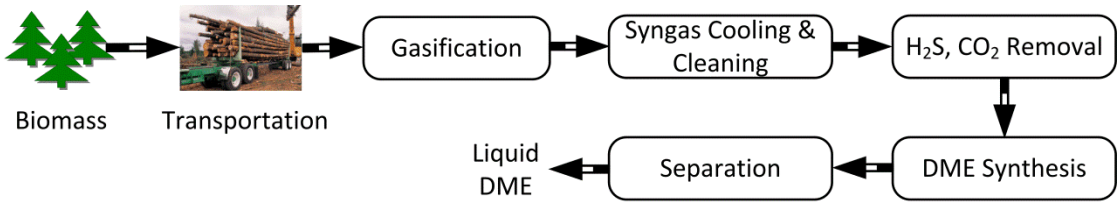

Figure 1.1: Simplified process flow diagram for biomass to DME process (Larson, Jin, & Celik, 2009)

1.2. Background

Semicontinuous separation is a recently developed process intensification strategy which can be used to perform multiple separations with less equipment than normally required. The system utilizes a single distillation column coupled with one or more middle vessels, operating in a forced cycle with sequential operating modes, to effect the required separations (Adams & Seider, 2009a).

Semicontinuous processes have been developed for ternary non-azeotropic distillation, azeotropic distillation, extractive distillation and semicontinuous distillation with chemical reaction (Adams & Seider, 2006, 2008a, 2009b; Monroy-Loperena & Alvarez-Ramirez, 2004; Phimister & Seider, 2000a, 2000b, 2000c). However, in this section we present a review of the fundamental aspects of semicontinuous non-azeotropic ternary distillation systems as this semicontinuous process is applied in this research.

The use of semicontinuous distillation for the separation of ternary mixtures was first proposed by Phimister & Seider, 2000a. They considered the separation of n-hexane, n-heptane and n-octane into three nearly-pure products, with target purities of 98 mol%, using a single distillation column integrated with one middle vessel (MV) as shown in Figure 1.2. The semicontinuous system is configured with the MV both feeding the distillation column and receiving a liquid side stream from the column while operating under a cyclic policy. The following three modes are repeated sequentially in an operating cycle:

i. Mode 1 – This mode commences with the MV containing the equimolar hydrocarbon mixture. As cycle continues the lightest (n-hexane) and heaviest (n-octane) components are continuously removed in the distillate and bottoms with the intermediate component (n-heptane) concentrating in the middle vessel. Tanks T2, T3 and T4 represent product collection vessels. The flow rate of distillate and bottoms products diminishes during the course of Mode 1 to maintain product purities as the concentration of n-hexane and n-octane in the MV decreases. Once the MV target purity is attained Mode 1 ends.
ii. Mode 2 – N-heptane at its target purity is discharged to its product collection tank until the MV is nearly emptied
iii. Mode 3 – Upon completion of mode 2 the MV is recharged with fresh feed and the cycle repeats.

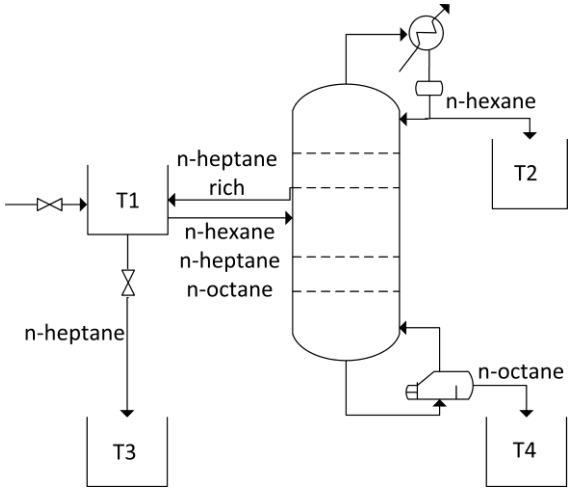

Figure 1.2: Process schematic of ternary semicontinuous distillation process of Phimister and Seider (Adams & Pascall, 2012)

The semicontinuous system using this operating policy has the advantage in that start-up and shutdown of the column are avoided compared to batch distillation since the feed to the column and the side stream to the MV are maintained throughout the entire cycle. However, due to the absence of steady-state conditions and wide operating range (feed composition and product flow rates) coupled with mode transitions, the design of the control system is critical in maintaining separation and operational objectives. Throughout the entire cyclic campaign the distillate and bottoms products must be maintained at desired purities while avoiding flooding and weeping conditions in the column. Phimister & Seider, 2000a, investigated three dual composition control strategies used for achieving the objectives of the ternary semicontinuous systems:

i. The *"LV"* (reflux rate manipulated to control distillate composition with the boil up rate varied to control the bottoms composition) configuration was shown to be ineffective for the semicontinuous system. At the end of the cycle where distillate and bottoms flow rates are small (column operates close to total reflux), the distillate and bottoms streams are ineffective at level control. Hence, L and V must be used for level control and are momentarily unavailable for composition control.
ii. The *"L/D, V/B"* (the reflux ratio varied to regulate distillate composition and the reboil ratio is manipulated to control bottoms composition) was also shown to render the semicontinuous system inoperable. As the distillate (n-hexane) and bottoms (n-octane) are removed the reflux and reboil ratios increase significantly towards the end of Mode 1. Consequently, the midpoint of each manipulated variable is difficult to locate with small changes in the distillate and bottoms rate resulting in large changes in the reflux/reboil ratios.
iii. The *"DB"* configuration (distillate flow rate manipulated to control distillate composition with the bottoms flow rate manipulated to control bottoms composition) while inoperable for continuous systems was shown to be effective in maintaining product purities and achieving the required separation. Phimister & Seider, 2000a reported that while setpoint tracking of product purities could not be achieved throughout the entire cycle the level controllers

were able to maintain the reflux and sump volumes within operational limits. Two alternatives of the *"DB"* configuration were considered. In the first configuration, the feed to the column is maintained at a constant rate with the reflux and sump levels maintained using the reflux rate and boilup rate respectively, while in the second configuration the feed rate is manipulated to control the sump level.

The semicontinuous system was simulated using material, equilibrium, summation and heat balances (MESH) assuming constant physical properties (such as densities and enthalpies of pure components), pseudo-steady-state heat and summation balances, constant pressure, constant molar overflow, negligible vapour holdup, perfect tray mixing and adiabatic operation (Adams & Pascall, 2012). A comprehensive discussion on the integration strategy employ can be found in Adams and Pascall, 2012. The design parameters for the semicontinuous system were estimated using modified Fenske and Underwood equations such that the vapour velocities remained within 70-90% of the flooding velocity throughout the cycle. The Underwood equations are used to estimate the minimum reflux ratio over the range of expected feed compositions while the minimum number of trays is estimated using conditions near the end of the operating cycle during which the column operates at or near total reflux (Phimister & Seider, 2000a). Finally, the trajectories provided in their work were based on a control system which assumed instantaneous composition measurements calculated from tray temperatures.

Later, the seminal work on ternary semicontinuous distillation was extended by Adams & Seider, 2008 to include chemical reaction for the recovery of speciality chemical, ethyl lactate from water by-product and unreacted ethanol and lactic acid. The semicontinuous system consists of a MV and distillation column configured as shown in Figure 1.2 coupled with a CSTR and pervaporation unit. The process operates under a cyclic campaign with three operating modes, similarly to that of Phimister and Seider:

i. Mode 1 begins with the middle vessel containing the quaternary reaction mixture (ethyl lactate, water, ethanol and lactic acid) to be separated. As the cycle progresses, ethanol and water are recovered in the distillate, lactic acid recovered in the bottoms product with ethyl lactate concentrating in the MV. The bottoms product rich in lactic acid is recycled to the CSTR while the ethanol-water rich distillate is sent to the pervaporation unit where water is removed and the dehydrated ethanol sent to the CSTR. At the same time, the CSTR is charged with an equimolar fresh feed of ethanol and lactic acid and the reaction continued with Mode 1 ending when an ethyl lactate purity of 98 mol% is attained.
ii. In Mode 2, ethyl lactate product is discharged from the middle vessel with the column remaining in operation.
iii. Once discharging is completed, Mode 3 commences with the near-equilibrium reactor mixture discharged to the MV and the cycle repeated.

The semicontinuous process utilized the MESH equations similar to that of Phimister and Seider with several enhancements (Adams & Pascall, 2012). Adams and Seider assumed a constant pressure drop across the column as opposed to a constant pressure. Physical properties and vapour-liquid equilibria were calculated rigorously using function calls to Aspen Properties. Additionally, improvements to the integration algorithm were applied as discussed in Adams & Pascall, 2012. Adams & Seider, 2008, proposed the following model-based, feed-forward, feedback control strategy:

i. Reboil ratio is manipulated to control the ethyl lactate impurity in the bottoms using a proportional integral controller.
ii. Reflux ratio is manipulated to maximize the purity of ethyl lactate in the side stream using a model-based feed forward controller coupled with a feedback controller for corrective action as shown by Eq. 1.1

$$R_{ref} = f\left(x_{F,EL}, R_{boil}\right) + K_c e_{S,EL} \qquad (1.1)$$

where R_{ref}, R_{boil}, $x_{F,EL}$, $e_{S,EL,}$ K_c are the reflux ratio, reboil ratio, ethyl lactate composition in the feed, reboil ratio, error (deviation from setpoint) and controller gain.

The feed-forward model is developed using the RadFrac distillation block in Aspen Plus with the design variables of the column consistent with the semicontinuous column. An optimization based approach is then used to determine the minimum reflux ratio which maximizes the purity of the side stream for various feed compositions and reboil ratios. The results obtained are then used to develop the model-based control law.

iii. Feed rate to the column is manipulated using feed-forward, model-based control based on feed composition. The feed rate is adjusted such that the internal liquid and vapour flow rates within the column are balanced preventing flooding and weeping.

iv. Side stream is controlled using the ideal side-draw control strategy in which the side stream flow rate is equal to the flow rate of ethyl lactate in the feed stream

Adams and Seider, demonstrated the effectiveness of the control strategy in achieving the separation objectives while remaining within operational limits. Additionally, the process was simulated for a range of production rates and a detailed economic analysis performed. The authors reported 17% lower lifetime costs for production rates in the range 0.3 to 2.0 million kg per year when compared batch and continuous processes (Adams & Seider, 2008a).

1.3. Objectives

Given the economic challenges which exist with biomass facilities the overall objective of this research is to design a semicontinuous system for the separation of bio-DME and assess its profitability compared to the conventional separation process. The overall research objective is achieved by the following steps:

i. Develop a dynamic model and associated control scheme for semicontinuous system which achieves separation objectives and captures mode transitions.

ii. Optimization of semicontinuous and continuous systems at various production rates to determine which separation strategy should be employed for a particular bio-DME plant size.

As the original, continuous separation section has three distillation columns, two semicontinuous systems are investigated and compared to the continuous system to determine the most economical configuration. In the first phase, the second and third distillation columns in the continuous system are replaced by a semicontinuous system using a single column tightly integrated with a middle vessel. The second phase investigates a semicontinuous system designed to effect the separations of the first and second distillation columns using a single distillation column coupled with a middle vessel.

1.4. Main Contributions

The contribution of this research is twofold.

1. **Development of cost-capacity relationships for semicontinuous and continuous DME separation system** - The economic results will be extended in future work to include the cost (capital and operating) for the entire processing facility together with harvesting and transportation costs in an enterprise wide optimization framework. This framework will consider the production processes (semicontinuous or continuous) for various biofuels and other decisions such as, land use and biomass feedstock to determine the optimal plant capacity for a biofuels distributed network in Canada.

2. **Continued development of semicontinuous theory** - In this work, the application of semicontinuous systems was extended to biofuel separation from reaction by-products. The application of semicontinuous system to separation of DME led to the development of a semicontinuous system for separation of a biphasic mixture using a partial condenser configuration, which has not been previously investigated. Additionally, temperature control configurations were developed for both semicontinuous systems studied eliminating the requirement

for costly composition analysers. This was the first time that temperature control has been utilized in semicontinuous systems. Dynamic simulation results illustrate the improved performance of the system in maintaining product purities and rejecting fresh feed disturbances.

1.5. Thesis Outline

The remainder of this thesis is organised as follows:

Chapter 2 – This chapter focuses on the development of a semicontinuous system for separation of DME, replacing the second and third distillation columns in the continuous process. Since the control system is fundamental to the operation of the semicontinuous system, several control configuration not previously examined, are investigated.

Chapter 3 – In this chapter we present the optimization approach utilized for the continuous and semicontinuous system, followed by an economic comparison of each system for a range of DME production rates

Chapter 4 – This chapter is devoted to the development of an alternative semicontinuous system wherein the separation of the first and second distillation columns in the continuous process is achieved. Also included is a detailed investigation of alternative control configurations followed by an economic assessment compared to the continuous system.

Chapter 5 – Here we summarize the results of this work and provide recommendations for future studies.

Chapter 2

TERNARY SEMICONTINUOUS DISTILLATION OF DME

The results in this chapter have been published in the following journal:

Pascall, A. and Adams, T. A. (2013), Semicontinuous separation of dimethyl ether (DME) produced from biomass. *Can. J. Chem. Eng*. doi: 10.1002/cjce.21813

2.1. Introduction

In previous studies, the semicontinuous systems were modeled using MESH equations with few simplifying assumptions as discussed in Chapter 1. However, in this work the semicontinuous system using rigorous pressure-driven dynamic simulations implemented in Aspen Plus Dynamics. As such the assumption of constant pressure drop throughout the system is eliminated.

The dynamic system model and comparisons of eight potential control strategies are presented in this chapter. Neither DME production nor many of the proposed control strategies have been examined previously for semicontinuous systems to the best of the author's knowledge.

2.2. Process Modeling

2.2.1. Continuous Process

The separation section, based on the proposed configuration of a switchgrass-to-DME facility by Larson et al., 2009 consists of a series of flash drums and distillation columns as shown in Figure 2.1.

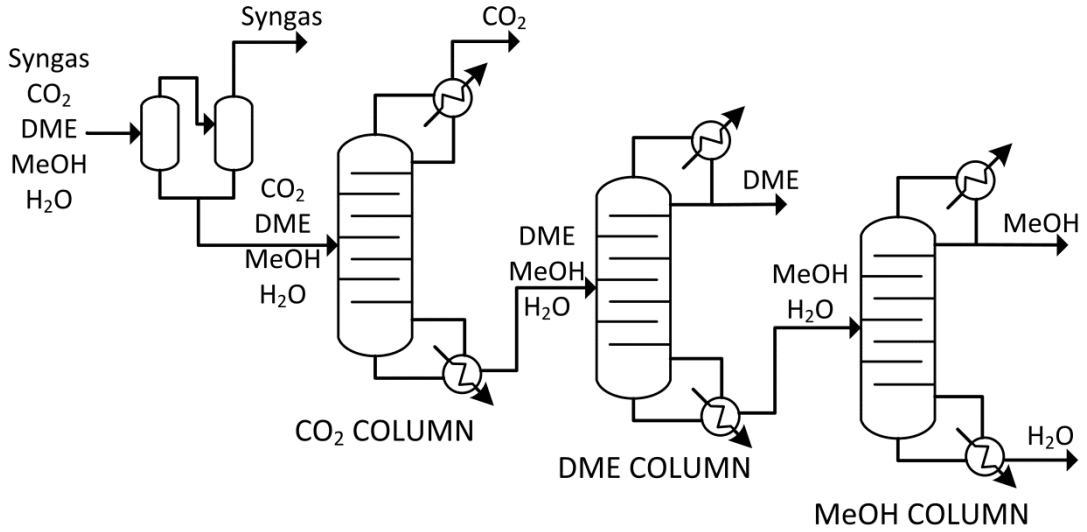

Figure 2.1: Continuous process for dimethyl ether separation

The reactor effluent, which contains unreacted syngas (carbon monoxide and hydrogen), reaction by-products (methanol, water and carbon dioxide) and DME, is sent to a series of flash drums where unreacted syngas is recovered and recycled to the DME reactor. The flash drum liquid products then undergo cryogenic distillation to remove dissolved CO_2. The bottoms product from the CO_2 column consisting of DME (81.57 mol%), methanol (14.43 mol%), water (3.98 mol%) with minimal CO_2 (0.02 mol%) at 10.0 atm and 328.54K is sent to the final two distillation columns. Here, DME is recovered at 99.95 mol% (the recommended standard for its use as a fuel (Arcoumanis et al., 2008; Ogawa et al., 2003) while the bottoms product is sent to the MeOH column where methanol and water are distilled to purities of 96[1] and 99.05 mol% (98.5 wt% assumed for this simulation) respectively at a system pressure

[1] A methanol purity of 96mol% was selected since it is sent to a downstream DME dehydration reactor and thus does not require high purity (van Dijk, 1998). By comparison, Grade AA methanol is 99.85 wt% pure (Fiedler et al., 2011).

of 10.0 atm. These process conditions were selected to be consistent with the work of Larson et al., 2009.

The separation section was simulated using Aspen Plus V7.3 with the RadFrac equilibrium-based model used for the distillation columns. The vapour-liquid equilibrium (VLE) was modelled using the Peng Robinson (PR) equation of state coupled with Wong Sandler (WS) mixing rule and the UNIFAC model for calculating the excess Helmholtz energy (a.k.a the PRWS-UNIFAC model). This property model was shown to accurately predict the VLE behaviour of the quaternary (CO_2, DME, MeOH, H_2O), subset ternary and binary systems when compared to experimental data (Ye, Freund, & Sundmacher, 2011).

2.2.2. Semicontinuous Process

2.2.2.1. Process Description

The semicontinuous process is designed to achieve the same separation objectives of the DME and MeOH columns using a single distillation column integrated with a MV. Using the configuration shown in Figure 2.2, DME is separated from the ternary mixture during a cyclic campaign involving three operating modes. The MV both feeds to and receives a side stream from the distillation column throughout each cycle. Consequently, the process exhibits non-stationary behaviour as the feed composition and flowrate to the distillation column changes throughout the cycle.

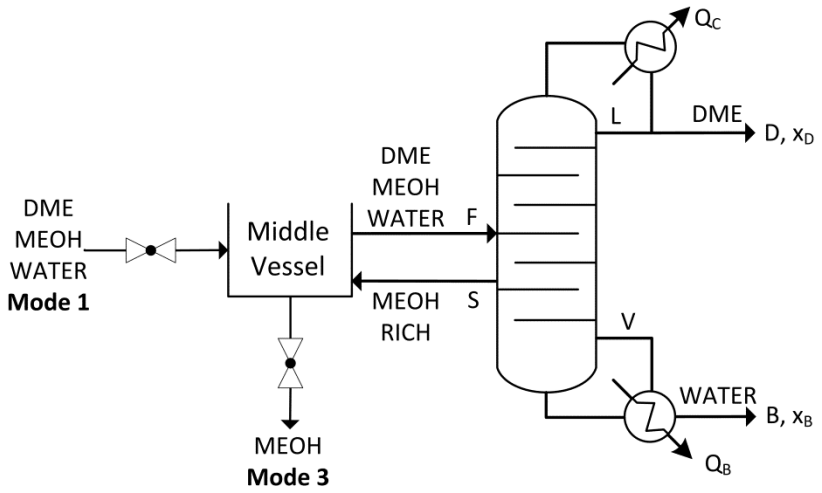

Figure 2.2: Semicontinuous process configuration

In Mode 1, the MV is charged with the ternary mixture which is of the same composition as the feed to the final two distillation columns in the continuous case. Once charging is complete, Mode 2 begins. During Mode 2, DME is recovered at 99.95 mol% in the distillate and water at 99.05 mol% in the bottoms in diminishing flow rates as the cycle progresses. The side draw has a high concentration of methanol and as DME and water are removed continuously, methanol concentrates in the MV until the desired purity is attained. On achieving a methanol purity of 96 mol% Mode 2 ends.

In Mode 3, the contents of the MV are quickly drained with the methanol product sent to the downstream dehydration unit. This mode ends when the MV is nearly emptied and the next cycle starts with Mode 1. In Modes 1 and 3 the feed to the column and side draw remain in operation such that there is no start-up and shut-down of the column, and together consume only a small fraction of the total cycle time. The semicontinuous process is simulated using the approach described in Section 2.2.2.3.

2.2.2.2. Control System Design

The control system is designed to ensure the following specification and operational objectives are met during mode transitions, feed composition and flow rate changes:

1. Distillate (DME) composition is maintained at 99.95 mol%
2. Bottoms (water) composition is maintained at 99.05 mol%
3. Flooding and weeping conditions in the column are avoided at all times

For the semicontinuous system there are seven degrees of freedom (DOF) correlating to seven manipulated variables: the condenser heat duty (Q_c); either the reboiler heat duty (Q_B) or boil-up rate (V); and the molar flow rates of the reflux (L), feed (F), distillate (D), side stream (S) and bottoms (B). Q_c is used to control the column pressure with the remaining DOFs used to control distillate composition (x_D), bottoms composition (x_B), reflux and sump levels. While several controller loop pairing configurations are possible only a few are considered for analysis based on an understanding of the process.

Eight control configurations are investigated using decentralized feedback control since it has been shown to be effective for various semicontinuous systems. Two traditional continuous control configurations commonly used for dual composition control (Skogestad, 1997) are not considered as they render the ternary semicontinuous system inoperable, namely *"LV"* (the reflux rate is manipulated to control x_D and the boil-up rate is varied to control the x_B) *and "L/D, V/B"* (the reflux ratio is manipulated to control x_D and the reboil ratio manipulated to control the x_B) (Phimister & Seider, 2000a).

Initially, it is assumed that all required stream compositions can be measured using composition analysers to explore an extensive number of control configurations. Later, inferential temperature control configurations are examined due to the increased cost (capital and maintenance) and time delay associated with composition analysers. The ability of the control configuration to achieve the separation objective while meeting specification and operational targets is then evaluated through dynamic simulation using Aspen Dynamics.

Configuration 1

Figure 2.3A shows the *"DB"* control configuration proposed by Phimister & Seider, 2000a for ternary semicontinuous separation systems. The feed rate to the column is flow controlled with a full liquid side draw returned to the MV. x_D and x_B are maintained by manipulating distillate and bottoms flow rates with reflux drum and sump levels controlled by reflux rate and reboiler heat duty.

Configuration 2

In this *"DB"* control configuration the feed to the column is not fixed but manipulated to control the reflux drum level as shown in Figure 2.3B. Sump level and product purities are controlled in the same manner as in configuration 1 with the reflux rate held constant. This structure has the advantage in that the column's internal flow rates are held fairly constant throughout each cycle.

Configuration 3

In control configuration 3, the sump level is controlled by manipulating the feed flow rate. However, as opposed to configuration 2, the reflux drum level is now controlled by manipulating the reflux rate as shown in Figure 2.3C. x_D and x_B are controlled in the same manner as configuration 1 and 2 with reboiler heat duty maintained constant throughout the cycle. This configuration proposed by Phimister & Seider, 2000a provided satisfactory performance for their ternary separation system of interest (separating three liquid hydrocarbons). Moreover, the delay experienced when sump level is controlled by manipulating reboiler heat duty is avoided with the added advantage of somewhat constant internal flow rates throughout each cycle (Phimister & Seider, 2000a).

Configuration 4

In the control configurations considered thus far the side stream flow rate (*S*) has not been utilized as a manipulated variable because of the low importance of maintaining the side stream at a constant composition. However, controlling the flow rate to achieve a higher purity recycle stream to the MV reduces cycle time (Adams & Seider, 2009a). (Adams & Seider, 2008a) implemented the ideal side-draw recovery arrangement where the side stream flow rate is controlled by:

$$S(t) = F(t)x_{F,MeOH}(t) \tag{2.1}$$

where $S(t)$ is the molar flow rate of the side draw, $F(t)$ is the molar flow rate of the feed stream, and $x_{F,MeOH}$ is the mole fraction of methanol in the feed. Eq. (2.1) is derived from the dynamic mass balance for methanol over the column assuming no holdup in the column, which is:

$$F(t)x_{F,MeOH}(t) = D(t)x_{D,MeOH}(t) + B(t)x_{B,MeOH}(t) + S(t)x_{S,MeOH}(t) \tag{2.2}$$

where *D* and *B* are the molar flow rates of the distillates and bottoms, and *x* are the mole fractions in the corresponding streams. Eq. (2.1) results from Eq. (2.2) for the

ideal case that no methanol is lost in the distillate and bottoms ($x_{D,MeOH} = x_{B,MeOH} = 0$) and that no impurities exist in the side draw ($x_{B,MeOH} = 1$). A control strategy according to Eq. (2.1) has shown to reduce loss of the intermediate species through the distillate and/or bottoms products ensuring a high purity side stream thereby reducing cycle time.

Figure 2.3D, shows the structure for configuration 4, where the ideal side-draw recovery is used to control the side stream rate with product purities and vessel level controlled in the same manner as in configuration 2.

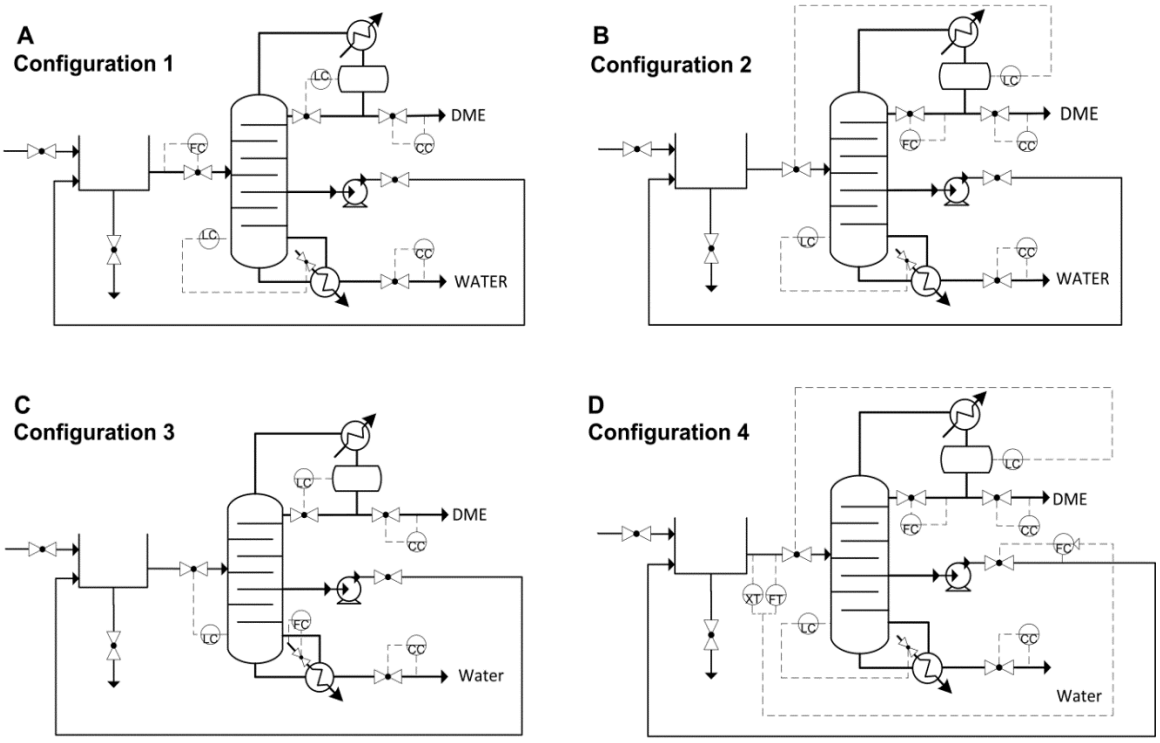

Figure 2.3: Control configurations 1, 2, 3 and 4

Configuration 5

Control configurations based on inferential temperature control are investigated to further improve the dynamic performance of the system. As shown in Figure 2.4A, a single tray temperature is controlled to maintain the distillate composition and another single tray temperature used to control the bottoms composition. The tray temperature

location is crucial to the accuracy at which product compositions are inferred (Shinskey, 1984) for the entire operating range.

Tray temperature locations are selected based on:

i. Invariant temperature criterion in which tray temperature is maintained at a constant value over the expected range of feed composition changes (Luyben, 2006a)
ii. Ensuring tray temperature is well correlated with composition for manipulated variable changes (Marlin, 2000)

This configuration has the added advantage in that the composition analyser for x_D is eliminated. However due to the possibility of offset in controlling x_B (see Results and Discussion), a cascade control structure is implemented. Here, the slave loop regulates the tray temperature by manipulating the bottoms flow rate while the master loop utilizes a composition analyser to adjust the tray temperature setpoint. The temperature analysers are assumed to have a dead time of one minute while the composition analysers have a three minute measurement lag (Luyben, 2006b).

Configuration 6

Thus far we have considered different arrangements of the *"DB"* control configuration. Here, we consider another control structure, *"LB"* control in which reflux rate is manipulated to control the x_D with bottoms flow rate used to control x_B. Additionally, temperature inferential and ideal side draw control schemes are implemented as shown in Figure 2.4B.

Control configuration 7

Figure 2.4C represents the *"DV"* control configuration with distillate and bottoms composition controlled by manipulating distillate flow rate and reboiler heat duty. This configuration also employs the temperature inferential and ideal side draw control schemes.

Configuration 8

This control configuration as shown in Figure 2.4D is similar to that of configuration 4 except that the reflux rate is not held constant. As the cyclic campaign progresses after charging of the MV, the column progressively moves away from its maximum operating capacity. The additional degree of freedom provided by the reflux rate is manipulated to ensure the column operates at its peak capacity without flooding. In conventional columns the flooding approach is detected by measuring the differential pressure across the column and controlled by regulating the reboiler duty, reflux or feed throughput (Birky, McAvoy, & Modarres, 1988; Lipták, 2005; Shinskey & Foxboro, 1977). In this configuration the reflux rate is adjusted to control the column's differential pressure such that it operates at its maximum capacity near flooding throughout the cycle.

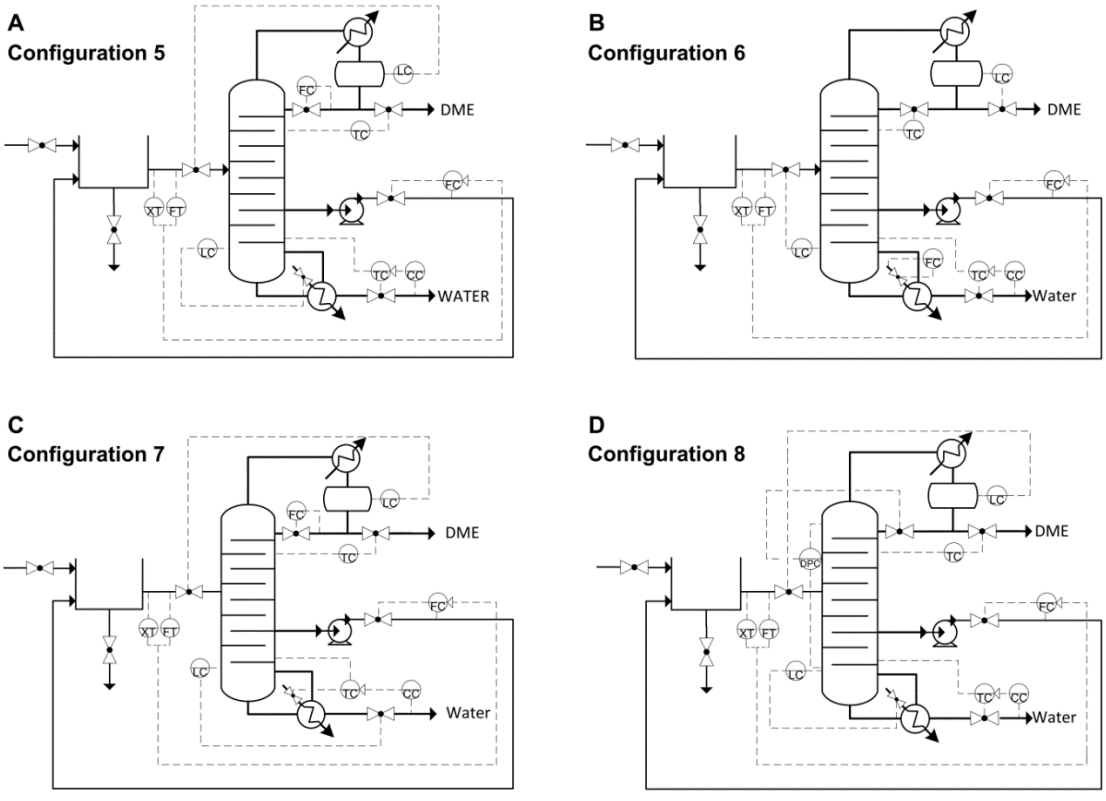

Figure 2.4: Control configurations 5, 6, 7, and 8

2.2.2.3. Simulation

In order to perform dynamic simulations of the semicontinuous system and associated control system in Aspen Dynamics, an equivalent steady-state flowsheet must first be created in Aspen Plus V7.3. In Aspen Plus, the semicontinuous distillation column is modelled using the equilibrium-based RadFrac unit with the PRWS-UNIFAC equation of state model. The column has 25 stages with an assumed Murphree efficiency of 85% (Tock, Gassner, & Maréchal, 2010) (assumed constant for all trays), condenser pressure fixed at 10 atm and a pressure drop of 0.1 psi per tray. Feed and side stream locations are selected such that distillate (DME) and bottoms (water) specifications are met while minimizing the reflux/reboil ratios. Distillate and bottoms specification of 99.95 and 99.05 mol% are attained using the design spec/vary function in the RadFrac unit. Once these have been completed, the equipment can be configured for export to the dynamic simulator.

The reflux drum and sump are sized according to commonly used design heuristics (Luyben, 2006b) while the control valves are designed with a pressure drop of 3 atm (Luyben, 2006b). The column diameter is then calculated using the Aspen Plus tray sizing function with the feed rate adjusted to achieve the required column diameter. The control configurations are evaluated using the minimum standard diameter for distillation columns, 1.5ft. (Aspen Technology Inc, 2011). Higher DME production rates can be achieved by increasing the feed and side stream rates (Adams & Seider, 2008a) with the appropriate standard sized column diameter selected to prevent flooding and weeping.

As the charge volume increases the operating cost per DME produced decreases as the transition modes (Mode 1 and 3) form a smaller fraction of the total cycle time. However, with larger charge volumes the capital cost increases significantly. The resulting tradeoff in the TAC forms an optimization problem (see Chapter 3). For this particular case the MV is sized with an initial molar hold up of 100 kmol (96% of maximum level) with the operating pressure set at 13 atm such that the required pressure of the feed to the column is attained after pressure drop losses.

The resulting steady-state simulation is then exported to Aspen Dynamics as a pressure-driven simulation and serves as the initial condition for the dynamic model. The dynamic simulation is first initialized, the side stream routed to the MV and the selected control scheme configured. Figure 2.5 shows the Aspen Dynamics structure for the semicontinuous system utilizing the control scheme in configuration 5.

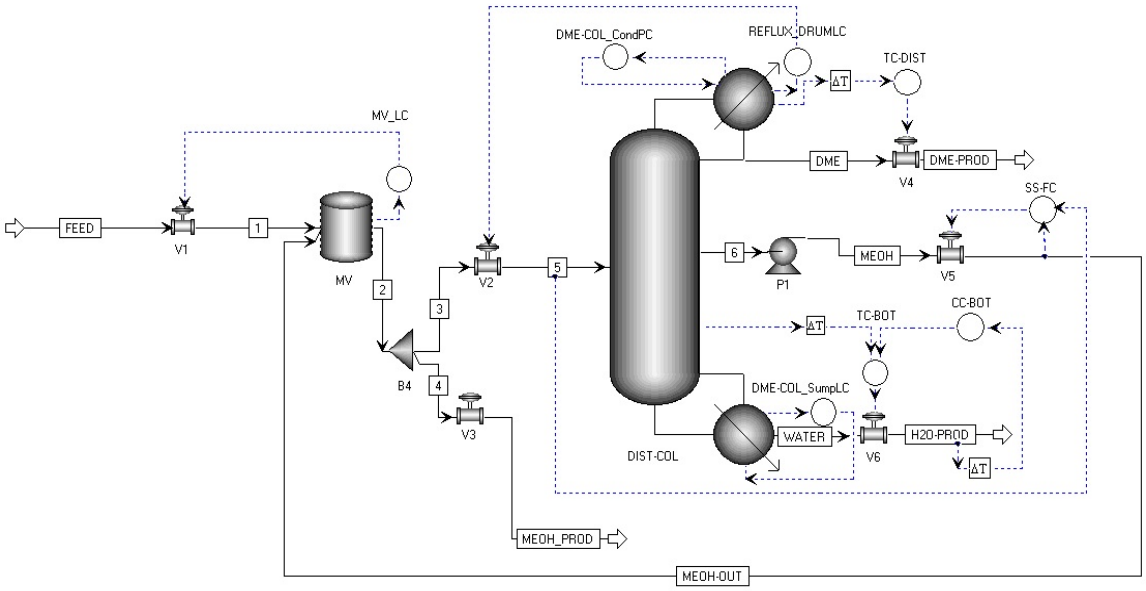

Figure 2.5: Aspen dynamics configuration for semicontinuous distillation of DME, MeOH and water

Temperature, composition and pressure loops are configured with proportional integral (PI) control while level and side stream flow controllers are P only. Controllers are tuned by hand such that the integral squared error (ISE) for DME in the distillate and water in the bottoms composition are minimized. Transition through the various modes of the cyclic campaign is accomplished by creating an event-driven task which controls the operation of the feed (V1) and methanol product (V3) valves. At the start of Mode 1, V3 is closed however V1 is fully opened until the required molar volume is charged to the MV. Once this mode is complete V1 is closed and Mode 2 commences with methanol concentrating in the MV. On achieving the target purity in the MV, V3 is fully opened, discharging methanol to the downstream unit until a liquid height of 10% is attained at which the cycle repeats.

2.3. Results and Discussion

2.3.1. Control Performance

In this section the effectiveness of the proposed control configurations for separation of the ternary mixture of DME (81.57 mol%), methanol (14.43 mol%) and water (3.98 mol%) with minor impurities (CO_2 – 0.02 mol%) are evaluated.

Although control configuration 1 has been shown to perform satisfactory in other semicontinuous systems in which the three species are approximately equimolar, when applied to this separation system the operational constraints are violated. As the cycle progresses DME and water holdup within the MV decreases while the methanol holdup and composition increases. Since the feed composition to the column decreases in DME and water, product flow rates are minimized to maintain product purities. This leads to higher internal flow rates under a constant feed flow rate resulting in flooding of the upper section of the column 81 minutes into the first cycle as shown in Figure 2.6. The Fair correlation (Fair, Steinmeyer, Penney, & Crocker, 1997) is used to calculate the flooding approach for each tray throughout the cyclic campaign.

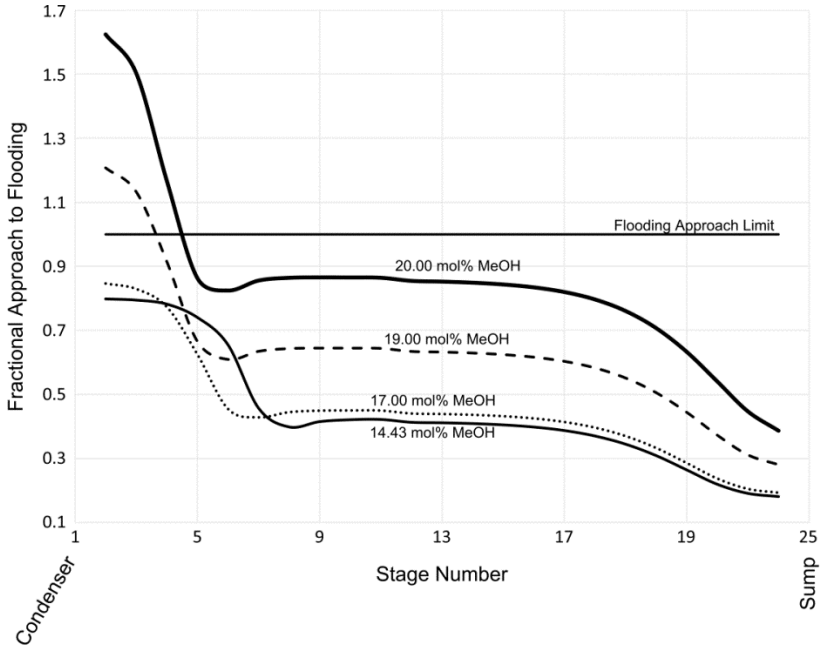

Figure 2.6: Flooding profile in semicontinuous distillation column for control configuration 1 after 81 minutes

Thus, the feed flow rate to the column should be manipulated to ensure flooding is avoided throughout the cycle. This is achieved through configurations 2 and 3. As shown in Figure 2.7 both configurations are able to achieve the desired separation without exceeding flooding limits.

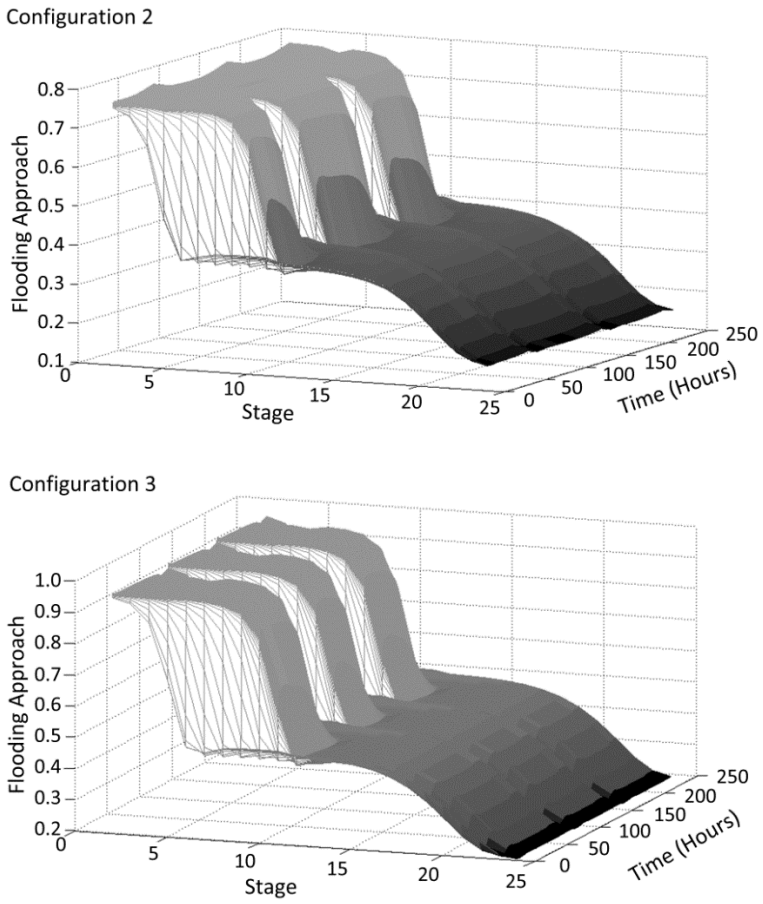

Figure 2.7: Flooding approach profile for control configurations 2 and 3

Additionally, throughout each cycle, the gas velocity through the sieve perforations in the top (stage 2), bottom (stage 24) and middle (stage 11) sections are greater than minimum velocity avoiding weeping (Figure 2.8). The minimum velocity (a.k.a the weep point or weeping velocity) is calculated using Eqs. (2.3) and (2.4) (Mersmann, Kind, & Stichlmair, 2011).

$$F_{min} = \varphi \sqrt{0.37 d_H g \frac{(\rho_L - \rho_V)^{1.25}}{\rho_V{}^{0.25}}} \qquad (2.3)$$

$$u_{min} = \frac{F_{min}}{\sqrt{\rho_V}} \qquad (2.4)$$

where, F_{min} is the minimum gas load, φ is the relative free area, d_H is the tray hole diameter, g is the acceleration due to gravity, ρ_L and ρ_V are the liquid and vapour densities u_{min} is the minimum vapour velocity.

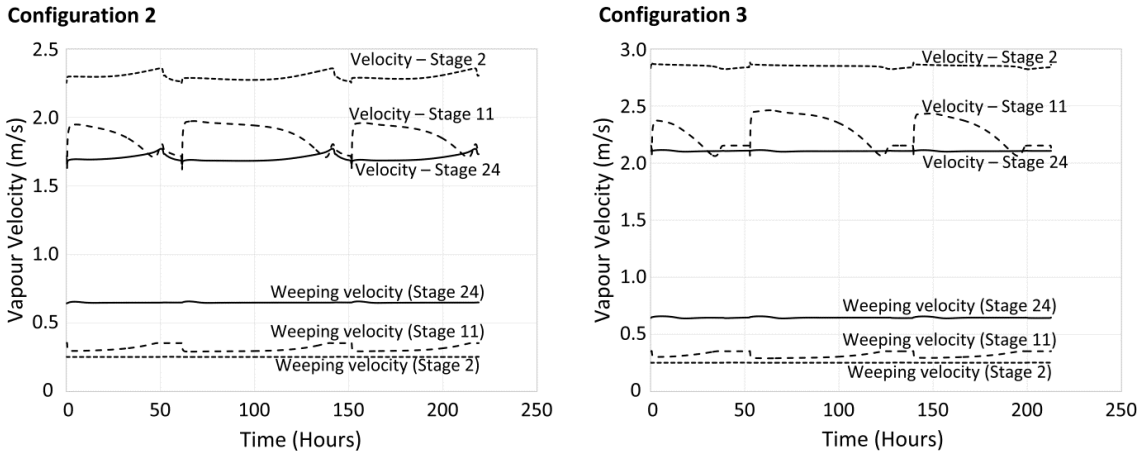

Figure 2.8: Weeping and operating velocities for configurations 2 and 3

Profiles for configurations 2 and 3 over three cycles are illustrated in Figure 2.9.
The cycles represented here occur after separation of the initial charge from the steady state simulation. As the MV is not completely drained at the end of mode 3, for each cycle the feed composition at the end of Mode 1 is slightly higher in methanol. Simulation results for both configurations demonstrate that despite achieving the methanol purity in the MV it is difficult to maintain the DME and water setpoint target throughout the cycle. Reducing the integral time for the composition controllers lessen the deviations as the cycle progresses, however, it results in valve saturation at the lower end (0%) significantly increasing the cycle time.

For configuration 3, larger fluctuations in sump level are observed when control is achieved by feed flow rate manipulations. This is primarily due to sump level being more responsive to heat input as oppose to feed flow rate and delays in tray liquid holdup in the bottom section of the column. Due to the interaction between the level and composition loops, larger fluctuations are observed in water purity throughout each cycle.

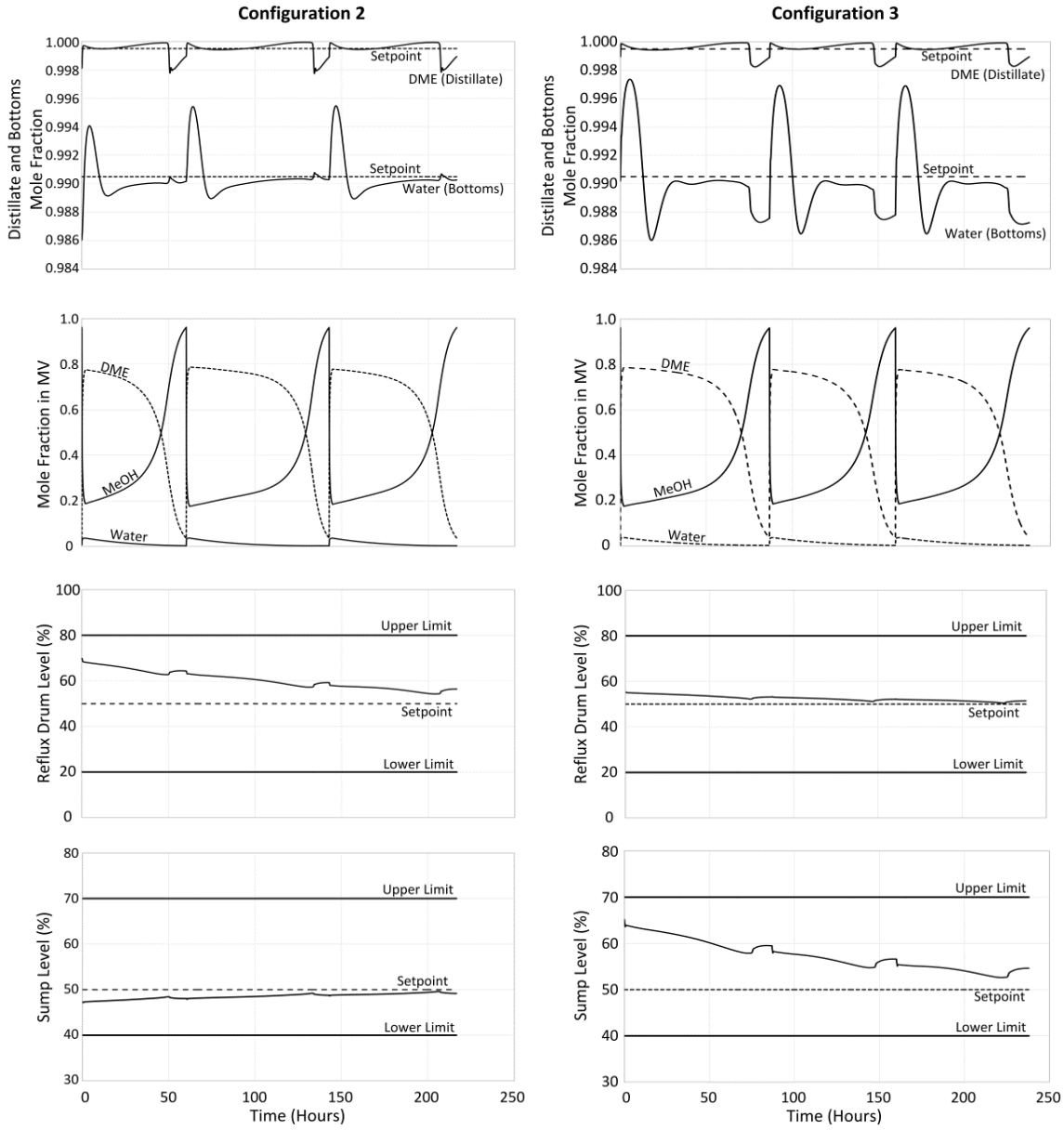

Figure 2.9: Composition and level profiles for control configurations 2 and 3 for three cycles

When the ideal side-draw control is applied (configuration 4), setpoint tracking for DME and water purities are greatly improved as shown in Figure 2.10. This control strategy ensures that methanol losses to the DME and water streams are minimized, resulting in a methanol-rich side stream throughout the cycle. As shown in Figure 2.10 and Table 2.1, this strategy reduces the cycle time by 19.4% when compared to

configuration 2 in which the side stream is not controlled. Additionally as illustrated in Figure 2.11, separation is achieved without flooding or weeping occurring.

Table 2.1: Control performance comparison and operating cost per DME produced for all control configurations

Configuration	Average cycle time (hours/cycle)	Integral squared error – DME purity setpoint	Integral squared error – Water purity setpoint	Operating cost per kg DME ($/kg)
1	Cycle failure due to column flooding			
2	72.10	5.07×10^{-5}	3.88×10^{-4}	0.057
3	79.27	4.85×10^{-5}	1.69×10^{-3}	0.067
4	58.05	2.87×10^{-5}	9.03×10^{-5}	0.044
5	30.08	5.22×10^{-7}	6.74×10^{-6}	0.018
5a[1]	29.42	5.14×10^{-7}	6.86×10^{-6}	0.018
6	27.78	8.45×10^{-7}	9.13×10^{-4}	0.024
7	Product compositions cannot be met			
8	26.95	3.99×10^{-7}	1.99×10^{-6}	0.022

Note: 1 – Side stream controlled to a fixed flow rate

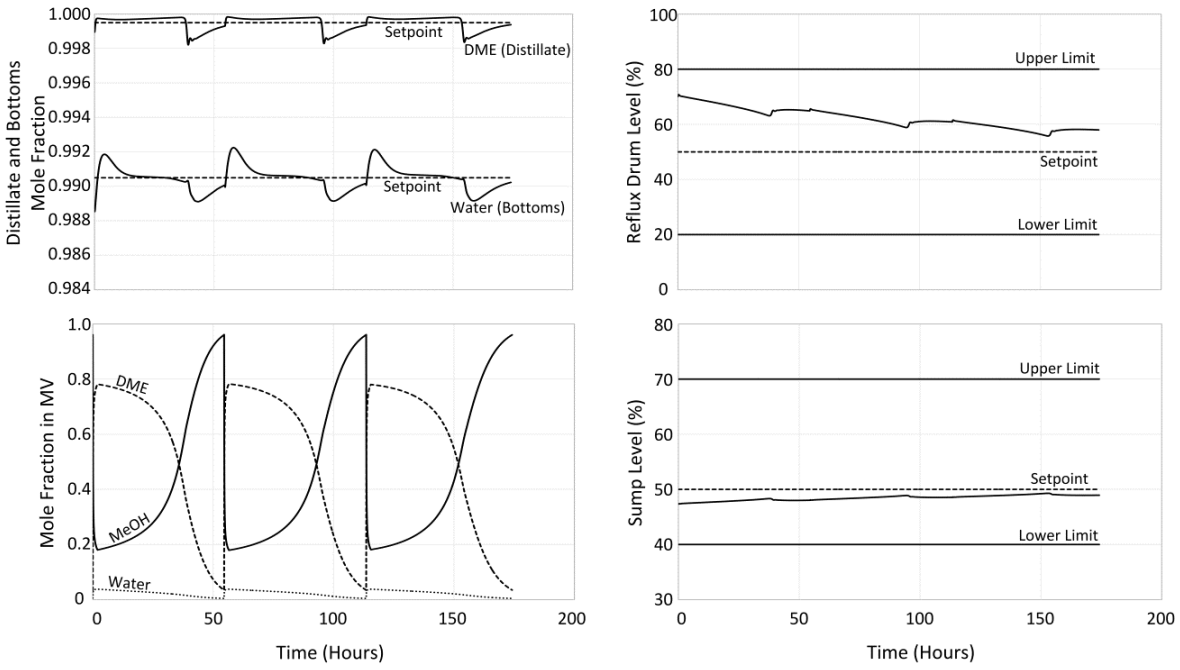

Figure 2.10: Composition and level profiles for control configuration 4

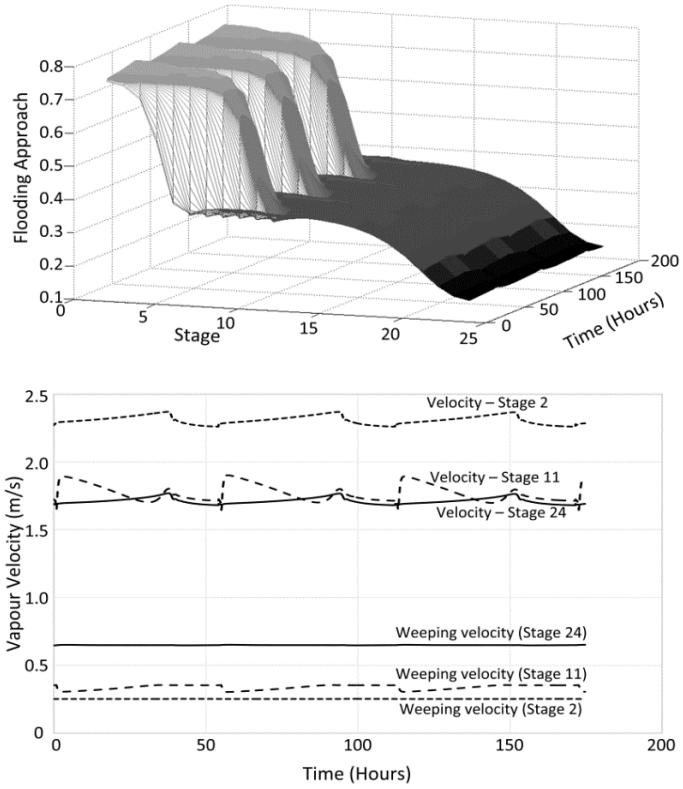

Figure 2.11: Flooding approach, vapour and weeping velocity profiles for control configuration 4

Tray Temperature Selection

The process for selection of tray temperature locations using the DB control scheme (configuration 5) as an example is presented here. In this section, we show that the approach is satisfactory but can result in offset, which can then be remedied using cascade control. Note that the Aspen Plus tray numbering convention in which stages are numbered from top to bottom with the reflux drum as Stage 1 is used in this analysis.

Invariant temperature criteria

Table 2.2 shows the temperature profile of various stages in the column for five feed sample composition which are likely to occur during a semicontinuous cycle. The feed compositions used in this analysis were obtained from simulation data for configuration 2. Snapshot 1 reflects the feed composition at the beginning of the cycle

with snapshot 5 reflecting the feed composition towards the end of the cycle. The temperature profile of the column for each feed composition snapshot was obtained using Aspen Plus. For each snapshot, the design spec/vary function was used to achieve the desired distillate and bottoms product specification. The *S/F* ratio, required for convergence of the column, is calculated using the ideal side draw approach Eq. 2.1.

According to the temperature invariant criteria, the best stages are those where the temperature does not change much with changes in feed composition. As shown in Table 2.2, in the top section, Stages 2 and 3 exhibit the smallest temperature variation over the range of feed compositions. Similarly, stages 23 and 24 exhibit the smallest variation in temperature in the bottom section. Note that stages 1 and 25 are not considered since they are not trays (they are the reflux drum and the reboiler, respectively). Stages 6-20 are not shown in the table for brevity because they exhibited large perturbations in temperature (>1°C) as feed composition changes.

Table 2.2: Temperature profile for stages at top and bottom of column for various feed compositions

Component	**Mole Fraction (kmol/kmol)**					**Temperature, Max – Min (K)**
	Snapshot 1	**Snapshot 2**	**Snapshot 3**	**Snapshot 4**	**Snapshot 5**	
Methanol	0.1443	0.4008	0.6503	0.8003	0.9503	
Water	0.0398	0.0365	0.0270	0.0190	0.0083	
DME	0.8157	0.5625	0.3227	0.1807	0.0415	
CO_2	0.0002	0.0001	0.0001	0.0000	0.0000	
Stage	**Temperature (K)**					
2	318.26	318.26	318.26	318.25	318.25	0.01
3	318.43	318.43	318.42	318.42	318.42	0.01
4	318.93	318.93	318.95	318.97	318.96	0.04
5	320.55	320.60	320.83	320.85	320.92	0.37
21	422.71	422.59	422.30	422.24	422.10	0.61
22	430.32	430.22	429.96	429.92	429.79	0.53
23	440.66	440.60	440.45	440.42	440.34	0.32
24	449.02	449.01	448.97	448.96	448.94	0.08

Temperature-composition correlation for manipulated variable changes

Stages 2, 3, 23 and 24 which best satisfy the temperature invariant criteria are then examined to determine how well each temperature correlates with its associated manipulated variable. In Aspen Plus, using the initial feed composition as the base case, the reboiler duty is held constant and the distillate flow rate varied at ±5% from the initial distillate flow rate. The resulting temperature-composition correlation is given in Figure 2.12A. Similarly, for the bottoms composition at the initial feed composition, the condenser duty is held constant and the bottoms flow rate varied at ±5% from the initial bottoms flow rate. The tray temperature and composition correlation obtained is shown in Figure 2.12B.

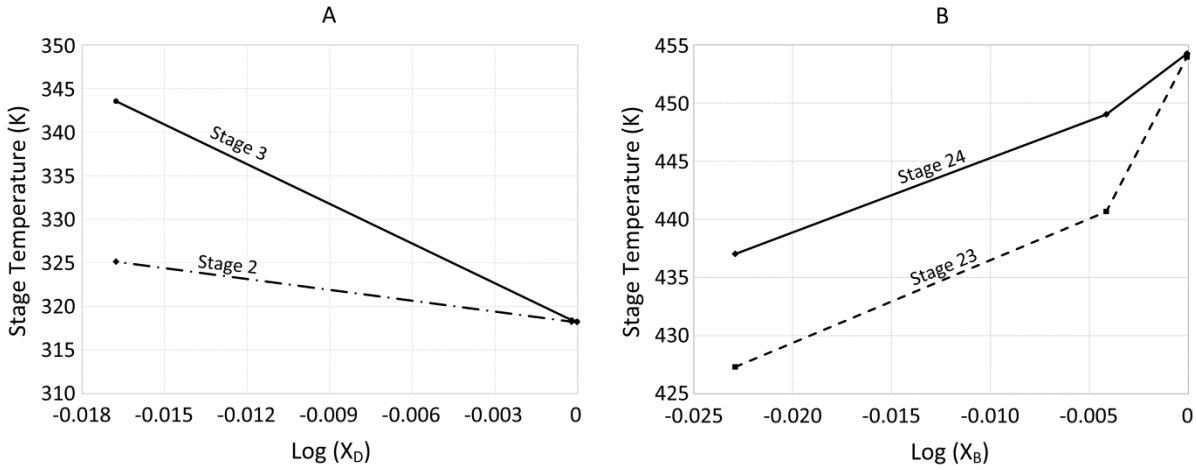

Figure 2.12: Correlation between tray temperature and distillate (A), bottoms (B) composition

Figure 2.12A shows that Stage 3 exhibits a larger temperature change over the range of distillate compositions when compared to Stage 2 (it has the largest slope). Hence, Stage 3 temperature was selected as the inferential variable for distillate composition. In the bottom section of the column Stage 23 has the larger slope in the region of operation ($\log(x_B) = -6.3 \times 10^{-5}$ or $x_B = 99.99$ mol% and $\log(x_B) = -0.00415$ or $x_B = 99.05$ mol%). As such Stage 23 was selected as the inferential variable for bottoms composition control.

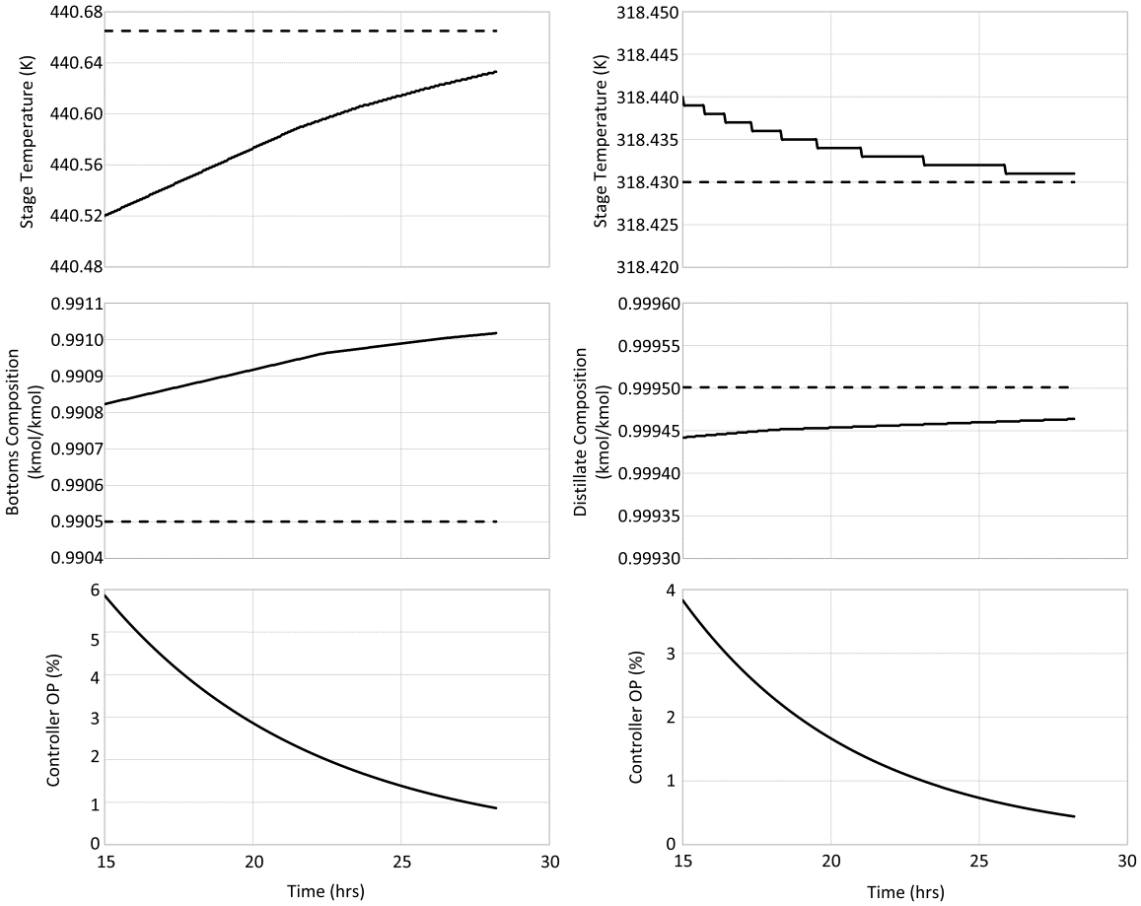

Figure 2.13: Composition and temperature profile for configuration 5 without cascade control for latter portion of first cycle

Next, stages 3 and 23 are evaluated using configuration 5 without cascade control. Figure 2.13 shows that during the cycle the bottoms product control valve closes to attain the required temperature setpoint, however, the actual bottoms composition is greater its setpoint composition. Since the valve closes while the composition is exceeded this would result in a larger cycle time. The composition offset is reduced by introducing a cascade control structure in which the tray temperature is corrected.

Unlike Stage 23, this offset is not experienced with Stage 3 inferential control as its temperature is held fairly constant (maximum deviation of 0.01°C as shown in Table 2.2) for all feed composition snapshots.

The temperature controllers are effective at maintaining the DME and water purity throughout the three cycles as shown in Figure 2.14, with the methanol concentrating in the side stream. Figure 2.15 shows that the methanol concentration on each stage remains fairly constant except during Mode 1. As Mode 1 commences the methanol concentration in the MV decreases rapidly corresponding to a decrease in the methanol flow rate to the column. The side stream, however, operates at a higher flow rate (Figure 2.14) and thus lower methanol purity.

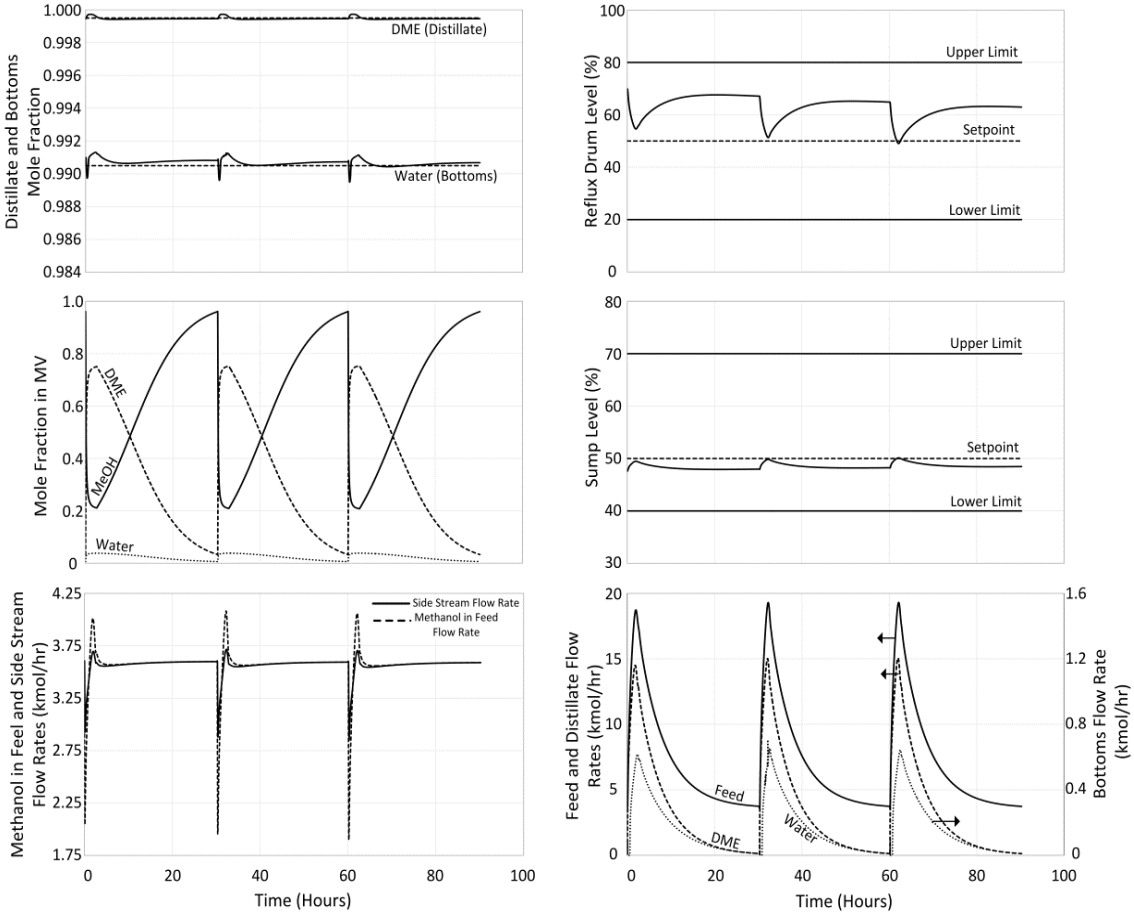

Figure 2.14: Composition, flow and level profiles for control configuration 5 for three cycles

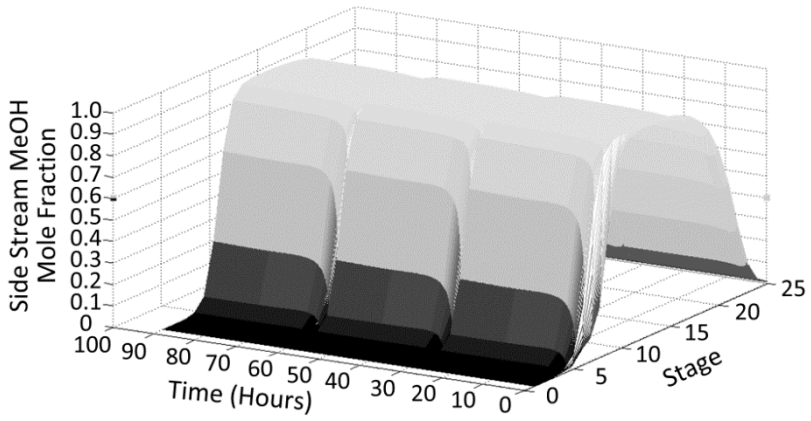

Figure 2.15: Methanol stage compositions and flow rate profiles for configuration 5 for three cycles

Figure 2.16 illustrates that unlike configurations 2, 3 and 4 the flooding profile varies throughout each cycle with the maximum flooding approach occurring at the beginning of the cycle (Mode 1). During Mode 1, the distillate product valve opens rapidly to maintain the temperature resulting in a decrease in reflux drum level and thus a sharp rise in the feed rate to the column. On the other hand, the bottoms composition control loop does not respond as quickly increasing the sump level and vapour flow rate and thus flooding approach within the column. As the cycle continues, the bottoms rate increases rapidly reducing the flooding approach within the column. In spite of these flow variations the vapour velocity in the top, middle and bottom sections of the column remain above the weep point throughout the cycles (Figure 2.16). The rapid change in reflux drum level and feed flow rate due to the composition loop response is not encountered in configuration 4 due to time delay of the analyser and tuning parameters. Tight tuning of the composition loops in configuration 4 result in oscillatory response and as such the composition configuration has a slower response than the temperature inferential control scheme. Thus the temperature inferential control scheme outperforms the composition analyser control configuration as shown by the reduced cycle time and integral square error (ISE) for the DME and water purity setpoints in Table 2.1.

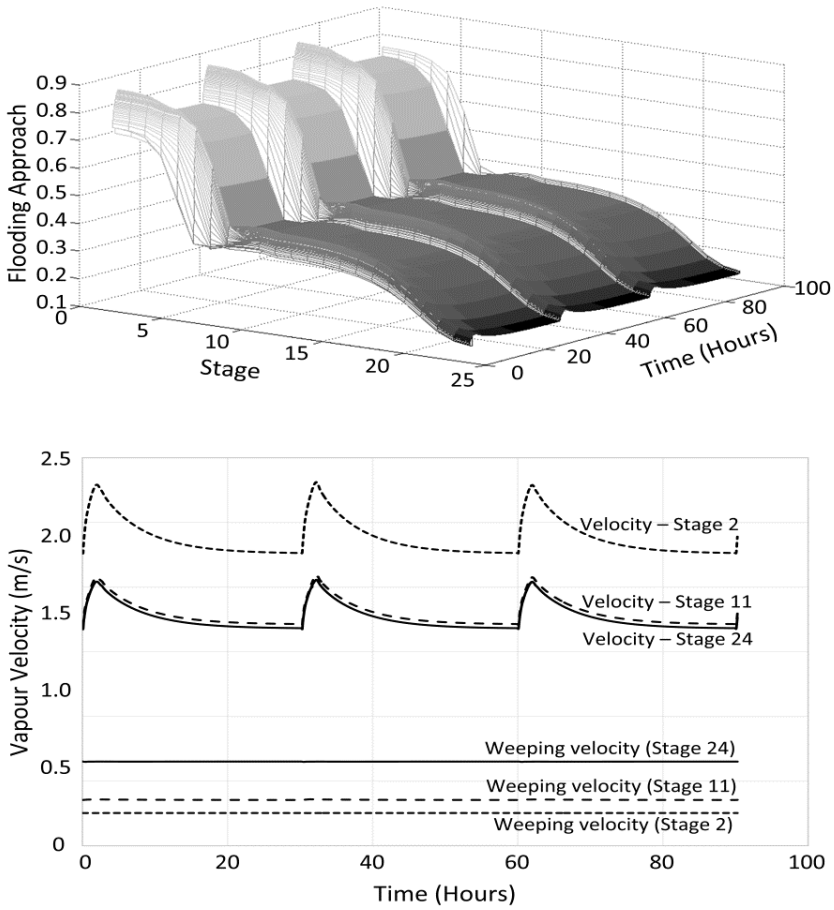

Figure 2.16: Flooding approach, vapour and weeping velocity profiles for control configuration 5 for three cycles

In configuration 5, the side stream approaches a steady state flow rate during Mode 2 as shown in Figure 2.14. However, after charging the middle vessel there is a delay in achieving this flow rate due to controller action and analyser dead time. This effect can be reduced by controlling the side stream at a constant flow rate setpoint, called configuration 5a. As shown in Table 2.1 and Figure 2.17 operating the side stream at a constant setpoint has little effect on the system profiles but results in a 2% decrease in cycle time and elimination of a composition analyser.

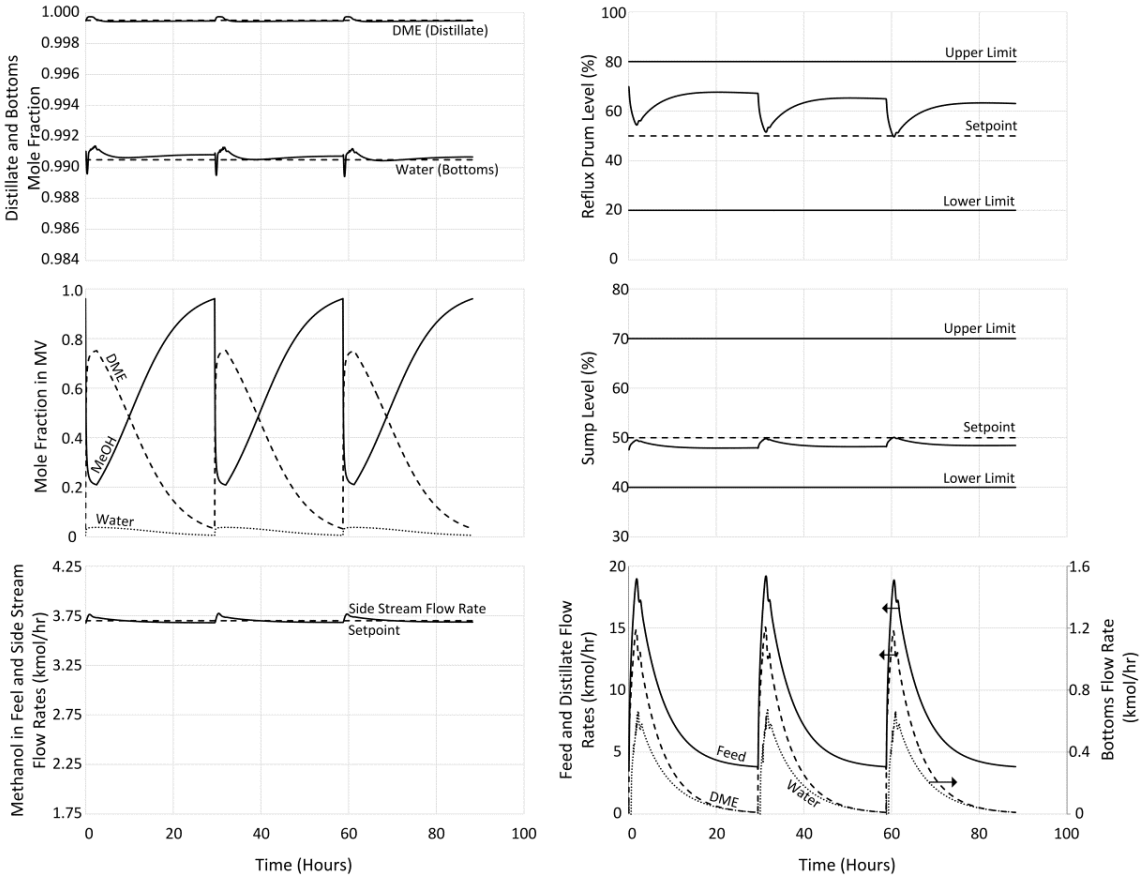

Figure 2.17: Composition, flow and level profiles for control configuration 5a with side stream controlled at a fixed setpoint for three cycles

In configuration 6 the DME purity is maintained throughout the cycle. However, setpoint tracking of the water product cannot be achieved. This response is similar to that obtained in configuration 3 where the delay due to tray liquid holdup and loop interactions results in large fluctuations as shown in Figure 2.18. Figure 2.19 illustrates the constant flooding approach and vapour velocity profiles maintained throughout the cycle as the boil-up rate remains fairly constant.

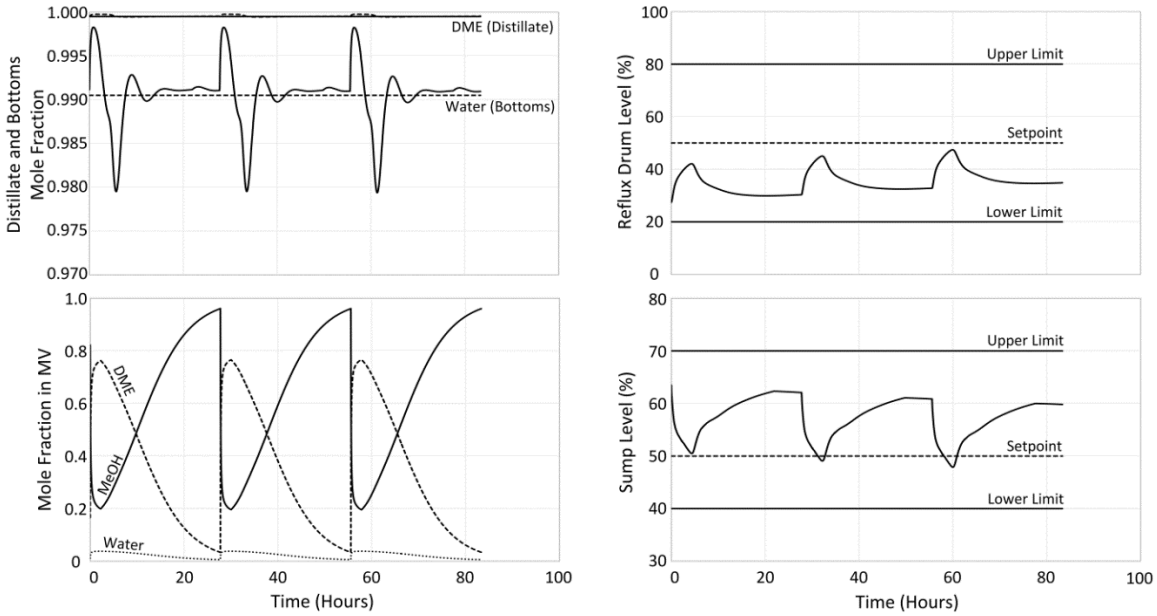

Figure 2.18: Composition and level profiles for control configuration 6 for three cycles

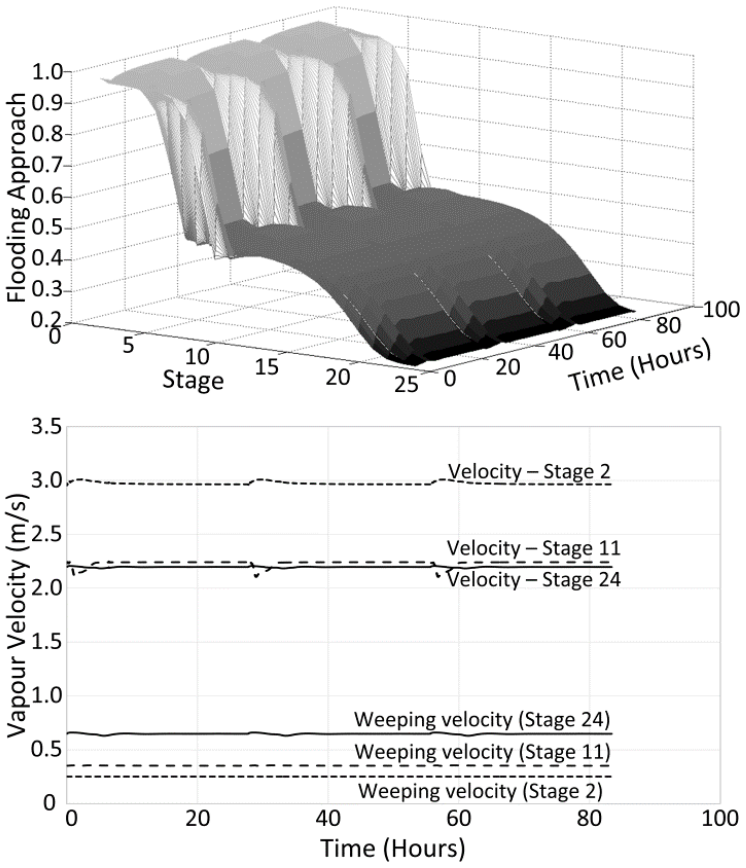

Figure 2.19: Flooding approach profile for control configuration 6 for three cycles

Control configuration 7 has shown to be inoperable for the semicontinuous system. The small water concentration in the feed necessitates a relatively high initial reboil ratio (44.2) to achieve the required stream purity. Controlling the sump level using the small bottoms flow rate with a large incoming flow (boil up and water product streams) is infeasible as shown in Figure 2.20. The fluctuations in sump level leads to oscillations in the water purity due to controller interactions. Evidently the variations in boilup rate lead to off-specification DME product.

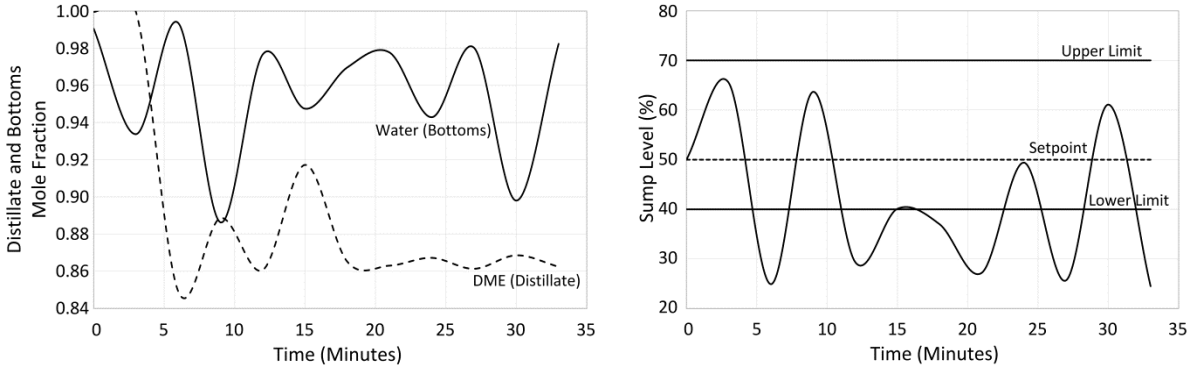

Figure 2.20: Composition and sump level profile for configuration 7 for a portion of the initial cycle from the steady-state simulation

As shown in Figure 2.22, the implementation of a differential pressure control loop ensures that the column operates at maximum capacity with a constant flooding approach profile throughout each cycle as compared to configuration 5. Furthermore, this control scheme leads to lesser fluctuations in vapour flow and thus velocity throughout the column compared to configuration 5. Configuration 8 also has the advantage in that off-specification products are avoided as shown in Figure 2.21 and cycle time is reduced. However, this is offset by an increased operating cost per DME produced as shown in Table 2.1. The differential pressure controller is configured as P only with a low proportional gain to prevent flooding during Mode 1.

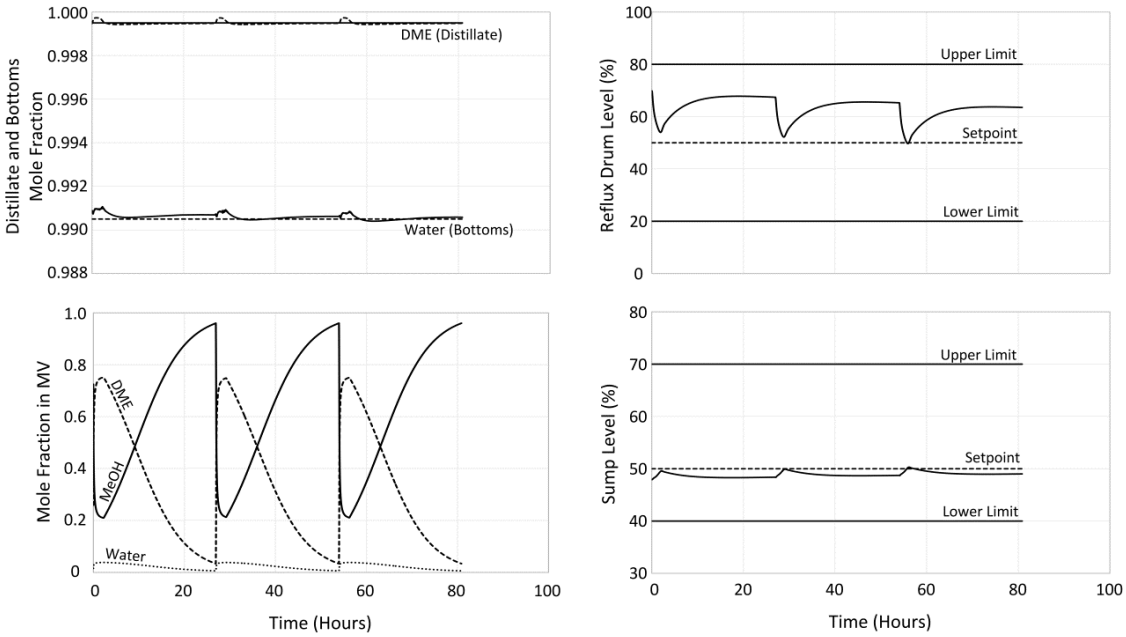

Figure 2.21: Composition and level profiles for control configuration 8

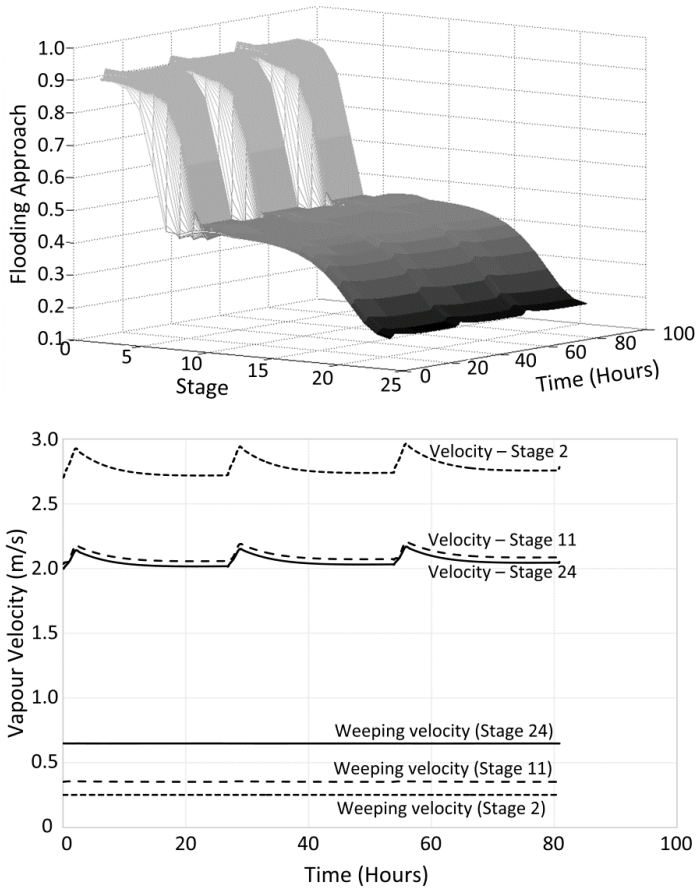

Figure 2.22: Flooding approach, vapour and weeping velocity profiles for control configuration 8

Based on the analysis of all possible configurations it can be seen that configuration 5, 5a and 8 provide the most satisfactory performance in maintaining product purities, cycle time and remaining within operational limits. Configuration 5a is selected as the control scheme for the DME-MeOH-Water semicontinuous separation system based on preliminary costing performed. Since the semicontinuous process is cyclic, another important consideration is attainment of a stable limit cycle. In this system *a priori* knowledge of the state variables during the stable limit cycle is not known, and as such the initial guess of the state variables are derived from the continuous simulation. While this initial guess state does not immediately result in a stable limit cycle, after a few cycles it converges to this stable limit as shown by the reflux and sump levels trajectories in Figure 2.23. Table 2.3 shows the tuning parameters for each control loop in configuration 5a.

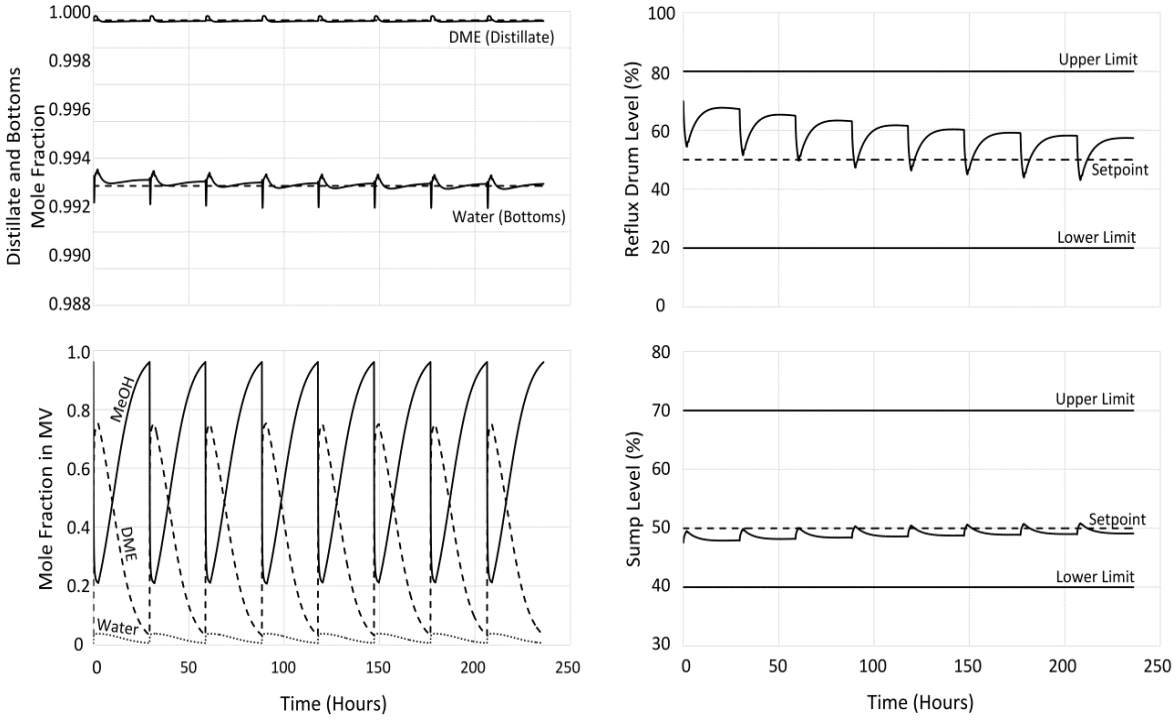

Figure 2.23: Composition and level profile for configuration 5 for eight cycles with side stream controlled at a constant setpoint

Table 2.3: Controller tuning parameters for configuration 5 with side stream controlled at constant setpoint

Control loop	Controller gain - K_c (%/%)	Controller integral time – τ_I (mins)
Reflux drum level	2.0	-
Sump level	2.0	-
Distillate temperature	35.0	80
Bottoms temperature	7.0	250
Bottoms composition	5.0	200
Side stream flow	2.5	-

2.3.2. Disturbance Rejection

The seven best control configurations were studied to determine how well each one is able to reject disturbances. We considered the response of the several control configurations to a step change in the fresh feed composition. The performance of the various configurations to a -10% step change in DME mole fraction in fresh feed (DME/MeOH/H_2O/CO_2: 73.41%/20.50%/6.07/0.02%) and +10% step change in DME mole fraction in the fresh feed (DME/MeOH/H_2O/CO_2: 89.73%/9.50%/0.75/0.02%) is given in Figure 2.24 and Figure 2.25 (the other species are increased or decreased proportionally). The disturbance is applied during the charging mode (mode 1) of the second cycle.

Configurations 2 and 3 can reject a 10% increase in DME mole fraction in the fresh feed with reduced offset in the bottoms composition as illustrated in Figure 2.24. However, for a 10% decrease in the DME mole fraction in the fresh feed the distillate valve closes to maintain the DME purity specification and reaches (0%) saturation. This result in failure of the cycle as DME is not removed resulting in the middle vessel concentration remaining fairly constant as the cycle progresses.

On the other hand, configuration 4 is capable of handling both ±10% changes in the DME mole fraction in the fresh feed as shown in Figure 2.24. For the -10% case the mole fraction of water in the fresh feed is approximately 1.5 times that of the base

case requiring a larger valve travel after the charging cycle. This results in a larger offset obtained in the bottoms composition.

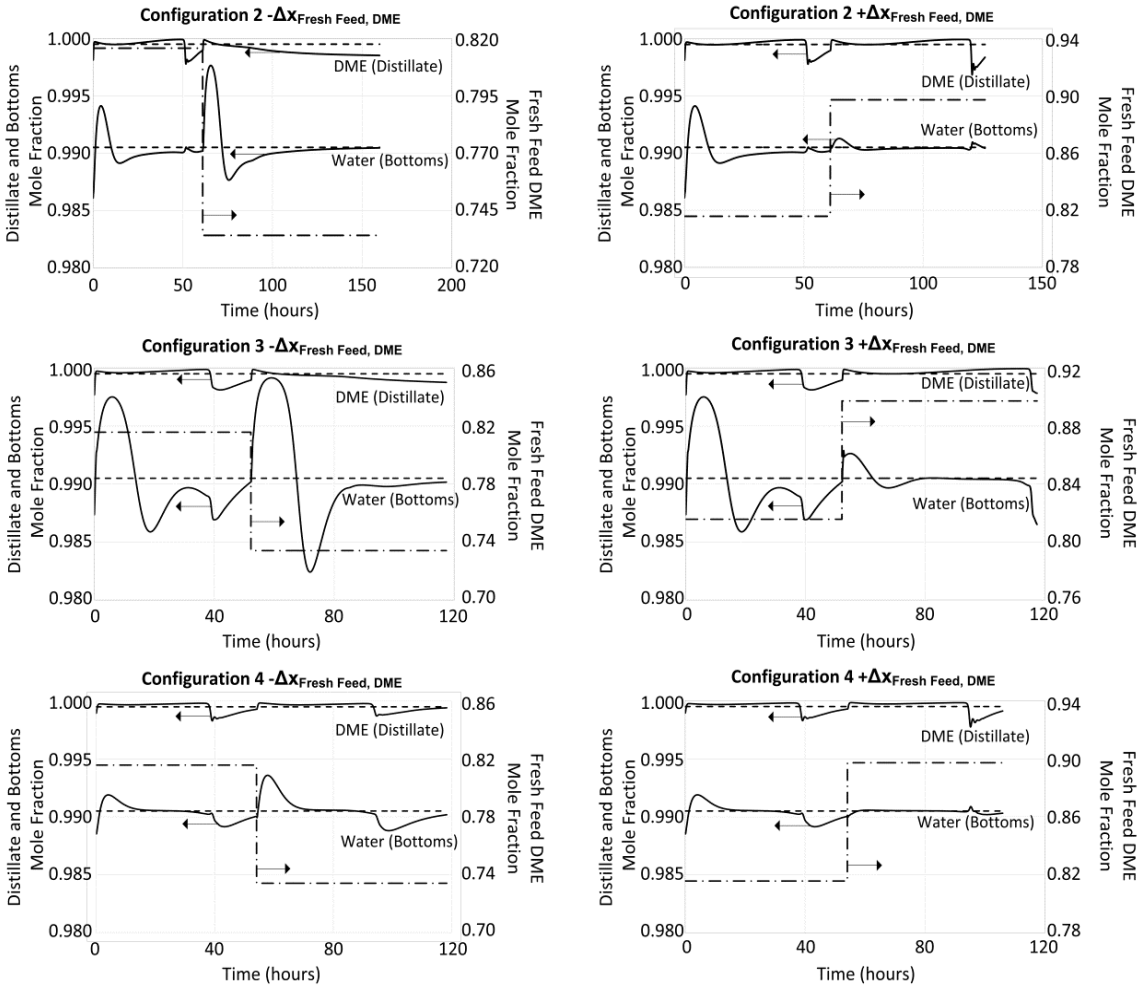

Figure 2.24: Performance of control configurations 2, 3 and 4 for ±10% change in DME mole fraction in fresh feed

Temperature inferential control configurations 5, 5a and 8 effectively reject disturbances in fresh feed composition as displayed in Figure 2.25. These three control configurations are able to maintain the distillation and bottoms purities close to their respective setpoints throughout the cycle. Unlike the previous temperature inferential control configurations, configuration 6 is capable of rejecting the -10% change in DME mole fraction in the fresh feed but is unable to handle a +10% change. For a +10% change the bottoms valve closes to maintain the water purity

specification and reaches (0%) saturation. The bottoms product is no longer controlled and with the purity falling sharply as the cycle progresses as shown in Figure 2.25.

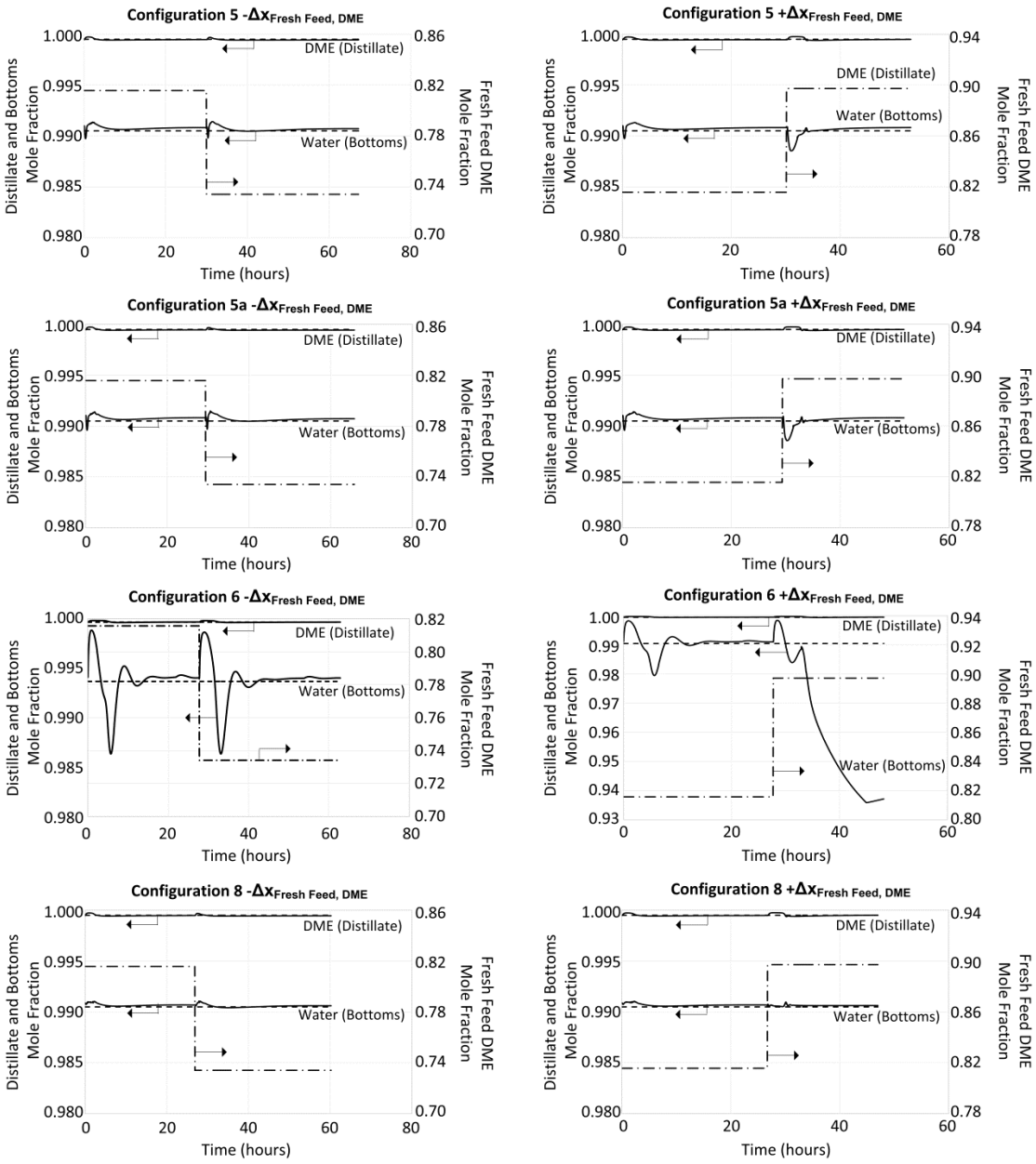

Figure 2.25: Performance of control configurations 5, 5a, 6 and 8 for ±10% change in DME mole fraction in fresh feed

2.4. Conclusion

In this chapter the design of a semicontinuous system for separation of a DME, methanol and water mixture in a single distillation column coupled with a middle vessel has been studied. Eight control configurations utilizing composition or temperature inferential control are investigated. Our analysis shows that configuration 5a (consisting of two temperature inferential PI control loops with the side stream controlled at a fixed flow rate), provides effective control in maintaining product purities over the range of feed composition and flow rate changes. This control configuration also allows the feed rate to the column to be manipulated preventing flooding and weeping conditions while the system converges to a stable limit cycle. Furthermore, this control configuration can effectively reject disturbances in the form of changes of ±10% to the concentration of the middle component, DME from cycle to cycle.

Chapter 3

OPTIMIZATION AND ECONOMIC ANALYSIS

The results in this chapter have been published in the following journal:

Pascall, A. and Adams, T. A. (2013), Semicontinuous separation of dimethyl ether (DME) produced from biomass. *Can. J. Chem. Eng*. doi: 10.1002/cjce.21813

3.1. Introduction

The previous chapter has addressed the design of the semicontinuous system and the selection of an effective control strategy to achieve separation objectives while adhering to operational constraints. In this chapter the most economical designs for the semicontinuous and continuous system at various production rates are compared. Preceding this comparison, the separation systems are optimized considering both capital and operating costs.

The optimization of conventional two product distillation columns has been investigated by numerous researchers. Several strategies for optimization of discrete and continuous variables include: MINLP approaches based on rigorous tray-by-tray, aggregate or shortcut models (Bauer & Stichlmair, 1998; Grossmann, Aguirre, & Barttfeld, 2005) or stochastic optimization algorithms using black-box models (Cabrera-Ruiz, Miranda-Galindo, Segovia-Hernández, Hernández, & Bonilla-Petriciolet, 2011). In this research, the NQ curves optimization algorithms in Aspen Plus is utilized for optimization of structural and operational variables of the

continuous distillation columns. These built-in algorithms have the advantage in that the rigorous distillation model is utilized during optimization while adhering to column constraints.

Optimization of the semicontinuous system, however, is a more complex task compared to the continuous distillation system. For continuous distillation, the reflux and reboil ratios are fixed for the optimal design. However, in the semicontinuous system, the separation objectives are achieved via a trajectory of reflux and reboil ratios which are defined by the control moves of the PI controllers. As such in the optimization of the semicontinuous system, structural variables and reflux/reboil ratio profiles (i.e. controller tuning parameters) must be considered simultaneously. Additionally, in the semicontinuous systems studied, the structure of the model equations are not entirely know due to function calls to Aspen Properties. Thus, deterministic optimization methods which rely on derivative information cannot be used as derivative information is not available and finite difference approximations are computationally expensive (Gengembre, Ladevie, Fudym, & Thuillier, 2012). Despite this, there exist various derivate-free optimization strategies based on search heuristics requiring only objective function evaluations (Biegler & Grossmann, 2004).

Adams & Seider, 2008b, investigated stochastic algorithms using a bi-level approach for the optimization of complex chemical processes with tight constraints using semicontinuous distillation with reaction in the middle vessel as an example. The bi-level approach consists of an outer (global variables – design specifications) and inner (local variables – control decision variables) levels. During optimization, the selected inner level algorithm determines the optimal values of the local variables for a given set of global variables. The authors concluded that three algorithms were effective for optimization of complex processes: Univariate (outer level) – Unimodal progression (inner level), Univariate only and Particle swarm optimization (outer level) – Unimodal progression (inner level).

One difficulty in utilizing the bi-level approach using the Aspen Dynamics semicontinuous model lies in the computation requirements for determining the optimal inner loop variables for fixed design variables. As algorithms to handle integer variables and reduce the computational time associated with optimization of both design and control decision variables are still being addressed, a modified approach to the bi-level algorithm was adopted. In this work, a systematic approach was utilized for determining the design variables followed by optimization of the control decision variables using particle swarm optimization (PSO).

3.2. Optimization Methodology

3.2.1. Continuous system

The total number of stages (*N*), feed tray location, $R_{ref,}$ and R_{boil} were optimized to achieve minimum TAC for each column using a two stage approach.

In the first stage the column is constrained by purity specifications achieved using the design spec/vary function in Aspen Plus. Using the Aspen Plus NQ Curves analysis tool the objective function (total heat load adjusted by the specified reboiler/condenser cost ratio) is minimized. For each *N*, the optimal feed tray location, $R_{ref,}$, and R_{boil} which satisfies the purity specifications are determined. The energy cost vs. *N* data generated is utilized in the second optimization stage.

In the second stage, capital cost is determined using Aspen In-Plant Cost Estimator V7.3.1. The TAC is calculated for each *N* to evaluate the trade-off between operating and capital cost at each production rate examined. This allows the selection of the optimal design for different production rates between 3.0 and7.0 MMkg DME per year.

3.2.2. Semicontinuous system

In this semicontinuous system, the TAC depends on total number of stages, feed tray location, side stream location, charge volume (middle vessel size), reflux drum size, sump size and controller tuning parameters (which drive the process). A systematic

approach is used to evaluate the effect of total number of stages, charge volume, reflux drum and sump sizes prior to optimization of the controller tuning parameters. The feed and side draw locations are fixed throughout the evaluation and optimization process owing to the complexity of the system and could be examined further in future work. Once the structural design for each production case is finalized the control decision variables (controllers' tuning parameters) are then optimized.

For this system, the optimization goal is to determine the controller tuning parameters which minimize the operating cost per DME produced for each production rate case study. The controller tuning parameters (proportional and integral gains) determine the reflux and reboil ratios profiles required to maintain the DME and water purities throughout the cycle. In this study, the optimal tuning parameters are determined using a particle swarm optimization (PSO) algorithm which has been shown to be efficient in optimization of complex chemical processes such as semicontinuous systems (Adams & Seider, 2008b). PSO is a stochastic optimization algorithm motivated by social interaction (Poli, Kennedy, & Blackwell, 2007) and has the added advantage in that it requires no knowledge of the model structure, which is in an implicit form, in Aspen Dynamics.

In PSO a population of N_p=30 particles are initialized in the multidimensional search space with each particle represented by a d-dimensional position vector. The initial population consists of (Adams & Seider, 2008b):

i. One particle with a feasible set of tuning parameters (obtained by hand tuning)
ii. 20% of the particles initialized randomly near the first particle (within 10% of each tuning parameters' feasible range)
iii. Remaining particles initialized randomly in the search space

At the next iteration each particle adjusts its position according to its own previous velocity, its best fitness location and the population's global best location attained thus far (R.C. Eberhart & Shi, 2000). The PSO algorithm utilizing the velocity equation with constriction factor proposed by Clerc & Kennedy, 2002 and variations employed by Adams & Seider, 2008b is shown in Figure 3.1.

Begin
Initialize population: Particle, P_1 at initial guess, $0.2N_P$ particles randomly near P_1 within a distance $0.1(U-L)$, remaining $0.8N_P-1$ particles randomly initialized in search space
Initialize velocity: Velocity vector v_j of all particles randomly initialized within an upper limit, v_{max} and lower limit $-v_{max}$
Initialize particle's best position: $P_{j,best} = P_{j,initial}$

While termination condition is not attained **do**
For j = 1 to N_P
Evaluate objective function
Update $P_{j,best}$ and global best particle, P_{global}
Update the particle's velocity vector:
$v_j = \chi\,[(P_j + c_1 r_1[0,1](P_j - P_{j,best}) + c_2 r_2[0,1](P_j - P_{global})]$
Update particle's position
$P_j = P_j + v_j$
For i = 1 to d
If $v_{j,i} > v_{max,i}$
$v_{j,i} = v_{max,i}$
Else if $v_{j,i} < v_{min,i}$
$v_{j,i} = v_{min,i}$
End if
If $P_{j,i} > U_i$
$P_{j,i} = U_i$
$v_{j,i} = 0.1v_{j,i}$
Else if $P_{j,i} < L_i$
$P_{j,i} = L_i$
$v_{j,i} = 0.1v_{j,i}$
End if
Next i
Next j
Loop
End

Figure 3.1: Particle swarm optimization algorithm

In Figure 3.1, P_j is the particle's position vector, $P_{j,best}$is the vector of the particle's position, P_{global} is the position vector of the best particle in the population, v_j is the velocity vector for particle j, $v_{j,i}$ is the velocity of dimension i (controller tuning parameter) for particle j, $v_{max,i}$ is the maximum velocity for dimension i, U_i is the

upper bound for dimension i, L_i is the lower bound for dimension i with r_1 and $r_2$being a vector of random values between 0 and 1. The velocity update equation utilized the tuning parameter values recommended by Clerc (Russell C. Eberhart & Yuhui, 2001): constriction factor χ of 0.729 and, personal (c_1) and social influence (c_2) constants of 2.05.

The particle swarm optimization code is developed in a Visual Basic for Applications (VBA) program linked with Aspen Dynamics V7.3 using object linking and embedding (OLE) automation. The decision variable array for each particle is supplied to Aspen Dynamics where one cycle is simulated and the objective function (operating cost per DME produced) value is returned to the VBA program. In cases where constraints are violated (reflux drum, sump levels, offset in purity trajectory, bulk product purities and reflux and sump end conditions) penalty terms are added to the objective function. The algorithm is terminated when the maximum number of iterations (500) or convergence tolerance criteria (0.1 $/tonne DME) is attained.

3.3. Optimization Results

3.3.1. Continuous system

The optimized design and operating variables at the various case production rates are illustrated in Figure 3.2 and Figure 3.3.

3.3.2. Semicontinuous system

The semicontinuous simulation procedure using control configuration 5a were performed for 25 and 30 stages columns at a standard column diameter. While the 30 stages column resulted in a decrease in operating cost the significant increase in capital cost could not be offset resulting in a higher TAC. As such a 25 stage column was selected as the base case design for all production rates considered.

Side stream/Feed ratio

The side stream/feed (*S/F*) ratio which is specified during the design of the semicontinuous system in Aspen Plus impacts both the cycle time and economics of

the process. As *S/F* increases the temperature difference (ΔT) between the side stream and bottoms product increases while the difference between the side stream and column top decreases. This results in lower reflux and reboil ratios required to maintain product stream purities and thus lower internal flow rates. The feed flow rate to the column is then increased such that the column operates at its maximum capacity. For the 1.5ft. diameter column using configuration 5, with the side stream under flow control, as *S/F* is increased the cycle time and operating cost per DME produced decreases. However, as shown in Table 3.1, as the *S/F* ratio is further increased from 0.158 to 0.160 there is minimal decrease in operating cost with the cycle time increasing as the side stream purity becomes a dominant factor. As a result an *S/F* ratio of 0.158 is considered for the design of the semicontinuous system for each production rate case.

Table 3.1: Operating cost per DME produced, cycle time and side stream purity at various side stream-feed ratios

Side stream/feed ratio	Operating cost/kg DME produced ($/kg)	Side stream methanol purity –steady state simulation (mol%)	Cycle time (hours)
0.152	0.0121	94.5	20.07
0.154	0.0085	93.3	14.02
0.156	0.0073	92.1	12.60
0.158	0.0068	91.0	12.21
0.160	0.0067	89.9	12.50

Sump and reflux drum size

The effect of the vessel size on the economics of the system is evaluated by systematically first varying the sump size with the number of stages fixed at 25, *S/F* ratio at 0.158 and reflux drum fixed at initial size. As shown in Table 3.2 for the 1.5ft. diameter column, sump size has minimal effect on the operating cost per DME produced however as the sump volume is decreased so does the cycle time. This was due to the lower residence time of bottoms product within the column. Additionally, reduced sump height has the added advantage of decreased column height and capital cost.

Table 3.2: Operating cost per DME produced and cycle time at various sump heights

Sump height (ft.)	Cycle time (hours)	Operating cost/kg DME produced ($/kg)
3.0	12.21	0.0068
2.5	12.02	0.0067
2.0	12.02	0.0067

With the sump height fixed at 2.0 ft., the reflux drum size is increased and the effects analyzed. The reflux drum size is increased while still maintaining the length/diameter ratio of 2.0. Table 3.3 shows that the effect of the reflux drum size on operating cost per DME is negligible while the cycle time decreases with increasing vessel size. This is due to the larger surge volume available allowing a higher feed flow rate to be maintained as the cycle progresses. As cycle time decreases the yearly DME production increases however this is offset by higher capital cost.

This procedure is repeated for all distillation column diameters in 0.5 ft. increments prior to optimization.

Table 3.3: Operating cost per DME produced and cycle time at various reflux drum sizes

Reflux drum diameter (ft.)	Reflux drum length (ft.)	Cycle time (hours)	Operating cost/kg DME produced ($/kg)
3.0	6.0	12.02	0.0067
3.5	7.0	11.97	0.0067
4.0	8.0	11.90	0.0068

Middle vessel volume

The middle vessel volume (charge volume) is varied for the various reflux drum and sump size cases evaluated. Larger charge volumes results in lower operating costs per DME produced due to transition modes forming a smaller percentage of the cycle time. Nonetheless, larger charge volumes increase capital cost significantly and the TAC per DME produced. For column diameters of 1.5 ft. a 100 kmol charge volume

is selected while for diameters of 2.0 and 2.5 ft. a charge volume of 150 kmol is chosen.

Tuning Parameters

The tuning parameters (9 decision variables, including K_c for reflux level, sump level, DME temperature, water temperature, water composition and sidestream flow controllers and τ_I for DME temperature, water temperature and water composition controllers) are optimized using the VBA-PSO algorithm linked with Aspen Dynamics on a quad-core 3.40 GHz Intel Core i7-2600 PC with 4GB RAM and Intel quad core processor. Approximately 40 CPU-days are employed for the optimization of each of the eight individual semicontinuous systems considered (which vary by production rate), which are performed on 8 identical workstations in parallel for a total of approximately 320 CPU-days of computation time. The computational intensity arises from the large CPU-time required for each Aspen Dynamics simulation which takes approximately 4 minutes for each cycle. Although the PSO algorithm cannot guarantee that a globally optimal solution is obtained, the results are at least locally optimal within small tolerances. The resulting optimized operating cost at the various production rate cases are shown in Figure 3.3.

2.1. Economic Analysis

In this study, the total direct cost (equipment, piping, civil, instrumentation, electrical, paint and others) of the distillation columns, condensers, reboilers, reflux drums, tanks, reflux and side stream pumps are determined using Aspen In-Plant Cost Estimator V7.3.1. Operating costs were assumed to be only utility (steam and cooling water) costs. The cost of steam was estimated (Towler & Sinnott, 2012) using natural gas and electricity prices of $2.51/MMBtu (U.S Energy Information Administration (EIA - Official Energy Statistics from the US Government), 2012) and $ 0.0491/kWh (Independent Electricity System Operator (IESO), 2012) respectively. Cooling water cost was estimated (Towler & Sinnott, 2012) based on electricity price of $0.0491/kWh (Independent Electricity System Operator (IESO), 2012) and water make-up and chemical treatment price of $0.02/1000 US gal (Towler & Sinnott,

2012). These estimates are equivalent to costs of steam at 168 and 198°C of $2.03 and $2.14 per GJ of heating load and an equivalent cost of cooling water at 27°C of $0.28 per GJ of cooling load.

The continuous and semicontinuous system designs are evaluated using the TAC calculated using Eq. 3.1. In this work a payback period of 3 years is assumed which is equivalent to that used in previous similar studies (Al-Arfaj & Luyben, 2002; Luyben, Pszalgowski, Schaefer, & Siddons, 2004; Luyben, 2006b, 2010). For each case, an operating time of 8400 hours per year is assumed.

$$\text{TAC} = \frac{\text{Total Direct Cost}}{\text{Payback Period}} + \text{Annual Operating Cost} \qquad (3.1)$$

The total direct costs of the semicontinuous systems are considerably lower than the continuous system for all production rates as illustrated in Figure 3.2.

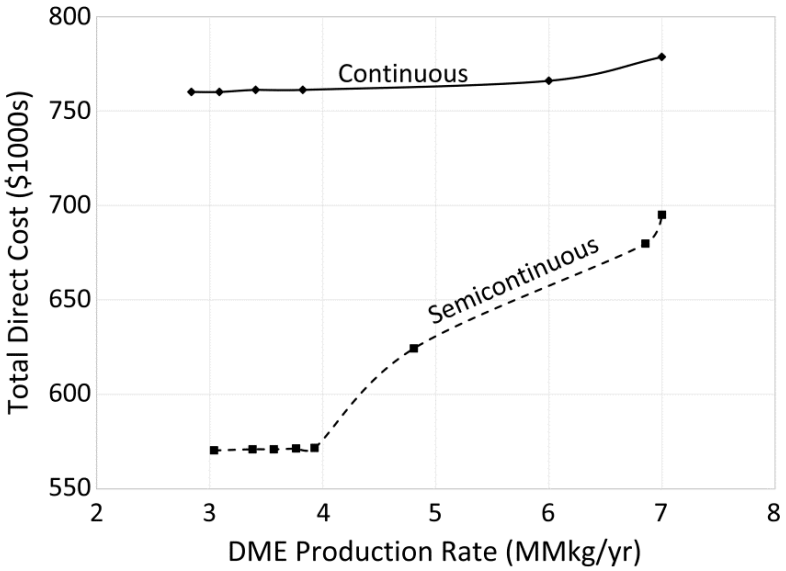

Figure 3.2: Total direct cost of continuous and semicontinuous systems at various production rates

This is anticipated as the semicontinuous system requires one less distillation column, condenser and reboiler. As the production rate increases however, the cost savings

decrease as the diameter of the semicontinuous column increases while the continuous column diameter remains the same (1.5 ft.) for all production rates.

The annual operating costs for the both systems are shown in Figure 3.3.

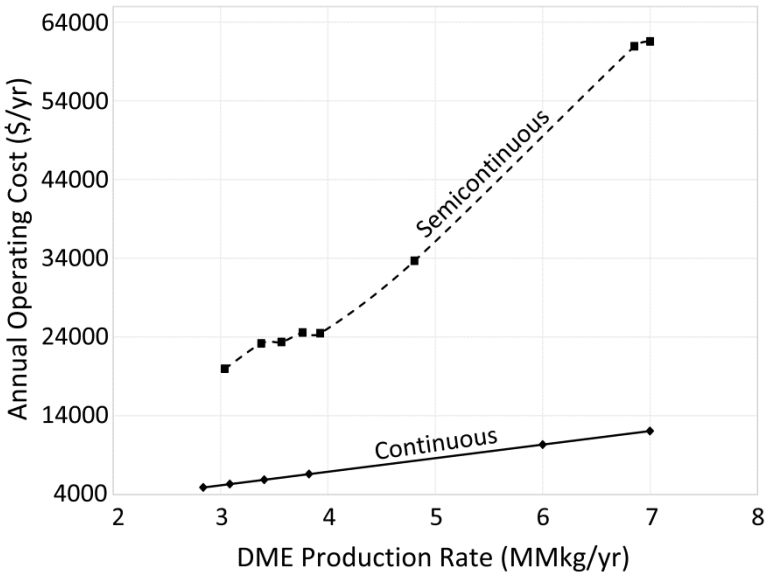

Figure 3.3: Annual operating cost of continuous and semicontinuous systems at various production rates

The operating costs for the semicontinuous system are significantly higher than the continuous case and increase as rapidly with increasing DME production. This is due to the low mole fraction of water in the feed stream requiring a high reboil ratio. As the cycle continues the reboil ratio increases to maintain the bottoms stream purity with the feed rate decreasing to prevent flooding within the column. At the lower feed rates the cycle time increases appreciably while the relatively constant internal column flows (vapour and liquid) results in higher operating costs per DME produced.

Comparing the semicontinuous and continuous systems the semicontinuous system has the lowest TAC for production rates less than 5.70 MMkg/yr as shown in Figure 3.4.

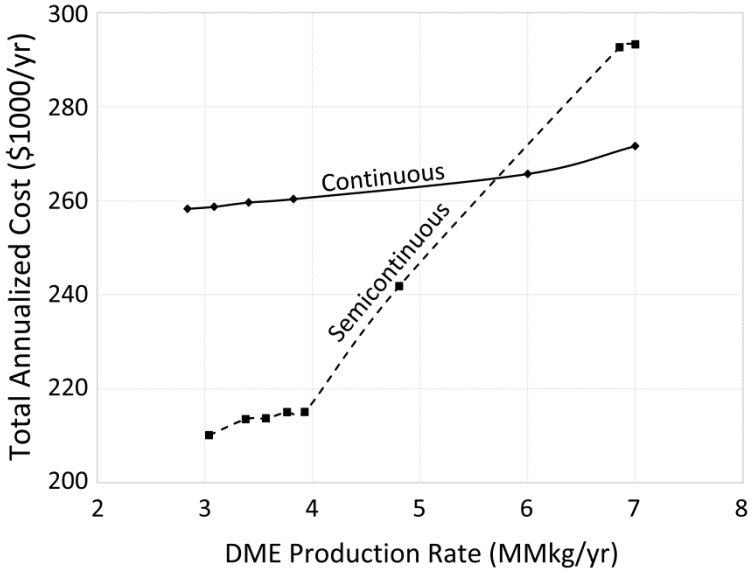

Figure 3.4: Total annualized cost of continuous and semicontinuous systems at various production rates

It is worth noting that while both systems were optimized the continuous system was optimized more efficiently in terms of design parameters and feed location while in the semicontinuous case variables such as feed and side stream locations were not optimized due to the complexity of the system.

3.4. Conclusion

The control system study was followed by optimization of the both the semicontinuous and continuous system over a range of production rates as presented in this chapter. In the semicontinuous case the control parameters were determined using PSO. However, due to the complexity and computation time required, not all of the design variables could be explored using this approach. Improved black-box optimization algorithms or development and use of reduced models can be advantageous for simultaneous optimization of design and control decision variables of the semicontinuous system.

Furthermore, economic comparison has shown the semicontinuous system to possess lower total annualized cost for production rates less than 5.70 MMkg/yr compared to the continuous case. On the other hand the operating costs of the semicontinuous system are higher than that of its continuous counterpart due to the low concentration of water in the feed stream. Overall the semicontinuous system looks promising for reducing the costs associated with bio-DME production for small scale distributed networks.

Chapter 4

SEMICONTINUOUS DISTILLATION OF DME FROM A VAPOUR-LIQUID MIXTURE

The results in this chapter have been submitted to the following journal:

Pascall, A. and Adams, T. A., Semicontinuous separation of bio-dimethyl ether from a vapour-liquid mixture. *Industrial & Engineering Chemistry Research*, submitted on April 22 2013.

4.1. Introduction

Although the results of the prior semicontinuous system are promising, there are additional semicontinuous strategies which could potentially be even better. The continuous process contains three distillation columns in series, and as detailed in the previous chapters the second and third columns are replaced by a semicontinuous process with a single column, with promising results. However, it may be possible to get even better results by replacing the first and second distillation columns with a semicontinuous system instead of the second and third. Therefore, it is the purpose of the present work to design, simulate, and optimize a semicontinuous process of this type to determine if there are any potential economic or energetic benefits to doing so.

The present work will investigate the semicontinuous separation of DME from a vapour-liquid feed using a partial condenser configuration. The development of a

semicontinuous system is an integrated design and control problem, and therefore the determination of an effective control system is essential to its understanding. Therefore, six control configurations using composition and two-point temperature control including an economic comparison with the conventional continuous system will be presented. All semicontinuous systems developed thus far (to the best of the author' knowledge) have employed total condensers and liquid-only feeds, and thus this is the first semicontinuous system using a partial condenser configurations and two-phase fresh feed to be studied. The two-phase nature of the feed mixture is particularly challenging because the existing control and design heuristics for semicontinuous systems with liquid-only feeds do not apply. Therefore, one of the central aims of this chapter is to develop new heuristics for this type of problem.

4.2. Continuous System

4.2.1. Process Description

The DME separation process is presented in Figure 4.1. The equipment configuration for the separation section is taken from the process developed by Larson et al. for DME production from switchgrass using the direct synthesis step (Larson et al., 2009).

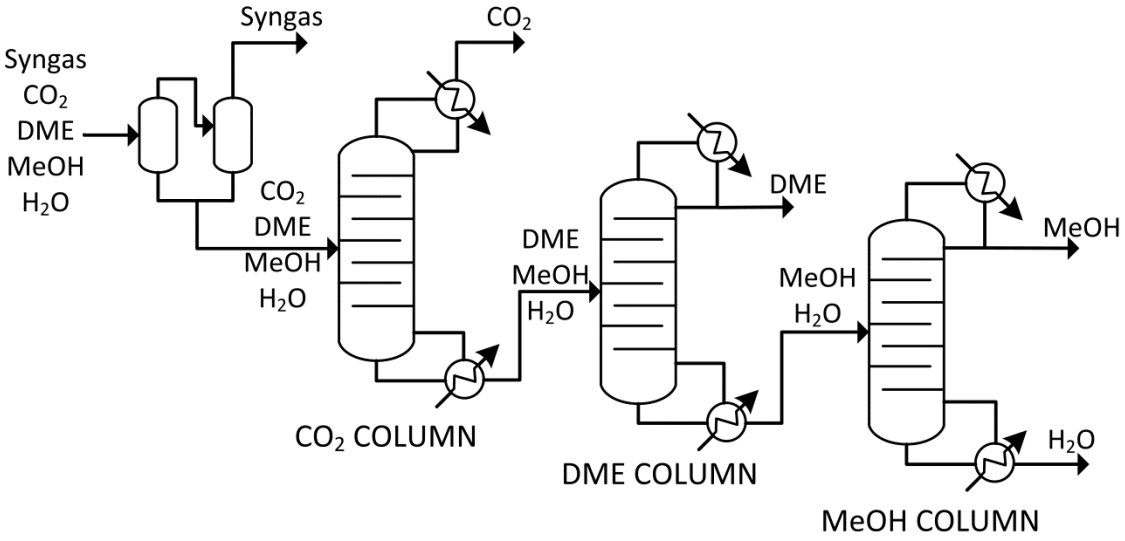

Figure 4.1: Equipment configuration for DME Separation Section

The gaseous product stream leaving the DME reactor is partially condensed and then sent to a series of flash drums where unconverted syngas is recovered. Following the flash separation steps, the effluent stream containing CO_2 (43.77 mol%), DME (37.98 mol%), methanol (6.62 mol%), water (1.82 mol%) and minimal syngas (H_2 - 3.81 mol% and CO – 6.00 mol%) is depressurized to 13.0 bar and sent to the distillation section.

In the first column, 99.99% of the CO_2 is recovered in the distillate (with a purity of 80.88 mol% CO_2) while a DME-MeOH-H_2O rich bottoms stream (0.02 mol% CO_2) is produced. The bottoms product is throttled to 10.0 bar and sent to the second distillation column where DME at 99.95 mol% (the proposed specification for its use as a fuel (Arcoumanis et al., 2008; Ogawa et al., 2003)) is obtained. In the DME column, 99.99 mol% DME is recovered in the distillate leaving a MeOH-H_2O rich stream (0.061 mol% DME) which passes to the third distillation column where methanol and water are recovered at 96 mol% and 99.05 mol% respectively (Pascall & Adams, 2013).

Simulation of the separation section was performed using Aspen Plus V7.3 with the Peng-Robinson-Wong-Sandler-UNIFAC (PRWS-UNIFAC) property method selected, because of its efficacy in vapor-liquid equilibrium prediction of the quaternary (CO_2, DME, MeOH, H_2O), ternary and binary sub-systems (Ye et al., 2011). The distillation columns were modelled using the rigorous equilibrium-stage RadFrac model with a Murphree efficiency of 85% assumed constant for all stages (Tock et al., 2010).

4.2.2. Optimization

The separation section was optimized for DME production at various rates in the range 1.0 – 7.0 MMkg/yr. The optimal number of stages (N), feed tray location, reflux (R_{ref}) and reboil (R_{boil}) ratios that results in the minimal total annualized cost (TAC) was determined for each column at the various production rates.

The optimal parameters for each column were determined via a two-phase approach. In the first phase Aspen Plus' NQ curves feature was used to generate the operating cost vs. *N* curve. The column is first constrained by purity specifications for the distillate and bottoms streams using the design specs/vary function in the RadFrac model. The NQ curve tool calculates the R_{ref}, R_{boil} and optimum feed stage location which satisfies the product specifications while minimizing the objective function (operating cost based on relative weighting of condenser and reboiler duty) for each *N*. The operating cost vs. *N* curve for each column is then employed in the second optimization phase.

The capital cost for each *N* using the optimal parameters determined in phase 1 is then determined using Aspen In-Plant Cost Estimator V7.3.1. The design which results in the lowest total annualized cost (TAC, which includes both the capital and operating cost) is selected for each DME production rate investigated.

4.3. Semicontinuous System

4.3.1. Process Description

The functionality of the CO_2 and DME columns from the continuous case (Figure 4.1) are achieved using the semicontinuous configuration with only one column shown in Figure 4.2.

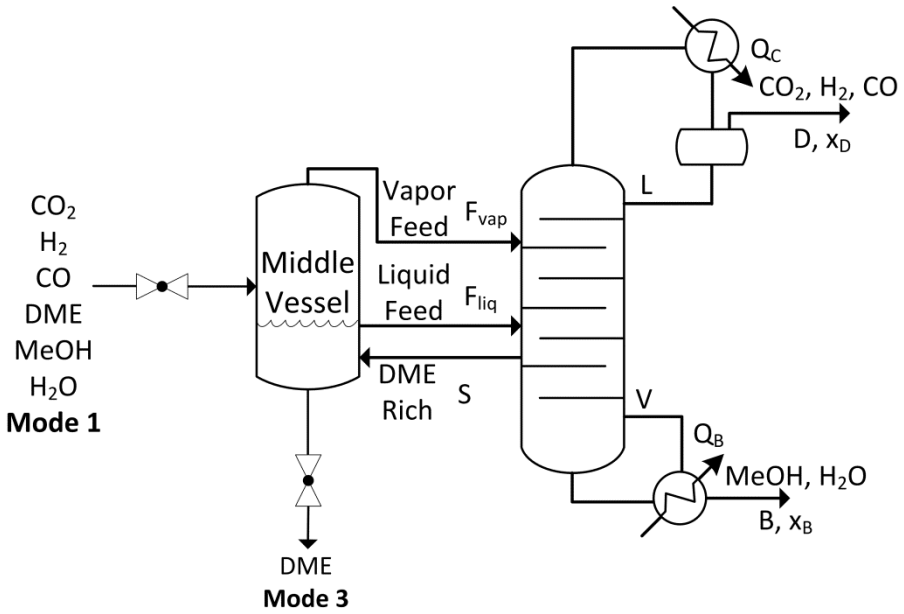

Figure 4.2: Semicontinuous process configuration

The proposed semicontinuous process produces CO_2 rich, MeOH-H_2O rich and DME products using a forced cycle with three operating modes. In Mode 1, the middle vessel (flash drum) is charged with the multi-component mixture of the same composition and state as the feed to the CO_2 column in the continuous configuration. Once the MV has been fully charged, Mode 2 commences. In this mode, CO_2 product with a DME impurity of 1.00 mol% and MeOH-H_2O product with a DME impurity of 0.061 mol% is recovered continuously as the cycle progresses. During this time, the CO_2, H_2, CO, MeOH and H_2O holdup in the MV decreases, and DME concentrates in the MV until the target purity specification is met. Once the DME target specification of 99.95 mol% is attained, Mode 3 begins. In Mode 3, the DME product is discharged until the MV is nearly drained and the cycle repeated.

It should be noted that during Mode 1 and 3 the feed stream to the column and side stream to the MV remain in operation so as to avoid shut-down and start-up of the distillation column. As the cycle progresses, the MV changes, and thus the composition to the column also changes. In addition, the distillate and bottoms flow rates decrease throughout the cycle as a result of controller actions to maintain target stream purities (see section 4.4.1). This demonstrates the non-stationary nature of the process. As such, the control system selected is essential in achieving the required objectives in the presence of these dynamic changes.

4.3.2. Control System Design

A control system for the semicontinuous system has to fulfill the following objectives during mode transitions and dynamic changes:

1. Specification objectives:
   i. DME impurity in CO_2 distillate stream is maintained at 1.00 mol%
   ii. DME impurity in MeOH-H_2O bottoms stream is maintained at 0.061 mol%

2. Operational objectives:
   i. Column stability – Pressure, reflux drum and sump levels are kept within certain bounds.
   ii. Flooding and weeping are avoided at all times during the cycle

An important aspect of the control system design lies in identifying the controlled and manipulated variables to meet the defined specification and operational objectives. There are eight manipulated variables (degree of freedom – DOF) available in this semicontinuous system: condenser heat duty (Q_c), reboiler heat duty (Q_B), reflux (L), vapor distillate (D), side stream (S), bottoms (B), liquid feed (F_{liq}) and vapor feed (F_{vap}) molar flow rates. The DOFs are used to control the DME impurity in the distillate (x_D), DME impurity in the bottoms (x_B), MV pressure, column pressure and reflux and sump levels with the additional DOFs used to optimize the cycle.

In a partial condenser column, besides Q_c (which is the conventional manipulated variable utilized in total condensers), D can also be utilized to control column pressure. However, the distillate composition is affected by manipulating D. Furthermore, the reflux drum level can be controlled by both Q_c and L but not with D as it has no effect on drum level. This is best understood by examining the mass balance of the reflux drum. The overall mass balance is of the form:

$$\frac{dM_L}{dt} + \frac{dM_v}{dt} = F_{in}(t) - L(t) - D(t) \qquad (4.1)$$

where F_{in} is the total vapor-liquid feed rate to the reflux drum and aM_L and M_v are the liquid and vapor hold up respectively. Using this overall mass balance, the liquid phase balance is shown in eq. 4.2.

$$\frac{dM_L}{dt} = F_{in,liq}(t) - L(t) + \sum_{i=1}^{i} \mathbb{N}_i(t) \qquad (4.2)$$

where $\mathbb{N}_i(t)$ is the interfacial mass transfer rate of each component i from the vapor phase to the liquid phase and $F_{in,liq}$ is the liquid flow rate in the feed stream and is given by:

$$F_{in,liq}(t) = \frac{Q_c}{\Delta H_v} \qquad (4.3)$$

with ΔH_v being the latent heat of vaporization of the overhead vapors from the column. Therefore, we obtain the following equation for the reflux drum liquid balance:

$$\frac{dM_L}{dt} = \frac{Q_c}{\Delta H_v} - L(t) + \sum_{i=1}^{i} \mathbb{N}_i(t) \qquad (4.4)$$

As shown in Eq. 4.4, the liquid hold up in the reflux drum is affected by the condenser heat removal and reflux flow rate but not the distillate rate.

The effect of Q_c on both level and pressure and the effect of D on pressure and composition results in strong interaction between pressure, composition and level control, thus increasing the difficulty in pairing and loop tuning compared to total condenser columns (Hori & Skogestad, 2007; Luyben, 2006b, 2012). While there are several loop pairing configurations that could potentially work, only variants of the *"DB"* (D is manipulated to control x_D with B varied to control x_B) and *"LB"* (L is manipulated to control x_D with B varied to control x_B) configurations are considered since they have been shown to be the most effective for semicontinuous distillation in prior studies (Pascall & Adams, 2013; Phimister & Seider, 2000a, 2000b, 2000c). These configurations are explained in detail in the next section.

Decentralized proportional-integral (PI) control was implemented for the six control configurations investigated due to its previous success in achieving good dynamic performance for semicontinuous systems while maintaining the simplicity of the control system. The main difference in the control configurations examined lies in the manipulated variable used for pressure control. Initially, composition control is used for all control configurations explored and later inferential temperature control employed due to the reduced cost and measurement time delay. A time-delay of 3 mins and 1 min have been assumed for the composition and temperature analyzers respectively (Luyben, 2006b). The performance of each control configuration in achieving the required specification and operational objectives is then evaluated using Aspen Plus Dynamics V7.3.

Configuration 1

Figure 4.3A shows the *"DB"* control configuration for the partial condenser semicontinuous system. In continuous distillation, the feed rate is often held constant to maintain a specified production rate, however, in semicontinuous systems this can lead to flooding of the column. As the cycle progresses, the holdup of CO_2, syngas, MeOH and H_2O in the MV decreases while DME holdup and thus DME composition increases. As the feed composition decreases in CO_2, MeOH, and H_2O, the distillate and bottoms rates are reduced by the controllers to maintain the DME impurity setpoint of each product stream. If the feed rate were to be held constant, this would result in increased internal flow rates and eventual column flooding.

In this configuration, F_{liq} is manipulated to control the reflux drum level, Q_B is varied to control sump level with Q_C utilized to maintain column pressure. x_D and x_B are maintained by manipulating the *D* and *B*. Additionally, the ideal side-draw recovery control strategy proposed by Adams & Seider, 2009a is implemented since the intermediate component losses in the distillate and bottoms streams is reduced. This results in a higher purity side stream to the MV thereby minimizing the cycle time. The ideal side-draw recovery strategy is derived from the dynamic mass balance for DME over the column assuming the ideal case of no DME accumulation in the column:

$$F_{liq}(t)x_{F_{liq},DME}(t) + F_{vap}(t)x_{F_{vap},DME}(t) = D(t)x_{D,DME}(t) + B(t)x_{B,DME}(t) + S(t)x_{S,DME}(t) \quad (4.5)$$

where F_{liq}, F_{vap}, *D*, *B* and *S* are the molar flow rates of the liquid feed, vapor feed, distillate, bottoms and side stream and *x* are the DME mole fractions in the equivalent streams.

Assuming no DME is lost in the distillate and bottoms i.e. $x_{D,DME} = x_{B,DME} = 0$ and no product losses in the side stream ($x_{S,DME} = 1$), the side stream flow rate is controlled according to:

$$S\,(t) = F_{liq}(t)x_{F_{liq,DME}}(t) + F_{vap}(t)x_{F_{vap,DME}}(t) \quad (4.6)$$

Configuration 2

In control configuration 2, the DME impurity in the product streams, column and MV pressures are controlled in the same manner as configuration 1. However, the reflux drum level is now controlled by manipulating reflux rate with F_{liq} varied to control the sump level and reboiler duty maintained at a constant rate as shown in Figure 4.3B

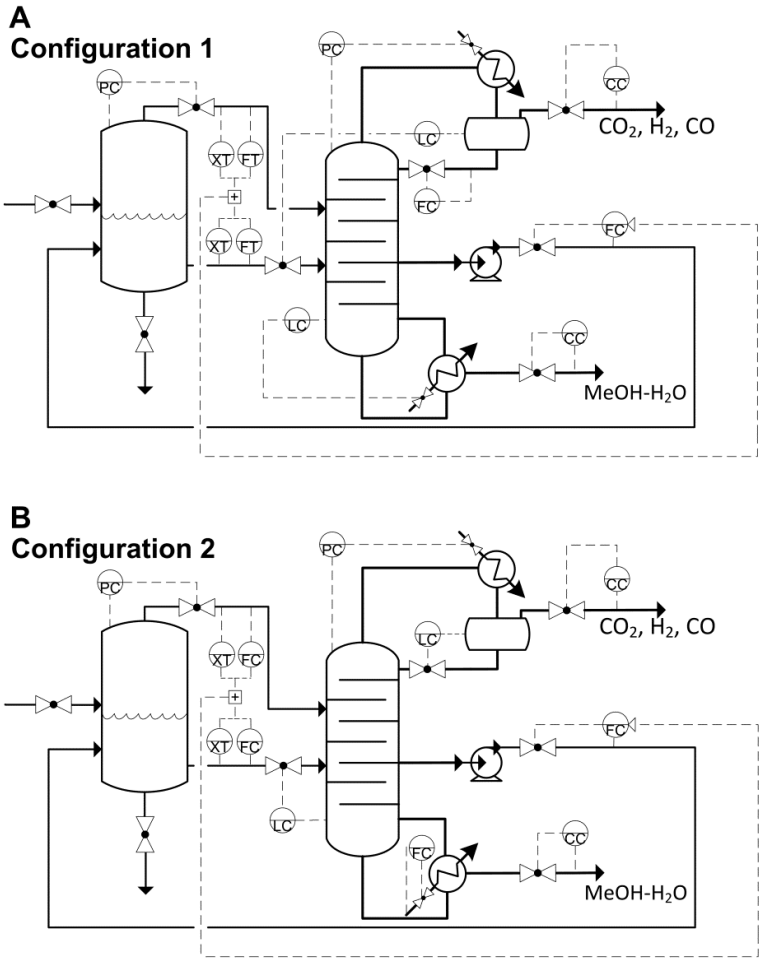

Figure 4.3: Control configurations 1 and 2

Configuration 3

Figure 4.4A represents the material balance *"LB"* control configuration with x_D and x_B controlled by manipulating the reflux and bottoms flow rate respectively. Unlike the previous two configurations the column pressure is controlled by manipulating the

vapor distillate rate. This method of pressure control is the most commonly used for conventional continuous partial condenser columns (Luyben, 2006b). Reflux drum and sump levels are controlled in the same manner as configuration 1 coupled with the ideal side-draw control strategy.

Configuration 4

This control configuration as shown in Figure 4.4B is the same as configuration 3 except that the reflux drum level is controlled using condenser duty with the reboiler duty held constant throughout the cycle.

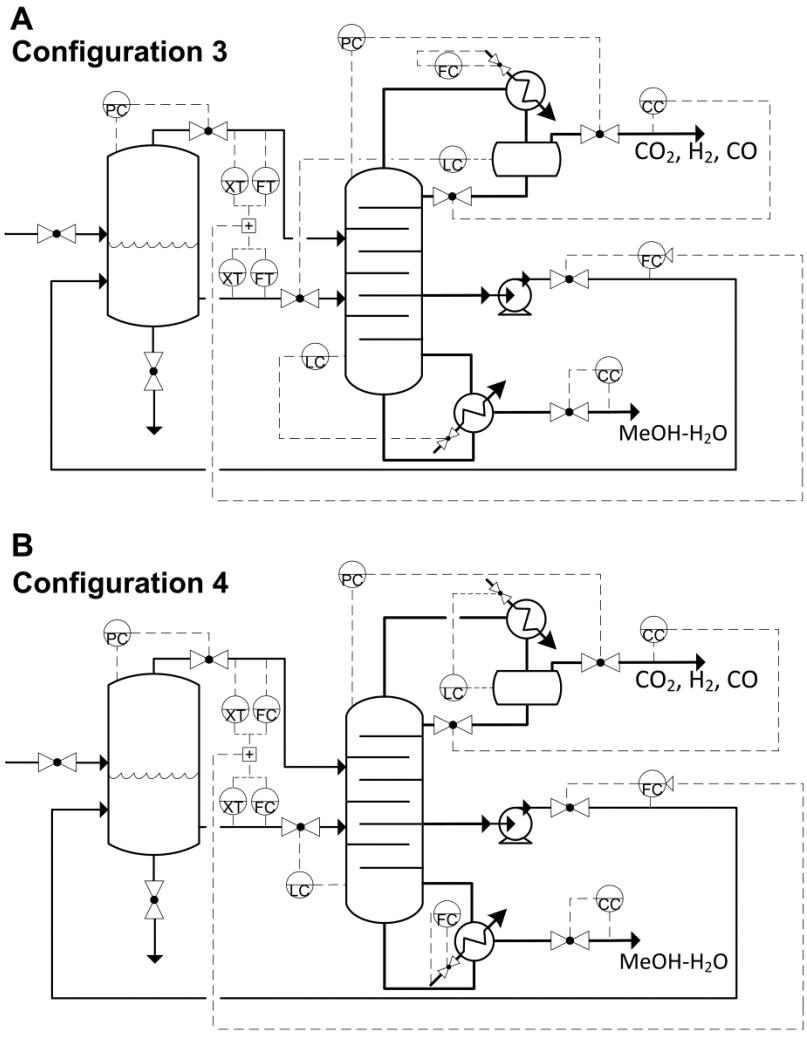

Figure 4.4: Control configurations 3 and 4

Configuration 5

Figure 4.5A illustrates an alternative *"DB"* control configuration wherein the column pressure is controlled using the reboiler heat duty. Hori & Skogestad, 2007 have shown the effectiveness of using reboiler duty to control column pressure for continuous systems and as such this structure has been considered for completeness. Now, the reflux rate is manipulated to control the reflux drum level with the condenser duty held constant. The ideal side-draw control strategy is also employed in this configuration.

Configuration 6

Configuration 6 as shown in Figure 4.5B is the same as the previous one except the reflux drum level is now controlled using the condenser heat duty.

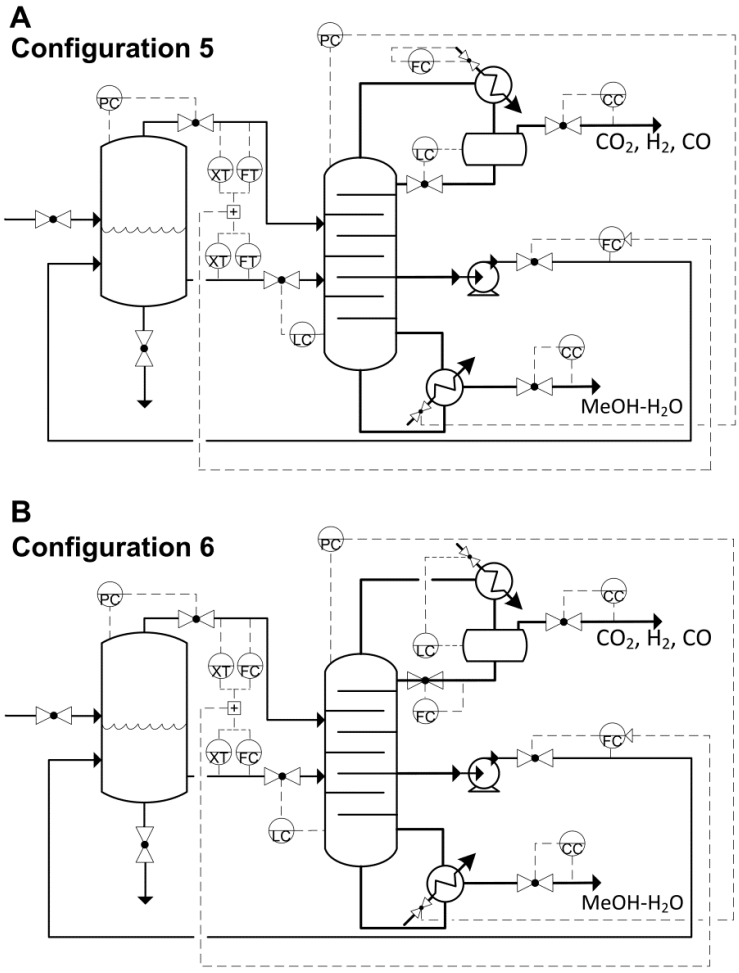

Figure 4.5: Control configuration 5 and 6

Temperature Control

Temperature control replaces the use of costly composition analyzers on the basis that holding temperature of a single tray constant results in invariable product purity (Yu & Luyben, 1984). The tray selected for temperature control is central to maintaining product composition (Shinskey, 1984) as the feed composition and flow rate changes throughout the cycle.

In previous work (Pascall & Adams, 2013), inferential temperature control has been applied successfully using the following tray temperature location selection criteria:

i. Invariant temperature criterion – Select the tray which produces the lowest variability in temperature for the projected range of feed composition disturbances (Luyben, 2006a).
ii. The temperature of the selected tray must be strongly correlated with composition for changes in its manipulated variable (Marlin, 2000).

Invariant Temperature Criterion

The first step in this analysis involves selecting a sample of feed compositions which are likely to occur during a semicontinuous cycle (in this case, the sample was taken from simulation results using composition-controllers). Liquid and vapor feed composition together with the vapor/liquid ratio at seven selected times using control configuration 1 are shown in Table 4.1. Snapshot 1 reflects the feed composition and F_{vap}/F_{liq} at the beginning of the cycle with snapshot 7 reflecting the feed composition and F_{vap}/F_{liq} towards the end of the cycle.

The composition control configurations employed do not achieve zero offset throughout the cyclic campaign. As such, temperature profiles at which "perfect control" is attained for the range of feed compositions to the distillation column cannot be obtained for evaluation of potential tray temperature locations. The column's temperature profile for approximate feed compositions (snapshot 1-7) were realized using an Aspen Plus simulation for the semicontinuous system (a steady-state simulation of MV and side stream distillation column). For each snapshot, distillate

and bottoms product impurities were attained using the design spec/vary function with reflux and reboil ratios used as manipulated variables. Convergence of the side stream column, however, requires specification of the *S/F* ratio, calculated for each snapshot using the ideal side draw strategy from Equation 4.6.

Table 4.1: Liquid and vapor feed composition during one semicontinuous separation cycle

Comp.	Composition (kmol/kmol)							
	Snapshot 1		Snapshot 2		Snapshot 3		Snapshot 4	
	Gas	Liquid	Gas	Liquid	Gas	Liquid	Gas	Liquid
DME	0.141	0.516	0.160	0.540	-	0.751	-	0.850
MeOH	0.001	0.103	0.001	0.102	-	0.059	-	0.036
H_2O	0.000	0.029	0.000	0.028	-	0.016	-	0.010
H_2	0.097	0.005	0.077	0.003	-	0.002	-	0.001
CO	0.148	0.010	0.125	0.007	-	0.004	-	0.003
CO_2	0.613	0.338	0.637	0.320	-	0.169	-	0.100
F_{vap}/F_{liq}	0.570		0.136		0.0		0.0	
	Snapshot 5		Snapshot 6		Snapshot 7			
	Gas	Liquid	Gas	Liquid	Gas	Liquid		
DME	-	0.900	-	0.961	-	0.996		
MeOH	-	0.024	-	0.009	-	0.001		
H_2O	-	0.006	-	0.002	-	0.000		
H_2	-	0.001	-	0.001	-	0.000		
CO	-	0.002	-	0.001	-	0.000		
CO_2	-	0.067	-	0.026	-	0.003		
F_{vap}/F_{liq}	0.0		0.0		0.0			

Figure 4.6 shows the temperature change for stages in the column's upper section except stage 2 (tray 1) due to the lack of sensitivity of temperature to composition at the column ends (Shinskey, 1984). Stages 3 are 8 are not included as these represent the vapor and liquid feed stages. As the composition of DME in the feed increases, Figure 4.6 shows that the temperature on the selected stage should increase to maintain the DME impurity in the distillate and thus cannot be kept fixed for the entire cycle.

This illustrates that unlike binary systems, tray temperature is not an accurate indicator of product composition for multi-component systems due to variations in the non-key components (Luyben, 2006a). Several approaches have been proposed to overcome this effect including: differential temperature, double differential temperature, composition estimator, cascade control and weighted average temperature (Yu & Luyben, 1984).

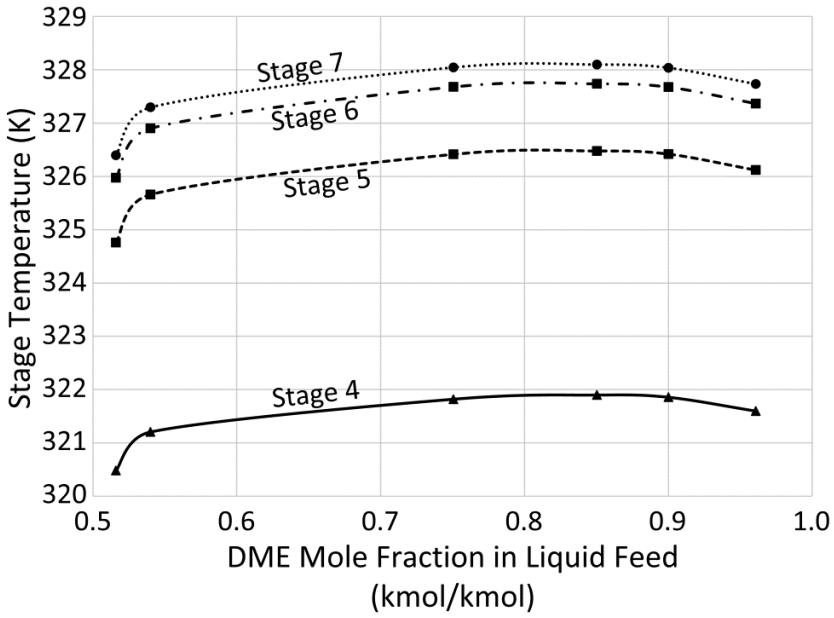

Figure 4.6: Temperature profile for stage in upper section of column for various feed compositions

Applying the invariant temperature criterion, various differential temperature locations in the upper and lower sections of the column were considered. Table 4.2 shows the temperature differentials which exhibit the least variation for the range of feed composition changes for all possible options examined.

Table 4.2: Differential temperatures for selected compositions at various feed temperatures

Stages	Differential Temperature (K)							
	Snapshot 1	**Snapshot 2**	**Snapshot 3**	**Snapshot 4**	**Snapshot 5**	**Snapshot 6**	**Snapshot 7**	**Max – Min ΔT**
S_7–S_6	0.42	0.39	0.37	0.36	0.36	0.37	0.33	0.09
S_5-S_4	4.27	4.45	4.59	4.58	4.56	4.52	4.13	0.46
S_7-S_5	1.64	1.64	1.63	1.62	1.61	1.61	1.49	0.15
S_{24}-S_{23}	0.52	0.50	0.49	0.49	0.50	0.49	0.49	0.03
S_{22}-S_{21}	0.04	0.03	0.03	0.03	0.03	0.03	0.04	0.01
S_{23}-S_{22}	0.11	0.10	0.10	0.10	0.10	0.10	0.10	0.01

Temperature-Composition Correlation for Manipulated Variable Changes

Temperature differentials S_7-S_6, S_7-S_5, S_{24}-S_{23} and S_{23}-S_{22}, best satisfy the first criterion and as such, are investigated to determine their sensitivity to changes in the manipulated variable for composition control. The differential temperature S_{22}-S_{21}, however, is not considered as the temperature difference is very small and thus too sensitive to noise.

For temperature control configurations 1, 2, 5 and 5 the DME impurity in the distillate and bottoms are maintained by the manipulated variables distillate and bottoms flow rate respectively. First, we examined the sensitivity of the differential temperatures S_7-S_6 and S_7-S_5 to changes in the distillate flow rate using the Aspen Plus steady-state simulation of the semicontinuous system. For each composition snapshot, 1, 3, 5 and 7, the distillate and bottoms product impurities were attained using the design/spec vary function with the reflux and reboil ratios as the manipulated variables, respectively. Additionally, the S/F ratio is specified using the ideal side draw strategy from Equation 4.6. The differential temperature and corresponding distillate composition is recorded for the base case and ±5% changes in distillate flow rate with the reboiler duty held constant. As illustrated in Figure 4.7, differential temperature S_7-S_5 is more sensitive (larger slope) to changes in the manipulated variable compared to S_7-S_6 for the expected range of feed composition. Hence, differential temperature S_7-S_5 is selected for distillate composition control.

Even though differential temperature S_7-S_5 best satisfy both criteria, towards the end of the cycle, offset will be experienced. This was confirmed through implementation in Aspen Dynamics and is due to the change in slope direction at the end of the cycle as explained in the following remarks. The DME impurity in the distillate stream is maintained by a reduction in the differential temperature setpoint from 1.64 (start of cycle) to 1.49K (end of cycle), as shown in Table 4.2. As shown in Figure 4.7, a lower DME impurity ($\log_{10}(x_D)$ becomes smaller) occurs as the distillate flow rate is reduced from the base case distillate rate to -5% change in distillate flow rate. Maintaining the differential temperature at 1.64K towards the end of the cycle requires a lower than required distillate flow rate as shown in Figure 4.7 – Snapshot 7. However, due to the change in slope, operating at a lower distillate flow rate gives a smaller ($\log_{10}(x_D)$ or lower DME impurity level in the distillate. The operation of this controller at a lower distillate rate with negative offset in impurity results in a larger cycle time hence, a cascade control structure in which temperature is corrected is introduced.

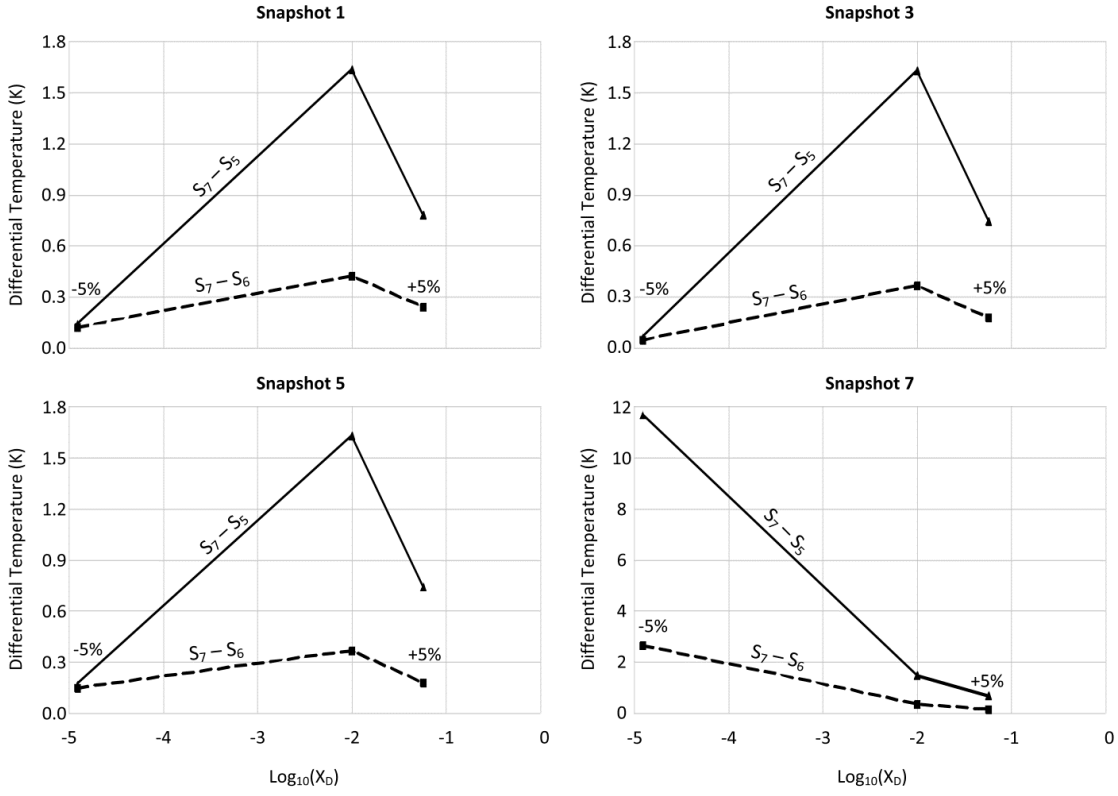

Figure 4.7: Correlation between differential temperature and distillate impurity composition for ±5% change in distillate flow rate at various feed compositions

Similarly, for the bottoms product for each composition snapshot 1, 3, 5 and 7 the base case is converged as previously described. The differential temperature and distillate composition for the base case and ±5% change in bottoms flow rate with condenser duty held constant are recorded. Differential temperature, S_{23}-S_{22} has a larger slope in the region $\log_{10}(x_B)$ = -6.89 or x_B = 1.29x10^{-5}% and $\log(x_B)$ = -3.22 or x_B = 0.061% than S_{24}-S_{23} for all feed composition cases. However, S_{24}-S_{23} exhibits a larger slope in all bottoms composition regions towards the end of the cycle (Snapshot 7) and for all feed compositions in the region of operation ($\log_{10}(x_B)$ = -1.32 or x_B = 4.82% and $\log_{10}(x_B)$ = -3.22 or x_B = 0.061%). Additionally, as S_{24}-S_{23} has a differential temperature greater than 0.1K (thus reducing its sensitivity to noise) it was selected for bottoms composition control.

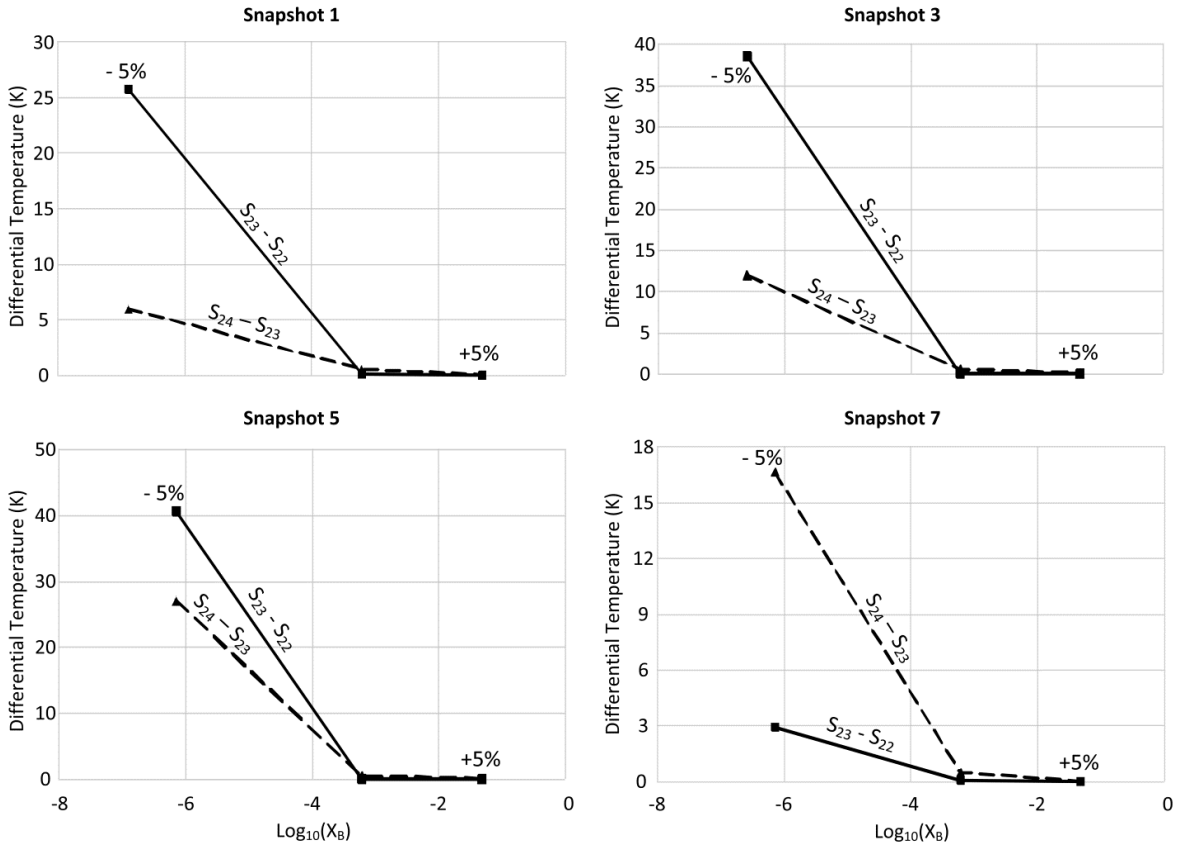

Figure 4.8: Correlation between differential temperature and bottoms impurity composition for ±5% change in bottoms flow rate at various feed compositions

Figure 4.9 shows the temperature control structure investigated for configurations 1, 2, 5 and 6. Configurations 3 and 4 are not discussed as they were later shown to be ineffective for the semicontinuous system (see Results and Discussion). The temperature control configurations have the advantages of avoiding additional corrections to compensate for pressure effects and eliminating the composition analyzer for x_B.

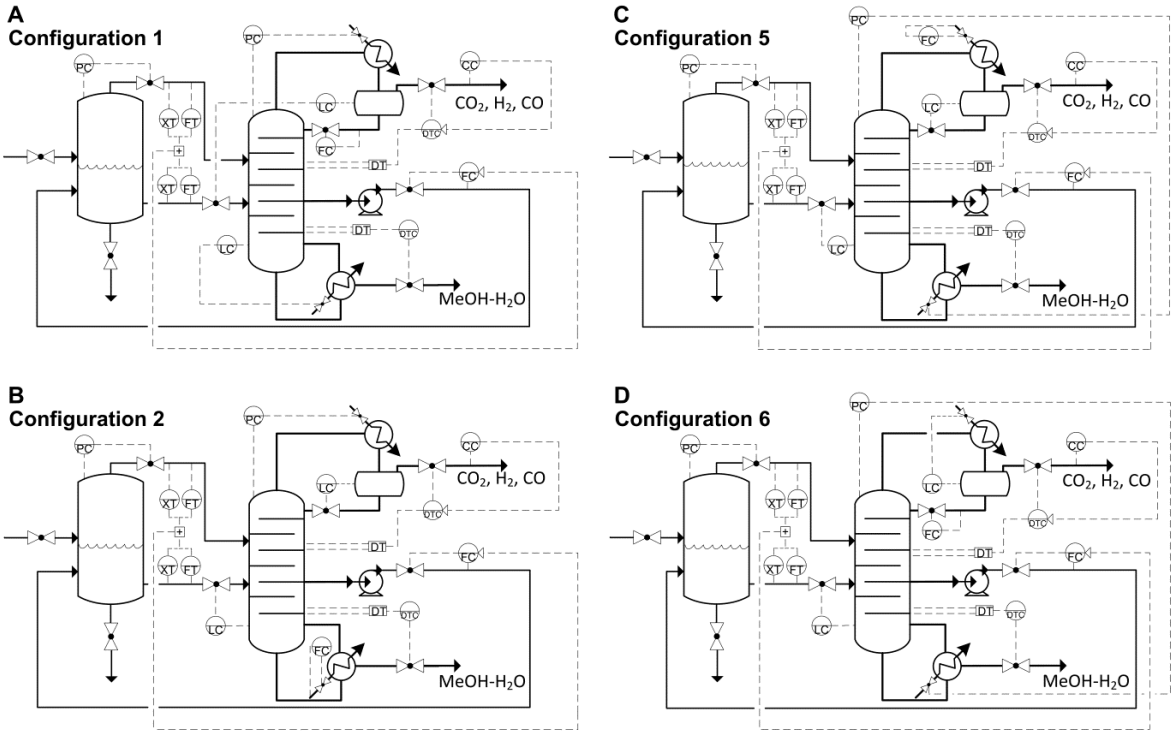

Figure 4.9: Temperature control for control configurations 1, 2, 5 and 6

4.3.3. Simulation

The dynamics of the semicontinuous system in achieving the operational and specification objectives through mode to mode transitions are analyzed using Aspen Dynamics V7.3. The initial operating conditions for the dynamic system are obtained from the resultant Aspen Plus steady-state simulation.

The semicontinuous distillation column is modeled using the RadFrac unit with 30 stages, an assumed Murphree efficiency of 85% (Tock et al., 2010) and condenser

pressure fixed at 13 bar with a pressure drop of 0.1 psi per tray. The design spec/vary function is used to obtain a DME impurity specification of 1.0 and 0.061 mol% in the distillate and bottoms products with the feed and side stream locations selected to minimize the reflux/reboil.

The control configurations are evaluated using a 1.5 ft column diameter (the minimum standard size for distillation columns (Aspen Technology Inc, 2011)) with accumulators (reflux drum and sump) and control valves sized according to heuristics (Luyben, 2006b). The MV is sized with an initial molar holdup of 62.5 kmol and liquid volume fraction of 75% at an operating pressure of 16 bar. This pressure is set such that the feed pressure to the column is maintained following pressure drop losses across the liquid and vapor feed valves. The configured steady-state simulation is exported to Aspen Dynamics and with the semicontinuous system and control system constructed as discussed in previous work (Pascall & Adams, 2013).

The configured Aspen Dynamics simulation is shown in Figure 4.10. The pressure, temperature and composition controllers were configured with proportional integral (PI) control with the side stream and level controllers as P only since tight control is not required. As heuristics for controller tuning for semicontinuous systems have not yet been developed, controllers are tuned such that the integral squared error (ISE) for DME impurity in distillate and bottoms products are minimized.

The mode-to-mode transitions are handled using Aspen Dynamics event-driven tasks which control the opening and closing of the feed (V1) and DME product (V4) valves. During the charging cycle V1 is 100% open with V4 closed. Once the charging mode is complete V1 is closed and Mode 2 (in which DME concentrates in the MV) commences. Once the DME purity of 99.95 mol% in the MV is attained V4 is opened to 100% discharging the DME product to the downstream unit until the MV liquid height is 10%.

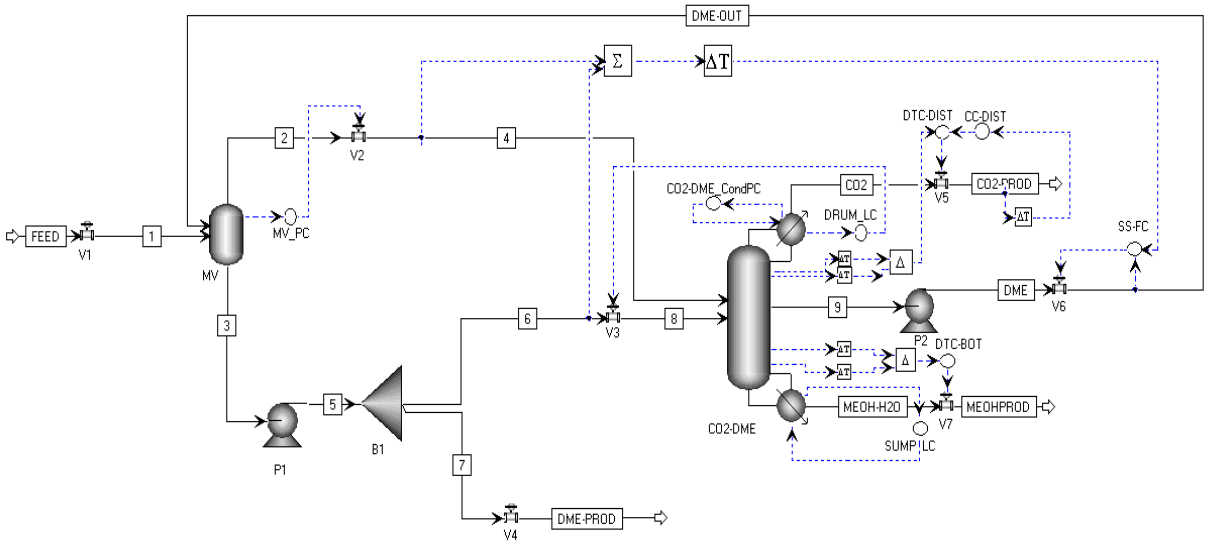

Figure 4.10: Aspen Dynamics implementation of temperature control configuration 1

4.3.4. Optimization

In the semicontinuous system there are several variables which can be optimized to reduce the TAC of the process including: total number of stages, feed and side stream locations, reflux drum, sump and middle vessel size and tuning parameters of controllers which drive the process. In this complex system, a systematic approach is first used to determine the structural parameters (middle vessel size or charge volume, sump and reflux drum size) with the total number of stages and feed and side stream locations fixed. Upon fixing the structural variables the tuning parameters are optimized to reduce the operationg cost per cycle as described in section 4.4.3 (Pascall & Adams, 2013).

4.4. Results and Discussion

4.4.1. Control Performance

The dynamic simulations results for the composition and temperature control configurations for separation of the multi-component, vapor-liquid mixture is presented.

Configuration 1 using composition control was shown to be effective in achieving the specification and operational objectives of the semicontinuous system. This is illustrated in Figure 4.11 and Figure 4.12. The mole fraction of DME in the MV at the end of Mode 1 is slightly higher than that of the fresh feed since the MV is not completely emptied at the end of Mode 3. The trajectories shown in Figure 4.11 and Figure 4.12 (and indeed all similar figures afterward) are for the last three cycles in a series of four cycles simulated, demonstrating that a stable limit cycle has been achieved. As mentioned earlier, the first cycle (not shown) is the cycle beginning from a guessed initial condition, where the initial MV charge is guessed and all initial tray compositions and flows are also guessed using the results of a hypothetical steady state simulation. These guessed conditions do not correspond to a stable limit cycle, but as the results show, after only one cycle, a stable limit cycle has been achieved. Furthermore, only the stable limit cycle is relevant. The profiles in Figure 4.11 illustrate that configuration 1 is able to maintain the impurity setpoint of the distillate and bottoms product while ensuring the reflux drum and sump levels remain within limits. However, during Mode 1, minor overshoot in the column pressure is attained. This is due to the rapid opening of the MV's control valve during to maintain the vessel's pressure during charging. The offset can be reduced by less aggressive tuning of the MV's pressure controller but results in overshoot of the pressure in the MV. As such the MV's pressure controller is tuned such that the overshoot in column pressure is reduced while ensuring the overshoot in the MV is < 1 bar.

In addition to maintaining product purities, pressure and levels, the control system ensure that flooding and weeping are avoided throughout each cycle as shown in Figure 4.12. Flooding calculations for each tray are calculated using the Fair

correlation (Fair et al., 1997) with the weeping velocity (minimum gas velocity) calculated by Equations 4.7 and 4.8 (Mersmann et al., 2011):

$$F_{min} = \varphi\sqrt{0.37 d_H g \frac{(\rho_L - \rho_V)^{1.25}}{\rho_V{}^{0.25}}} \qquad (4.7)$$

$$u_{min} = \frac{F_{min}}{\sqrt{\rho_V}} \qquad (4.8)$$

where, F_{min} is the minimum gas load, φ is the relative free area, d_H is the tray hole diameter, g is the acceleration due to gravity, ρ_L and ρ_V are the liquid and vapor densities u_{min} is the minimum vapor velocity.

The weeping velocity is calculated for the top (stage 2), side stream (stage 19) and bottom (stage 29) section of the column. The gas velocity through the sieve holes are greater than the weeping velocity indicating that weeping is avoided.

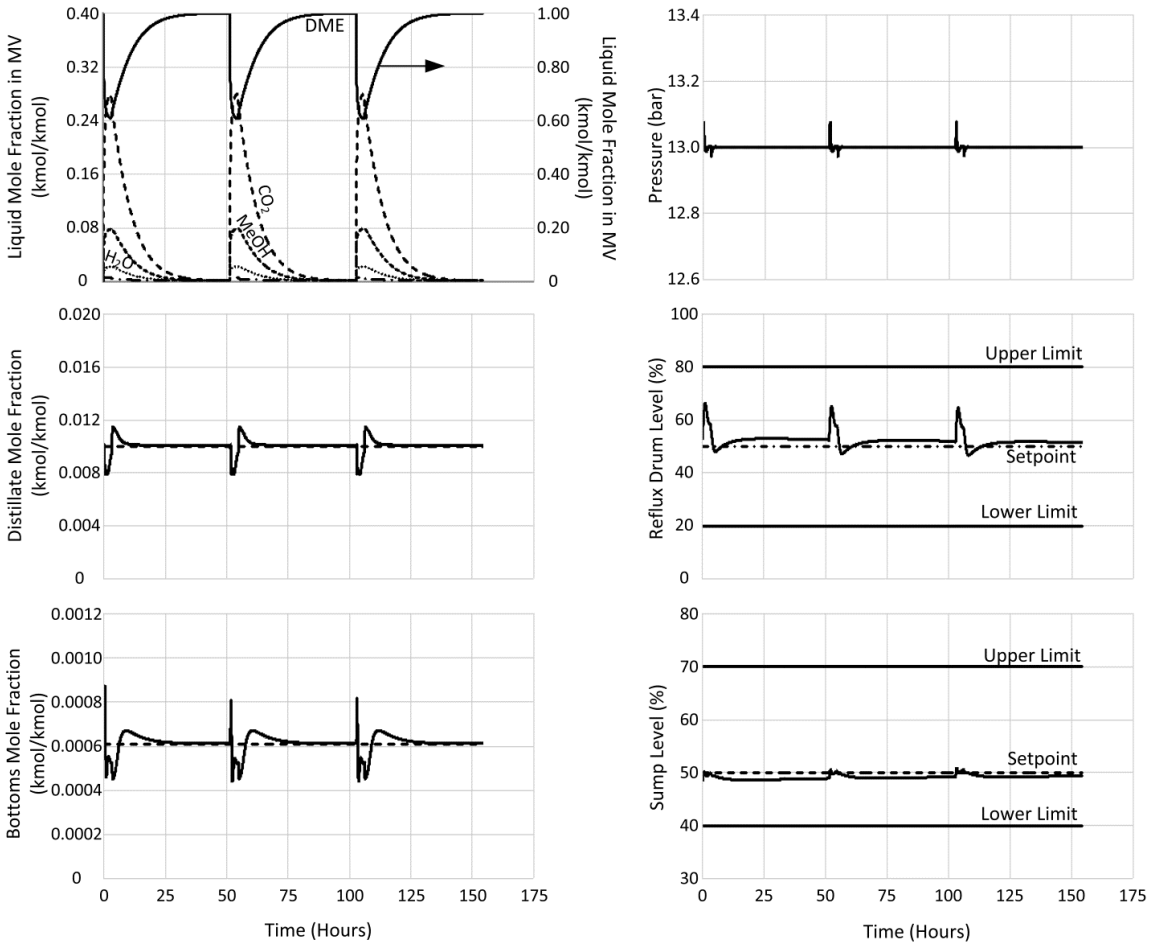

Figure 4.11: Composition, pressure and level profiles for composition control configuration 1

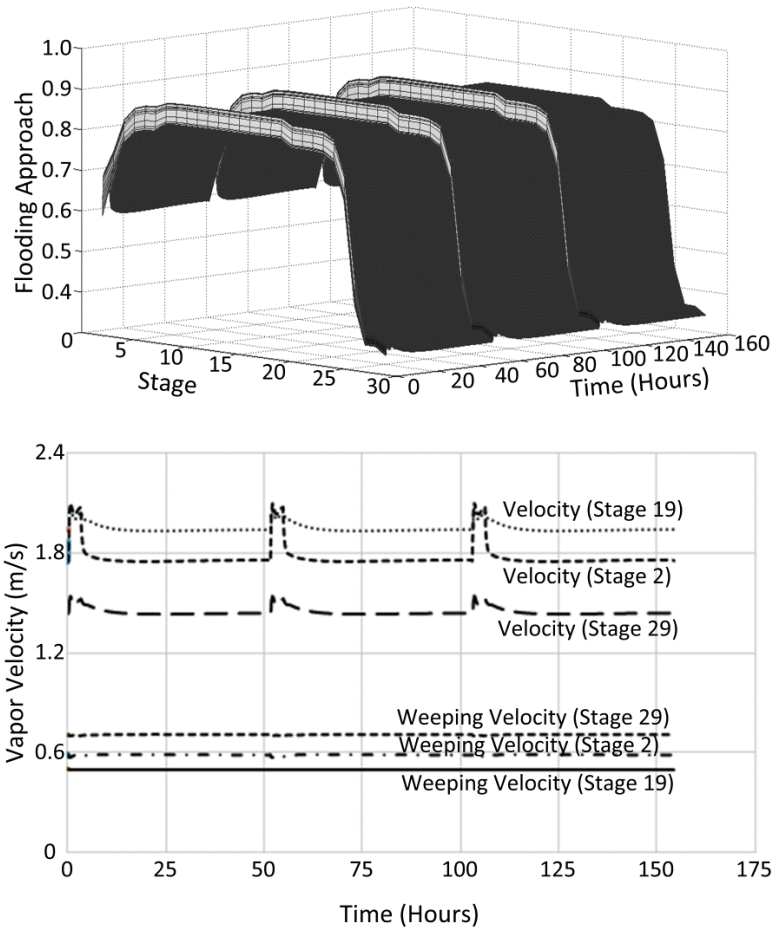

Figure 4.12: Flooding approach, vapor and weeping velocity profiles for composition control configuration 1

While composition control configuration 2 is able to achieve the required separation and operational objectives, a larger offset in bottoms impurity and sump level is experienced. The use of the feed rate to regulate sump level introduces a time delay due to tray hydraulics, resulting in fluctuations in the bottoms level. As a result, the bottoms composition is more responsive to heat input during Mode 1, where the sump holdup increases greatly. At a constant reboiler heat duty, the heat supplied is insufficient to maintain the DME impurity level in the bottoms product. This produces a large offset in the bottoms product with the product valve closing until the sump holdup decreases and its purity is within specification, as shown in Figure 4.13.

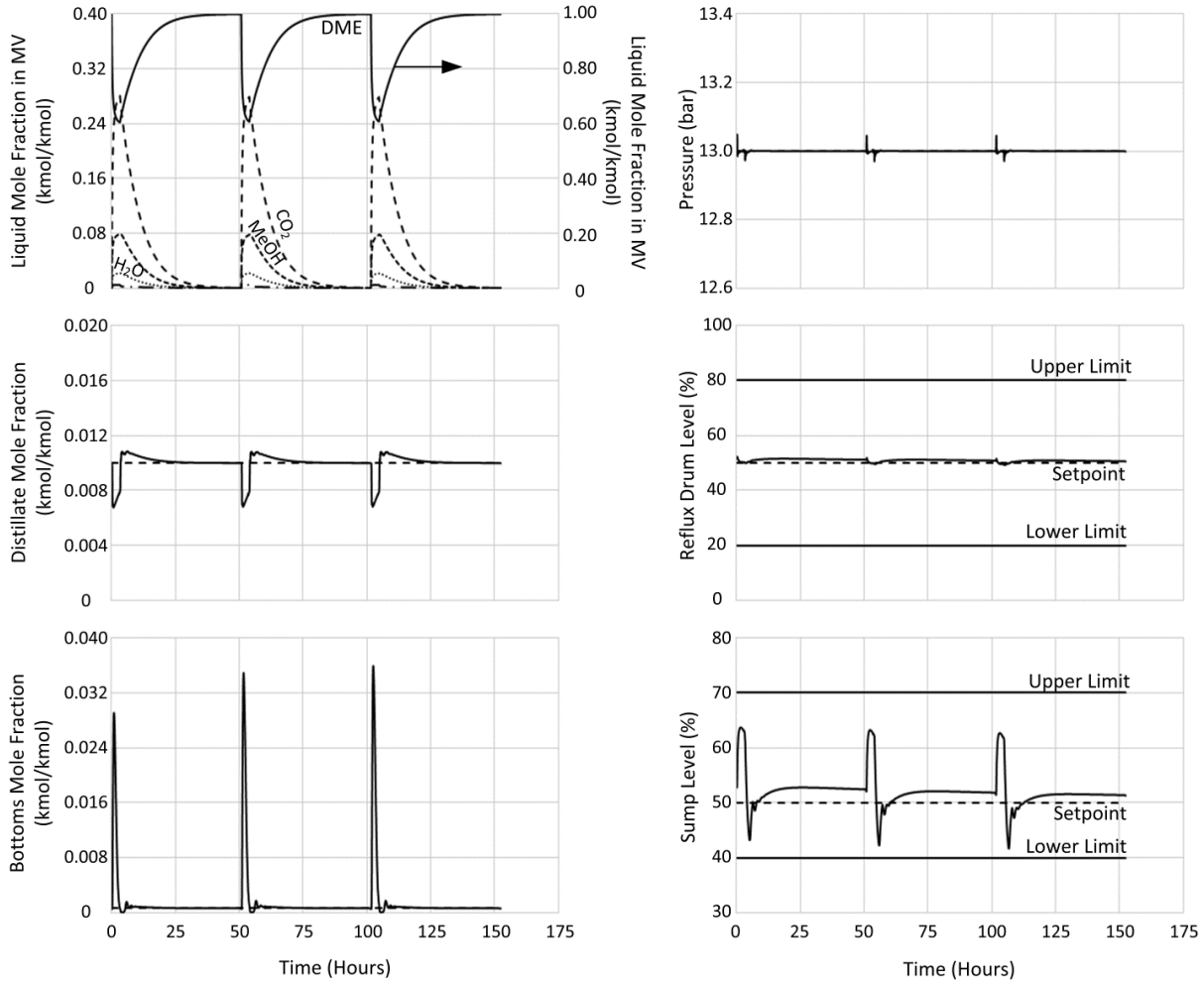

Figure 4.13: Composition, pressure and level profiles for composition control configuration 2

On the other hand, configuration 2 has the advantage of maintaining fairly constant flooding and velocity profiles as the boil-up rate remains almost constant. Stage 2, however, exhibits higher velocities during Mode 1 where the column receives a vapor feed from the MV.

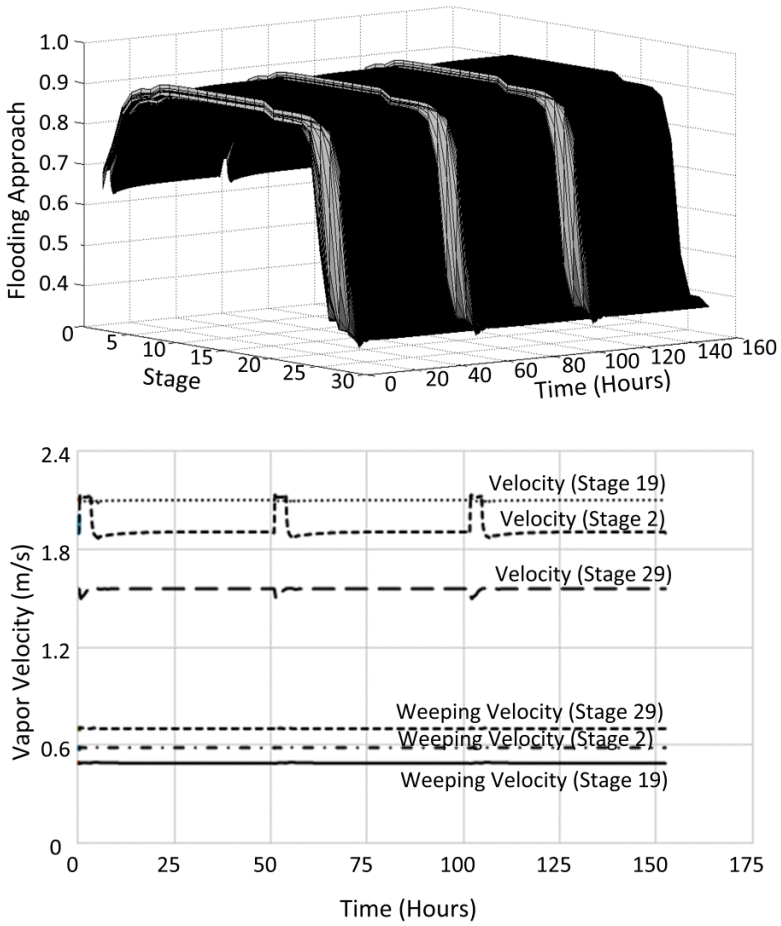

Figure 4.14: Flooding approach, vapor and weeping velocity profiles for composition control configuration 2

Although the use of distillate flow in controlling column pressure has shown to be effective in conventional continuous partial condenser columns, it renders the semicontinuous system inoperable for configurations 3 and 4. In configuration 3, as the cycle progresses, the distillate valves saturates at its lower range (0%) and as such is unable to regulate the column pressure, as shown in Figure 4.15. Due to the interaction between the pressure and composition loops, the rapid closure of the distillate valves results in a lower DME impurity in the distillate. As a result the reflux rate decreases, leading to an increase in reflux drum level and subsequent closure of the column's liquid feed valve. With no feed to the column and a constant condenser heat duty, the internal vapor, column pressure, and flooding approach decreases significantly, rendering the semicontinuous system inoperable.

In configuration 4, the opposite effect occurs as the condenser duty is no longer held constant but used to regulate the reflux drum level. As the cycle progresses, as the vapor flow to the column decreases, the distillate product valve again saturates at 0%. This results in a decrease in the reflux rate and subsequent decrease in condenser duty to control the reflux drum level. As the condenser duty decreases at a fixed reboiler duty, the column pressure begins to regulate and the distillate valve opens rapidly. This action increases the DME impurity in the product leading to increased reflux. Even though the cycle repeats itself with the pressure eventually increasing, the increased reflux rate leads to flooding of the column.

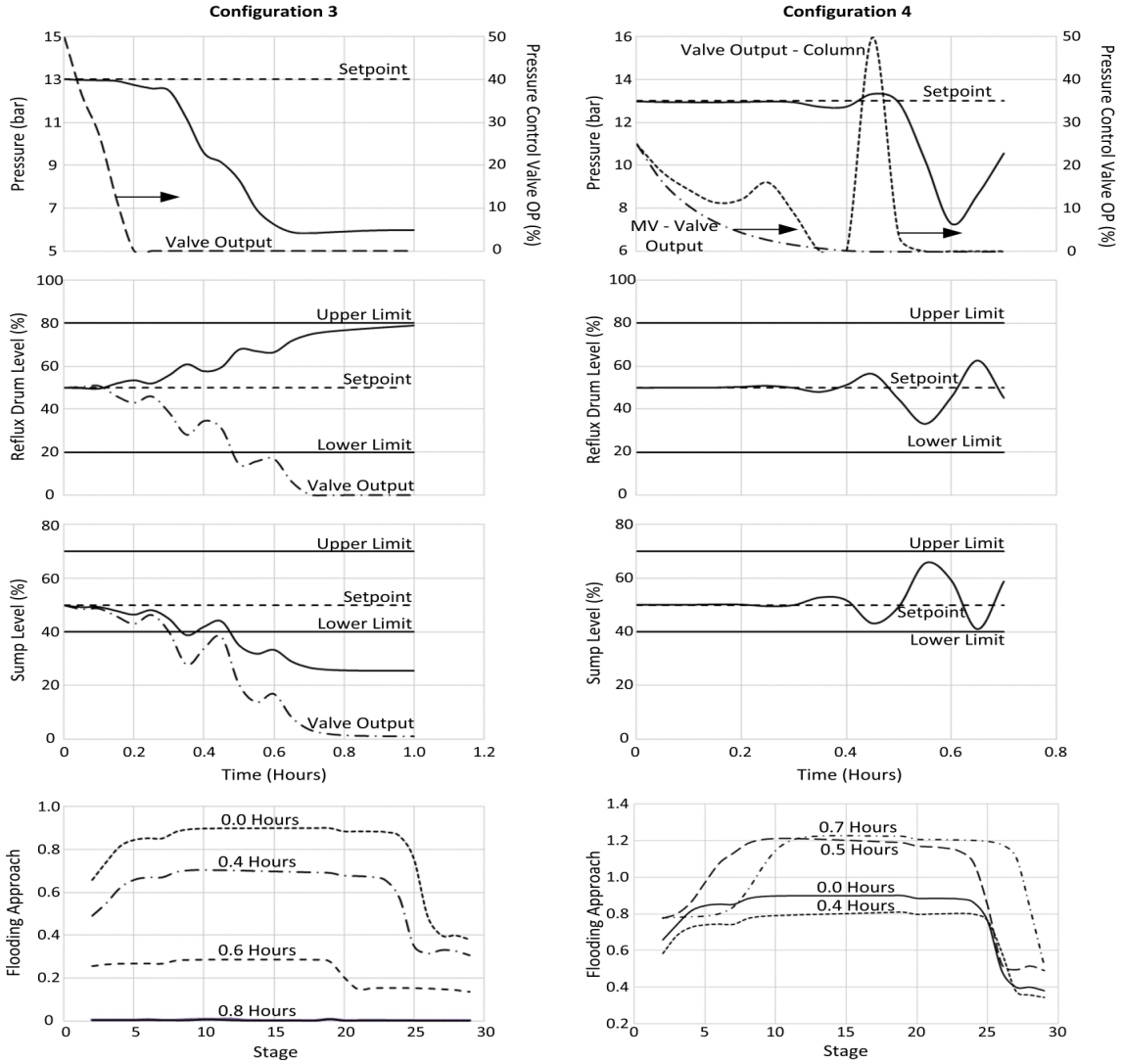

Figure 4.15: Pressure, level and flooding approach profiles for configurations 3 and 4

Figure 4.16 and Figure 4.18 illustrates that configurations 5 and 6 are able to maintain the column pressure while meeting the MV purity. However, the bottoms impurity exhibits the same response as configuration 2 where the setpoint tracking cannot be achieved at the beginning of the cycle. During the period in which the column receives a vapor feed from the MV (Mode 1 and part of Mode 2), the reboiler heat duty decreases to maintain the columns pressure. Since the pressure control loop is faster than level control due to liquid holdup delays, the sump level increases. The lower reboiler duty coupled with increased sump holdup results in off-specification bottoms product.

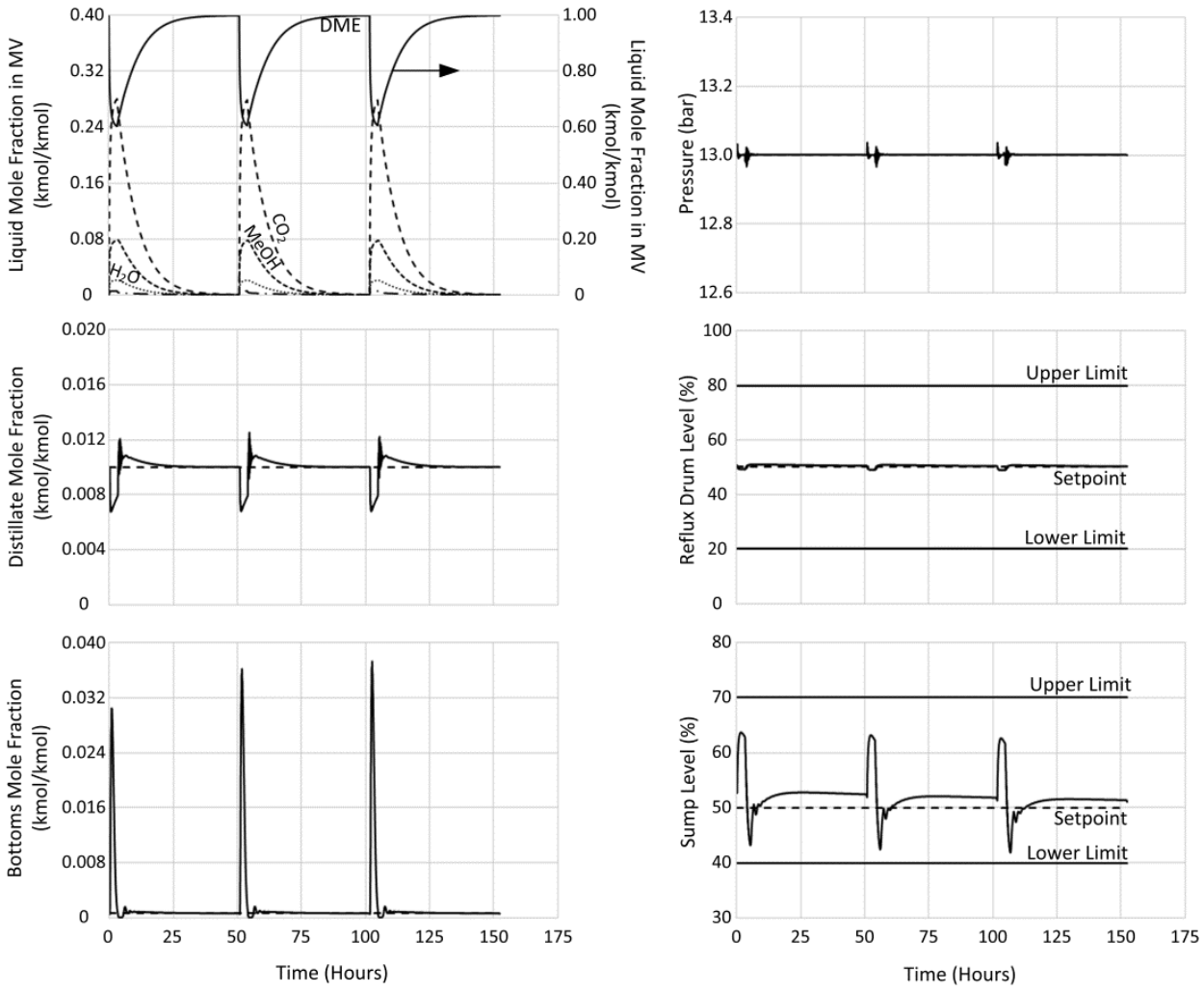

Figure 4.16: Composition, pressure and level profiles for composition control configuration 5

Although setpoint tracking of bottoms impurity cannot be achieved throughout the entire cycle for configurations 5 and 6, flooding and weeping conditions are avoided, as shown in Figure 4.17 and Figure 4.19.

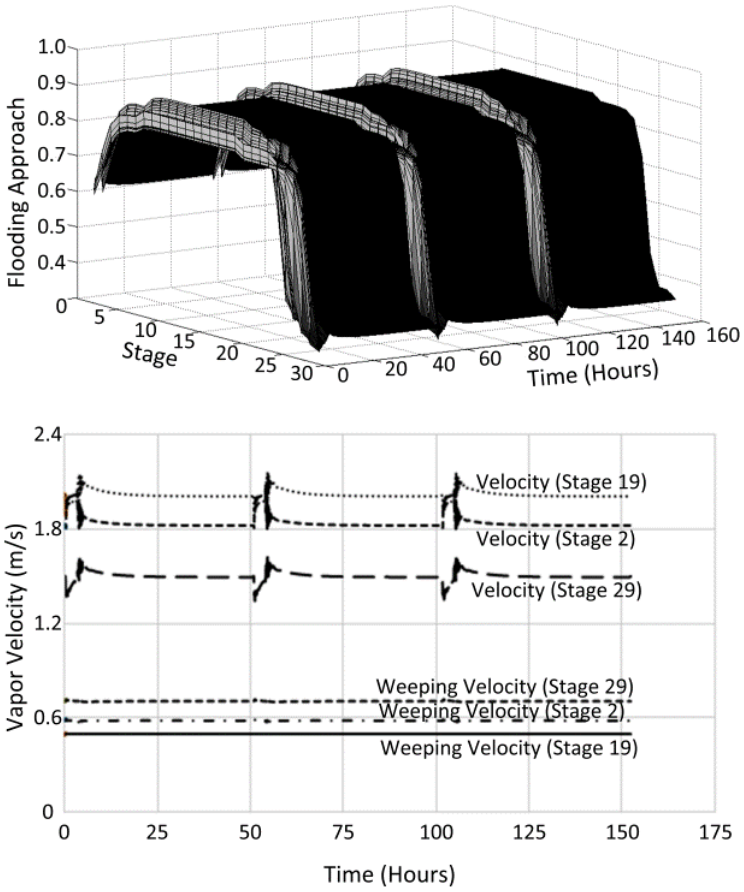

Figure 4.17: Flooding approach, vapor and weeping velocity profiles for composition control configuration 5

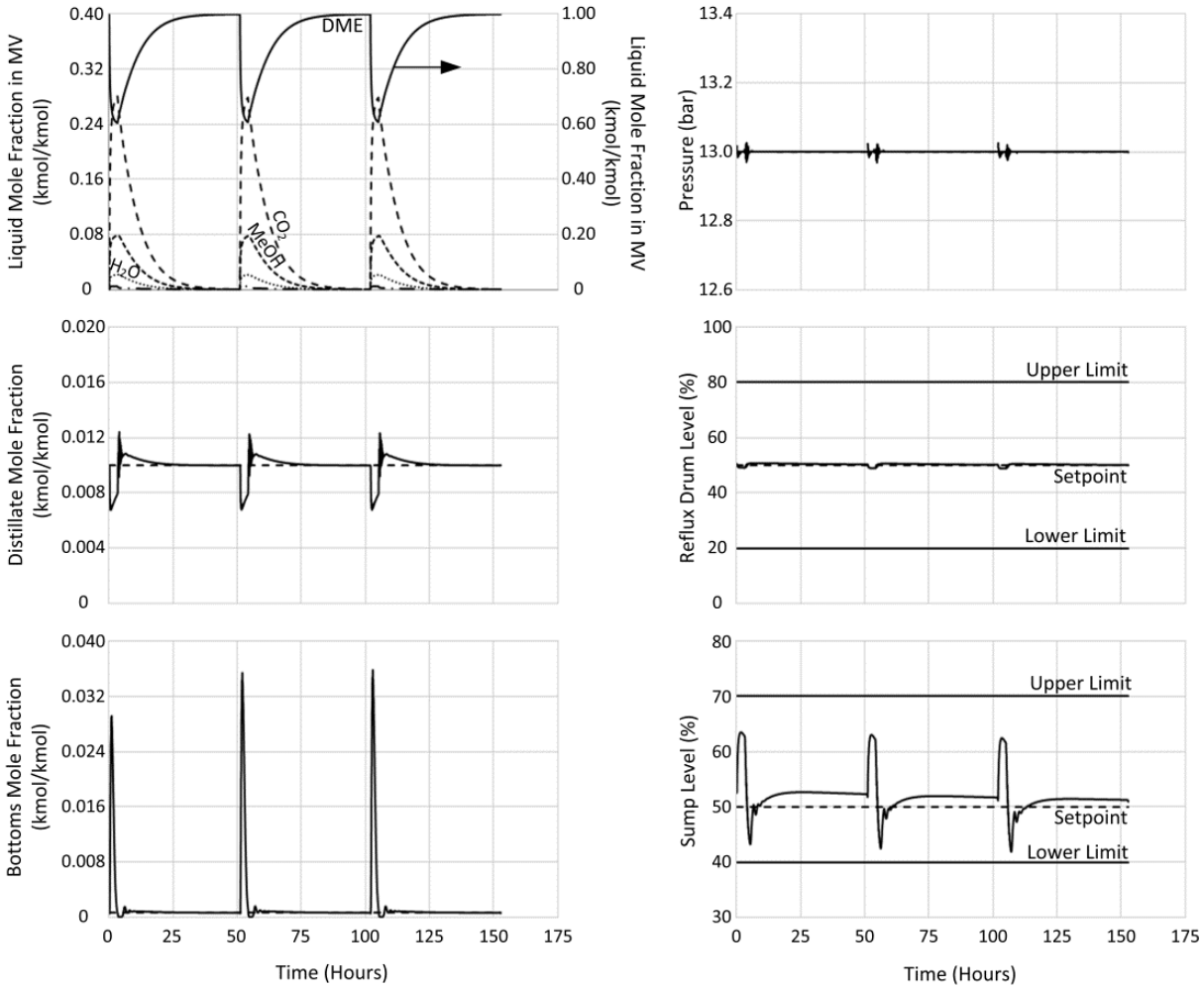

Figure 4.18: Composition, pressure and level profiles for composition control configuration 6

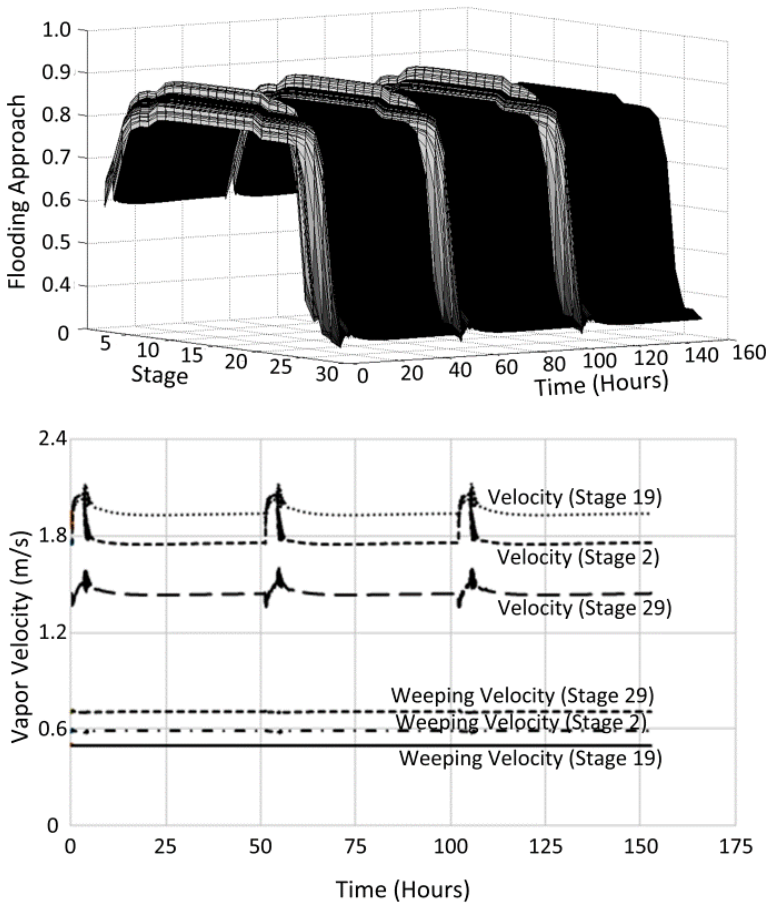

Figure 4.19: Flooding approach, vapor and weeping velocity profiles for composition control configuration 6

When temperature control is employed for configuration 1, setpoint tracking of DME impurity in the distillate and bottoms streams are greatly improved, as shown in Figure 4.20 and Table 4.3. Additionally, the internal flow rates within the column are maintained such that the weeping and flooding within the column are avoided, as shown in Figure 4.21. Similarly, the response for temperature control in configurations 2, 5 and 6 were similar to their respective composition control configurations with lower integral squared error (ISE) for distillate and bottoms products. The cycle time and product ISE for the temperature control configurations are summarized in Table 4.3.

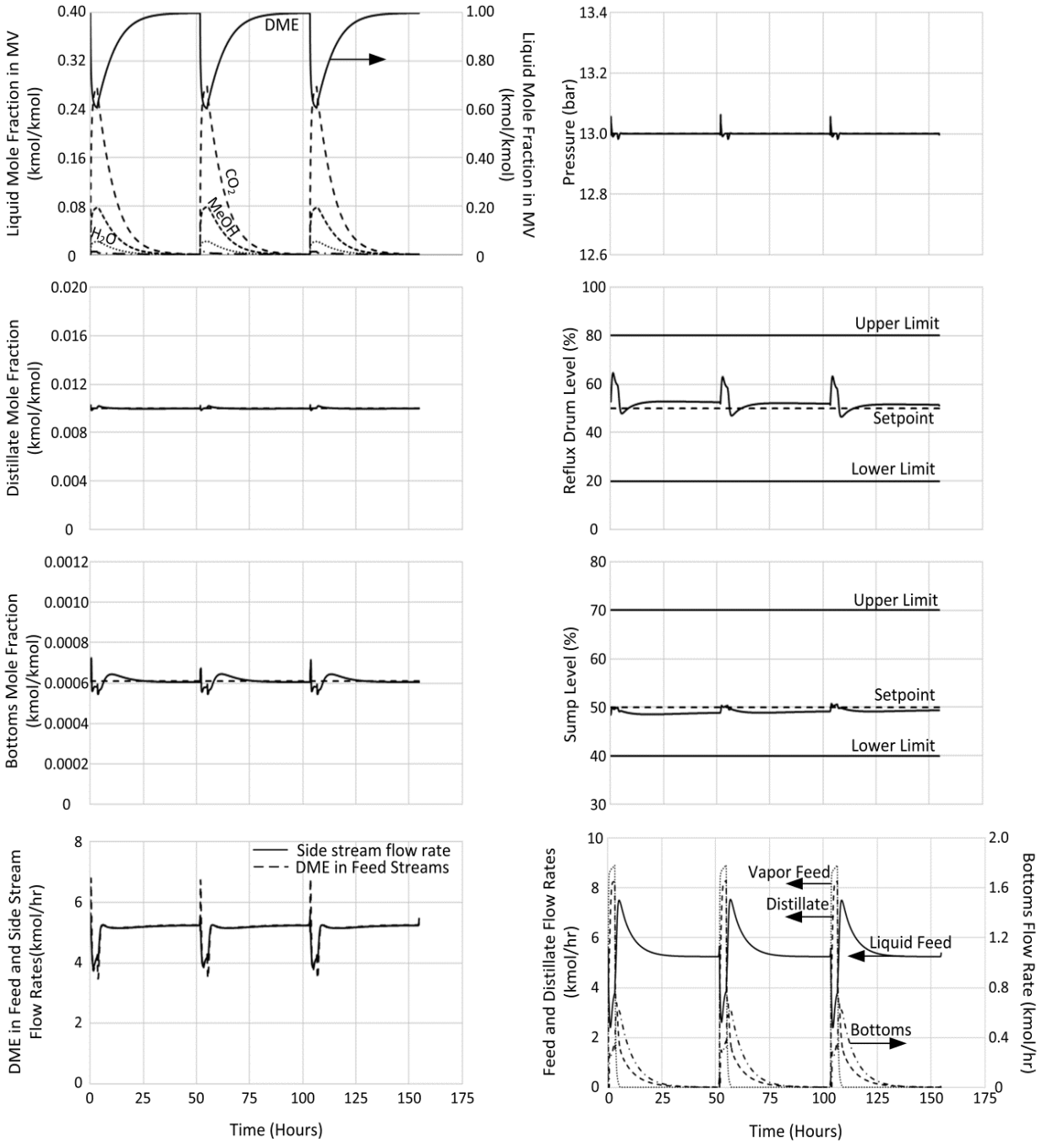

Figure 4.20: Composition, pressure, flow and level profiles for temperature control configuration

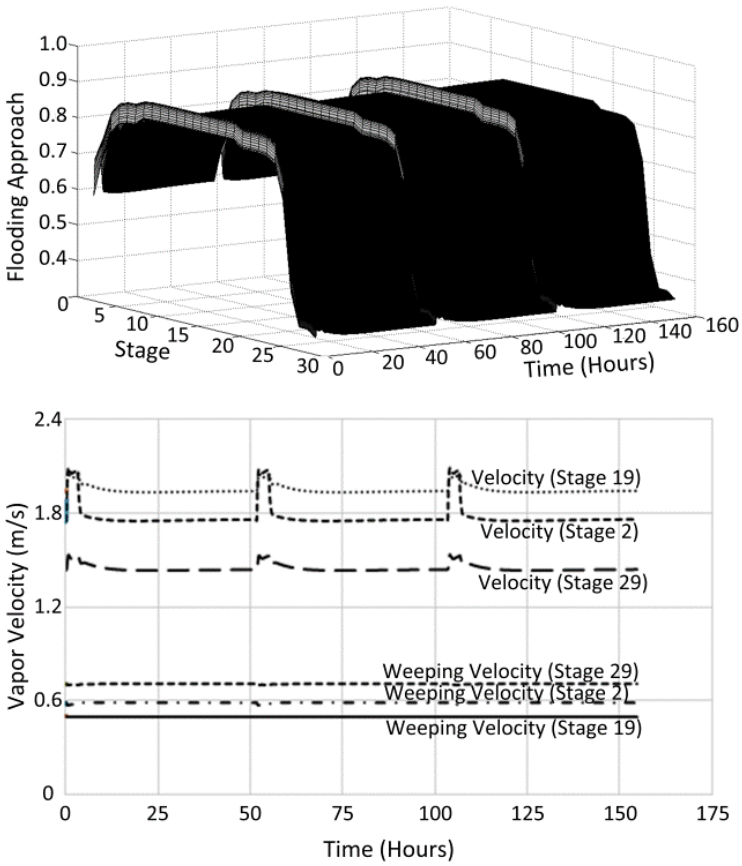

Figure 4.21: Flooding approach, vapor and weeping velocity profiles for temperature control configuration 1

Additionally, as shown in Figure 4.21 the side stream achieves a relatively constant flow rate as Mode 2 progresses. As such, the side stream can be controlled at a constant flow-rate setpoint, configuration 1a, eliminating two composition analyzers. Figure 4.22 show that operation under such a constant side stream flow rate policy (which we now call configuration 1a) has little effect on the system profiles.

Table 4.3: Control performance comparison for all control configurations

Configuration	Average cycle time (hr/cycle)	Average integral squared error per cycle – Distillate DME impurity	Average integral squared error per cycle – Bottoms DME impurity
Composition Control			
1	51.38	1.24×10^{-5}	9.07×10^{-8}
2	50.73	2.56×10^{-5}	1.07×10^{-3}
3	Cycle failure		
4	Cycle failure		
5	50.77	2.65×10^{-5}	1.17×10^{-3}
6	50.87	2.69×10^{-5}	1.08×10^{-3}
Temperature Control			
1	51.55	8.43×10^{-8}	1.86×10^{-8}
1a[1]	53.08	7.31×10^{-8}	1.66×10^{-8}
2	51.20	5.29×10^{-5}	7.32×10^{-4}
5	50.68	2.34×10^{-5}	1.40×10^{-3}
6	50.57	2.16×10^{-5}	1.45×10^{-3}

Note: 1 – Side stream controlled at a fixed flow rate

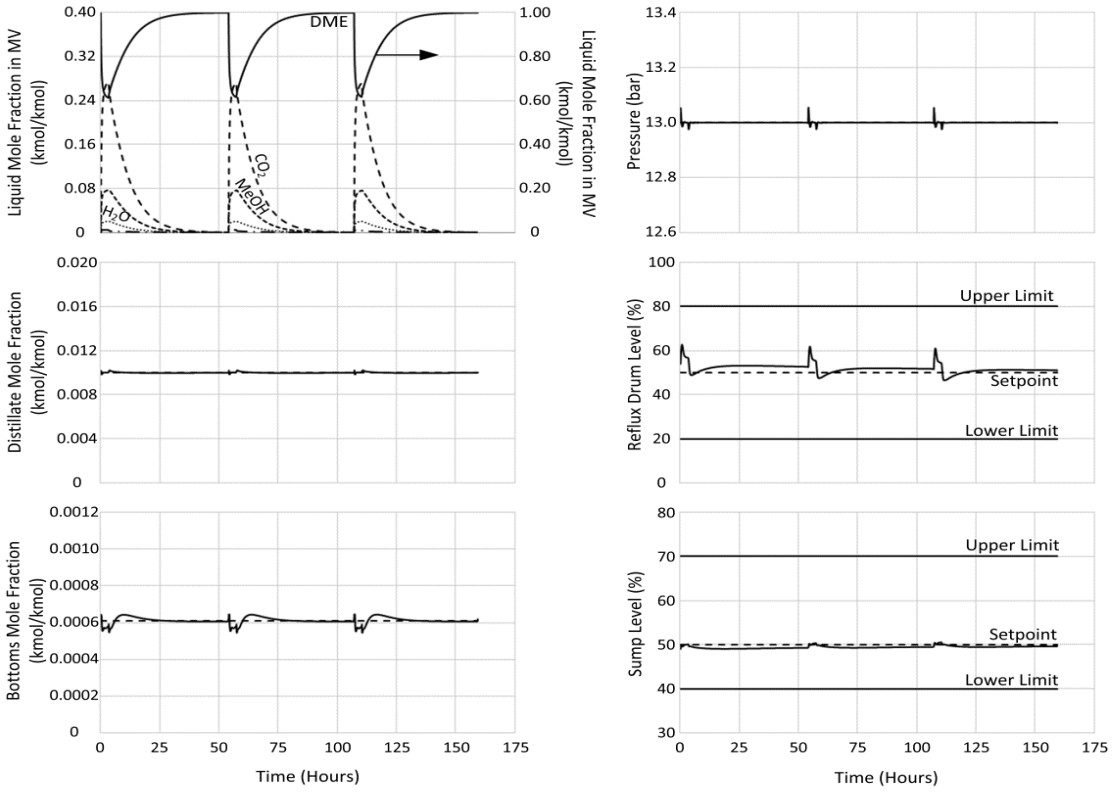

Figure 4.22: Composition, pressure and level profiles for temperature control configuration 1a

Configuration 1 and 1a based on temperature control give the best control performance (lowest product ISE) while adhering to operational objectives. Configuration 1a is selected as the control scheme for the multi-component vapor-liquid mixture separation as it eliminates the two feed composition analyzers.

4.4.2. Disturbance Rejection

The simulation results presented thus far have examined the operation of the column in achieving the desired product purities in the face of flow rate and feed composition changes. In this section, we consider the effect of two external disturbances to the semicontinuous system: fresh feed composition and temperature or vapor fraction changes.

Composition Disturbance

Composition control configuration 1 and temperature configurations 1 and 1a were subjected to +10% step change in DME mole fraction in the fresh feed (H_2/CO/CO_2/DME/MeOH/H_2O: 3.81% / 5.99% / 40.82% / 41.78% / 5.96% / 1.64%) and -10% step change in DME mole fraction in the fresh feed (H_2/CO/CO_2/DME/MeOH/H_2O: 3.81% / 5.99% / 46.72% / 34.18% / 7.29% / 2.01%).

As shown in Figure 4.23 and Figure 4.24 configuration 1 using both temperature and composition control can handle ±10% changes in DME mole fraction in the fresh feed. The temperature control configuration with the side stream operated under constant flow rate exhibits the lowest offset in distillate and bottoms composition under -10% DME feed composition disturbances (see Table 4.4). However, for a +10% DME change in mole fraction the bottoms product has a larger offset than temperature configuration 1 since the side stream is not adjusted for the increase DME flow to the column.

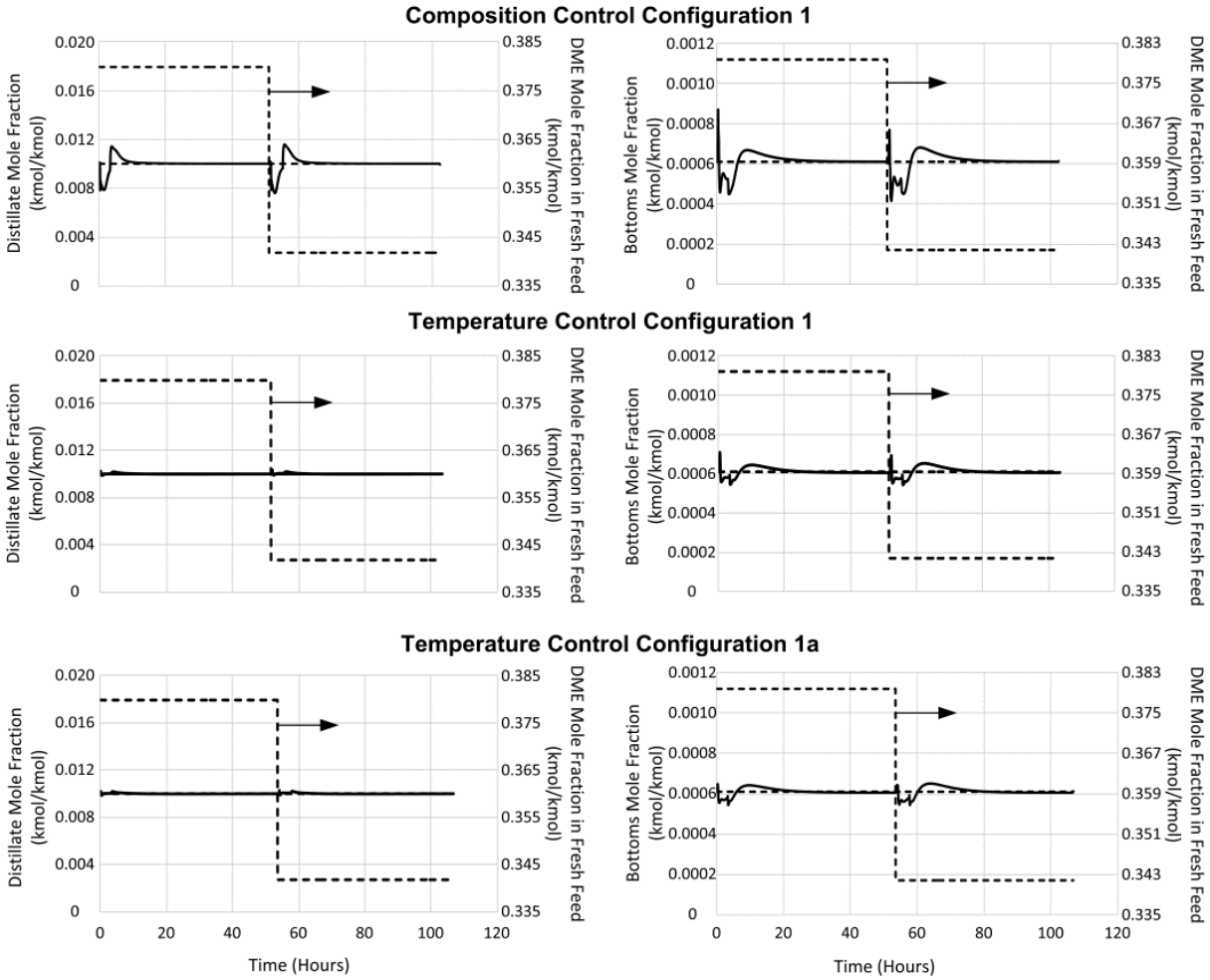

Figure 4.23: Performance of composition and temperature control configuration 1 for -10% change in DME mole fraction in fresh feed

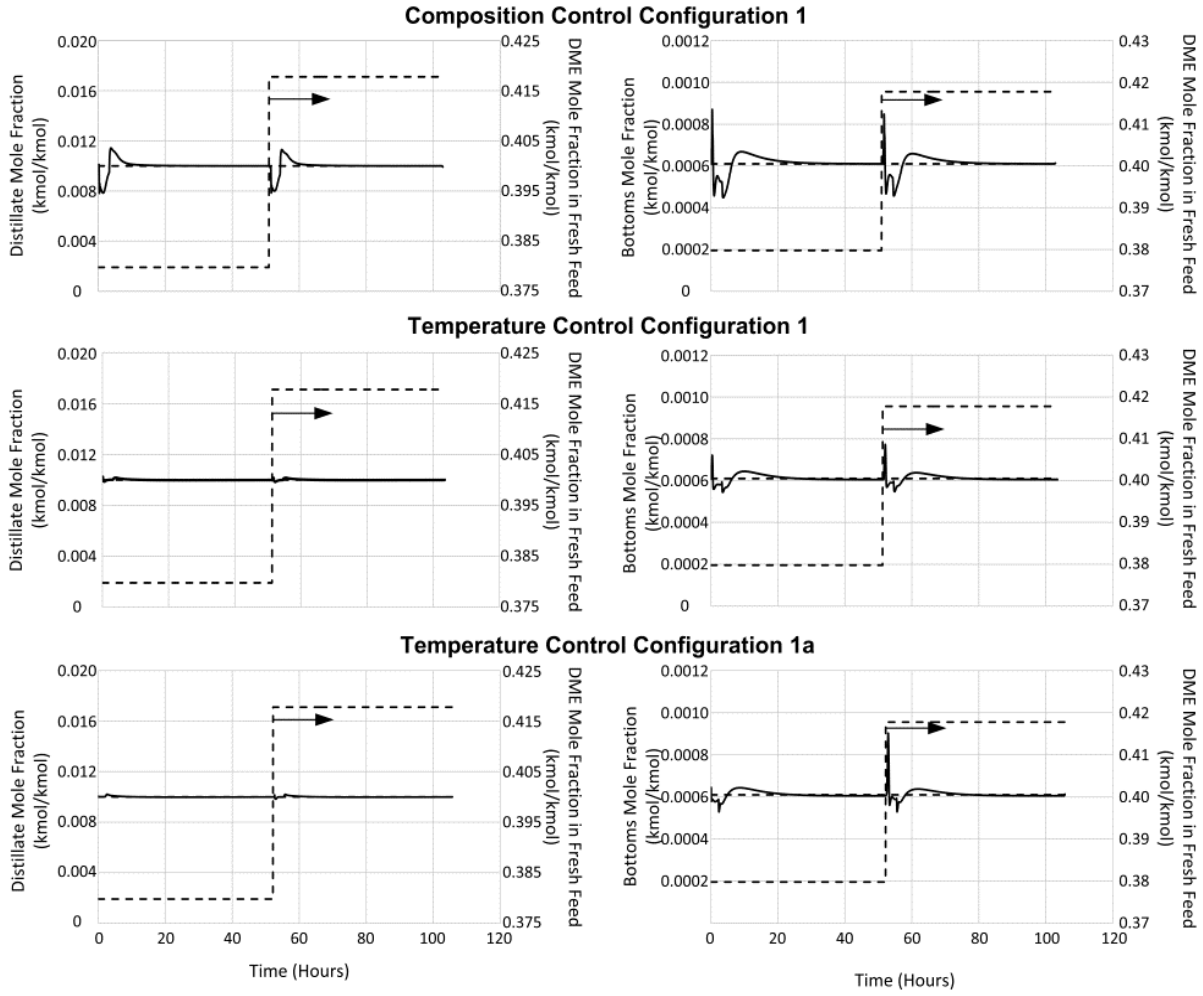

Figure 4.24: Performance of composition and temperature control configuration 1 for +10% change in DME mole fraction in fresh feed

Table 4.4: Control performance for cycle in DME mole fraction disturbance cycle

Configuration	-10% DME Mole Fraction		+10% DME Mole Fraction	
	ISE -Distillate	ISE-Bottoms	ISE -Distillate	ISE-Bottoms
Composition 1	1.45×10^{-5}	1.20×10^{-7}	1.07×10^{-5}	6.99×10^{-8}
Temperature 1	9.88×10^{-8}	2.40×10^{-8}	8.22×10^{-8}	1.82×10^{-8}
Temperature 1a	9.17×10^{-8}	2.24×10^{-8}	7.64×10^{-8}	3.44×10^{-8}

Temperature Disturbance

Composition control configuration 1 and temperature configurations 1 and 1a were subjected to a +10K (291.4 to 301.4K) step change in fresh feed temperature (+38.3% increase in feed vapor fraction) and a -10K (291.4 to 281.4K) step change in fresh feed temperature (-30.4% decrease in feed vapor fraction).

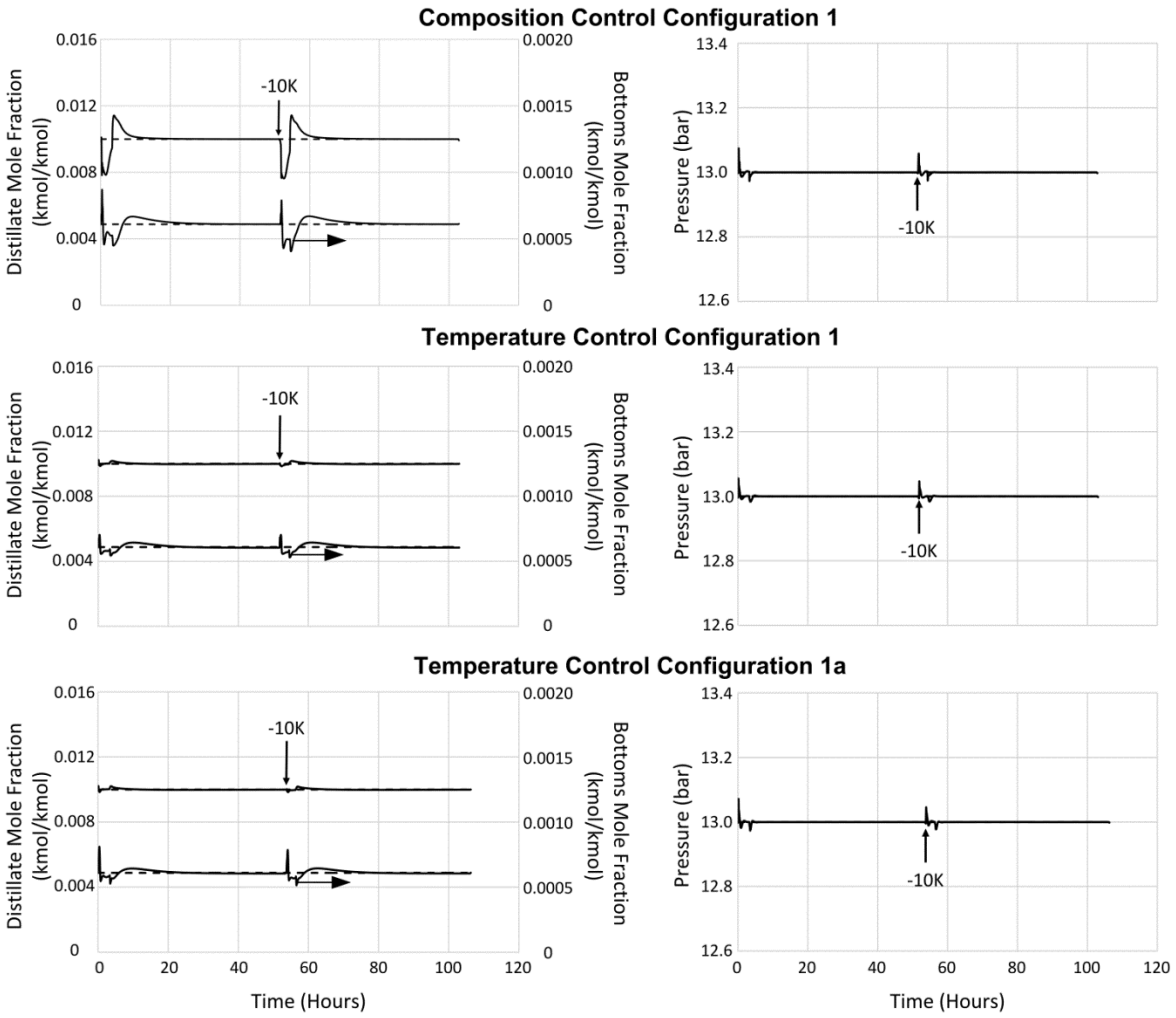

Figure 4.25: Performance of composition and temperature control configuration 1 for -10K change in fresh feed temperature

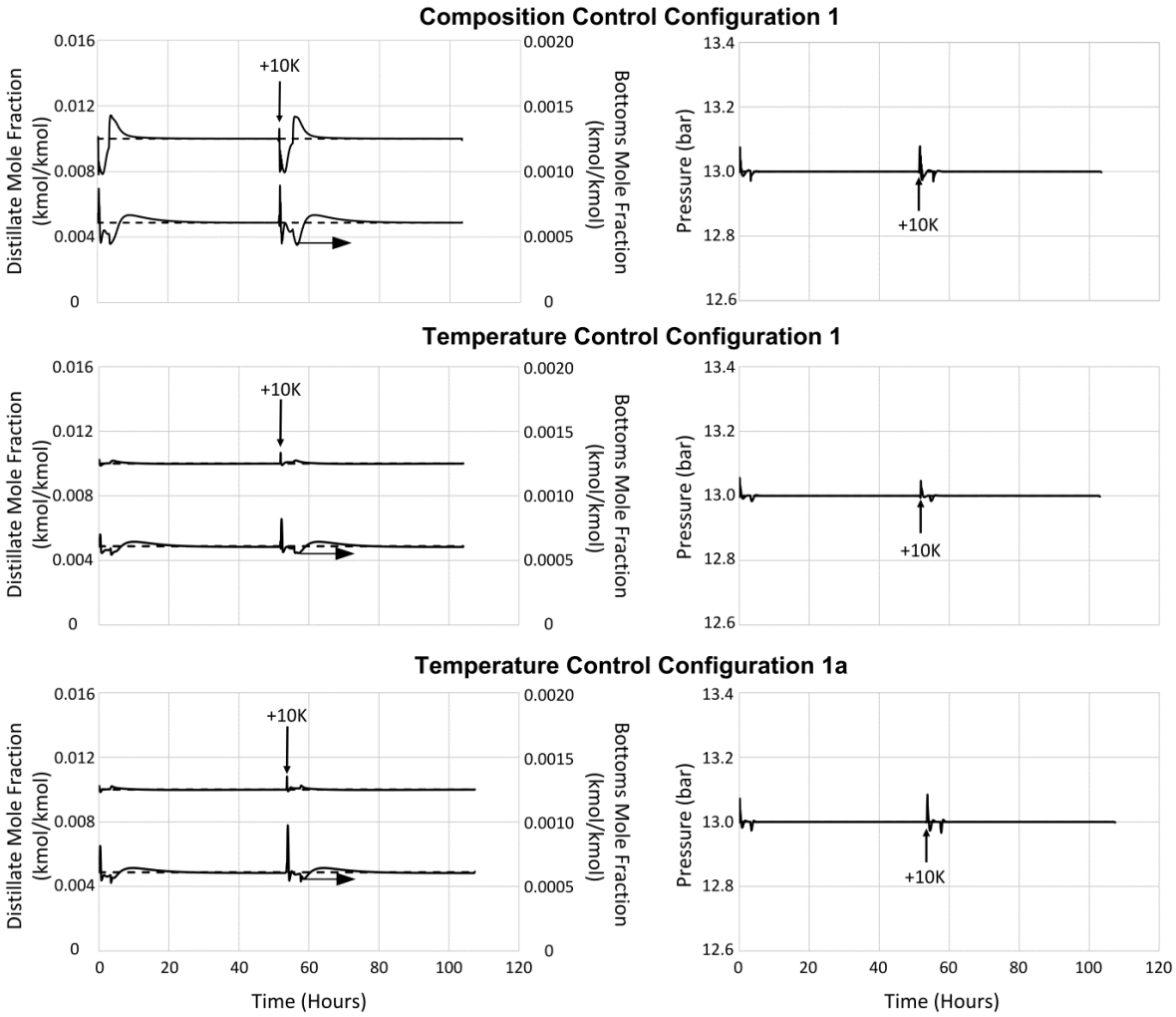

Figure 4.26: Performance of composition and temperature control configuration 1 for +10K change in fresh feed temperature

In addition to composition disturbances, configurations 1 and 1a effectively reject disturbances in the feed temperature (and thus vapor fraction) as illustrated by Figure 4.25 and Figure 4.26. Unlike the composition disturbance, temperature control configuration 1 is better able to handle feed temperature disturbance. In the case of temperature increase, the vapor fraction of the feed increases, thus increasing the vapor feed to the column during Mode 1 and Mode 2. As the side stream rate is held constant, this results in DME losses in the product streams increasing the ISE for each stream (see Table 4.5).

Table 4.5: Control performance for cycle in DME mole fraction disturbance cycle

Configuration	-10K Temperature		+10K Temperature	
	ISE -Distillate	ISE-Bottoms	ISE -Distillate	ISE-Bottoms
Composition 1	$1.30x10^{-5}$	$1.04x10^{-7}$	$1.16x10^{-5}$	$9.44x10^{-8}$
Temperature 1	$9.43x10^{-8}$	$1.98x10^{-8}$	$1.28x10^{-7}$	$2.61x10^{-8}$
Temperature 1a	$8.57x10^{-8}$	$2.50x10^{-8}$	$1.51x10^{-7}$	$4.76x10^{-8}$

4.4.3. Economic Analysis

Having demonstrated the efficacy of the semicontinuous system in achieving the separation objectives and handling feed disturbances, we now evaluate its economic viability. In this work the semicontinuous and continuous designs are evaluated using the TAC (Equation 4.9). An annual operating time of 8400 hours with a payback period of 3 years (Luyben et al., 2004; Luyben, 2006b; Pascall & Adams, 2013) are assumed.

$$\text{TAC} = \frac{\text{Total Direct Cost}}{\text{Payback Period}} + \text{Annual Operating Cost} \qquad (4.9)$$

The total direct cost (equipment, civil, electrical, piping, instrumentation and others) of the distillation columns, reboilers, condensers, reflux drums, middle vessel, reflux, side stream and feed pumps are determined using Aspen In-Plant Cost Estimator V7.3.1. The annual operating cost is based on the refrigerant, steam and cooling water requirements for the distillation processes. Refrigerant at \$7.9/GJ (Seider, Seader, Lewin, & Widagdo, 2009) of cooling load is used with the cost of steam and cooling water estimated. The cost of steam is calculated (Towler & Sinnott, 2012) using electricity and natural gas prices of \$0.0491/kWh (Independent Electricity System Operator (IESO), 2012) and \$2.51/MMBtu (U.S Energy Information Administration (EIA - Official Energy Statistics from the US Government), 2012) respectively. Cooling water cost is calculated (Towler & Sinnott, 2012) using electricity at \$0.0491/kWh and water make-up/chemical treatment at \$0.02/1000 US gal (Towler & Sinnott, 2012). These calculations correspond to price of steam at 147.6 and 168°C of

$0.53 and $2.03 per GJ of heating load and price of cooling water at 27^{o}C at $0.52 per GJ of cooling load.

Continuous system

The operating and direct cost, at various production rates, resulting from the optimization of the design (*N* and feed stream location) and operating variables (R_{ref} and R_{boil}) are illustrated in Figure 4.27.

Semicontinuous system

Prior to the economic analysis of the semicontinuous system, we investigated the effect of various design variables on the TAC. Owing to the complex nature of the system the integer design variables are fixed prior to evaluation of the continuous design variables (side stream/feed ratio, sump height and middle vessel volume). The number of trays is fixed at 28 (the total of the optimal CO_2 and DME columns for the continuous case) with the side stream and feeds locations fixed such that the reflux and reboil ratios are reduced in the steady state initialization case. The continuous design variables were determined by systematically varying one variable at a time.

Side stream/Feed Ratio

In the design of the semicontinuous system in Aspen Plus, the side stream split (*S/F* ratio) is specified to match the intermediate component using the ideal side draw approach. However, as shown in our previous work (Pascall & Adams, 2013), even slightly higher *S/F* ratios result in significantly reduced cycle time and operating cost per product produced. The reflux-reboil ratios and thus internal flow rates decreases with increasing *S/F* ratio as such the feed rate to the column can be increased to maintain operation at its maximum capacity.

Here we consider the effect of *S/F* ratio for a 1.5ft column for the semicontinuous separation column. Table 4.6 shows the strong effect of side-stream ratio on the reducing the cycle time and operating cost of this semicontinuous system using

temperature configuration 1a. At *S/F* ratios above 0.40 the product purities cannot be maintained thus *S/F* of 0.4 is considered for each variable studied.

Table 4.6: Operating cost per DME produced and cycle time at various side stream-feed ratios

Side stream/feed Ratio	Operating cost/kg DME produced ($/kg)	Cycle time (hours)
0.380	0.46	51.00
0.385	0.25	29.00
0.390	0.15	18.40
0.395	0.12	16.50
0.400	0.09	12.90

Middle Vessel Volume

The charge volume (middle vessel size) affects both the capital and operating cost of the system. Larger charge volumes reduce the operating cost per DME produced as the transition modes (1 and 3) form a smaller fraction of the cycle time. On the other hand, the increase in charge volume significantly increases the capital cost and TAC/DME produced. The middle vessel is sized using standard diameters with an L_R/D_R ratio of 3, Table 4.7. The middle vessel is selected using the steady-state initial feed flow rate as a guide. For example, using the 1.5 ft. diameter column, the feed rate to the column is 70.5 kmol. As such a 4.0 ft. diameter middle vessel was selected.

During the charging phase, the feed to the column is maintained, allowing the charge volume to be greater than the initial molar holdup of the vessel. As the charge volume increases while maintaining the same charge rate, the length of charging mode (mode 1) increases. However, on commencement of Mode 1, the feed rate (liquid and vapor) to the column first increases to a maximum and then decreases as the cycle progresses to maintain the reflux drum level and the pressure of the MV (Figure 4.20). As the vapor and liquid outlet rates decrease, the maximum charge volume is selected to avoid liquid overflow while maintaining the maximum pressure offset of +1bar. For each column diameter examined, various charge volumes are examined while

maintaining the same charge rate to the MV. Thus a charge volume of 110 kmol is used for column diameters of 1.5 ft and 250 kmol for 2.0ft columns.

Table 4.7 : Initial MV molar holdup for various vessel diameters

Diameter	Length (ft)	Initial molar hold up (kmol)
3.0	9.0	30.00
4.0	12.0	71.00
4.5	13.5	101.16
5.0	15.0	138.70
5.5	16.5	184.69

Sump Size

The effect of sump size is evaluated by reducing the sump height with the *S/F* ratio and charge volume fixed at 0.4 and 110 kmol respectively for the 1.5 ft diameter column. While the sump height has a minimal effect on the operating cost per DME produced as shown in Table 4.8, the capital cost of the column is reduced. Additionally, reduced sump height has the advantage of lower cycle time as the residence time of the bottoms product in the column is reduced.

Table 4.8: Operating cost per DME produced and cycle time at various sump heights

Sump height (ft.)	Cycle time (hours)	Operating cost/kg DME produced ($/kg)
5.5	17.25	0.07
3.0	17.25	0.07
2.0	17.20	0.07
1.0	17.10	0.07

Reflux Size

Pascall & Adams, 2013 showed that reflux drum size has negligible effect on the operating cost per product produced with the advantage of a decrease in cycle time. The decrease in cycle time is however offset by increasing capital cost.

Subsequent to optimization of the tuning parameters which drive the process, the economics of the partially optimized semicontinuous system is compared to the continuous process. As expected the total direct cost of the semicontinuous system is lower than that of the continuous process as less equipment is utilized. However, the operating cost of the semicontinuous system is greater than the continuous system outweighing the capital cost advantage. This results in higher TAC as shown in Figure 4.28.

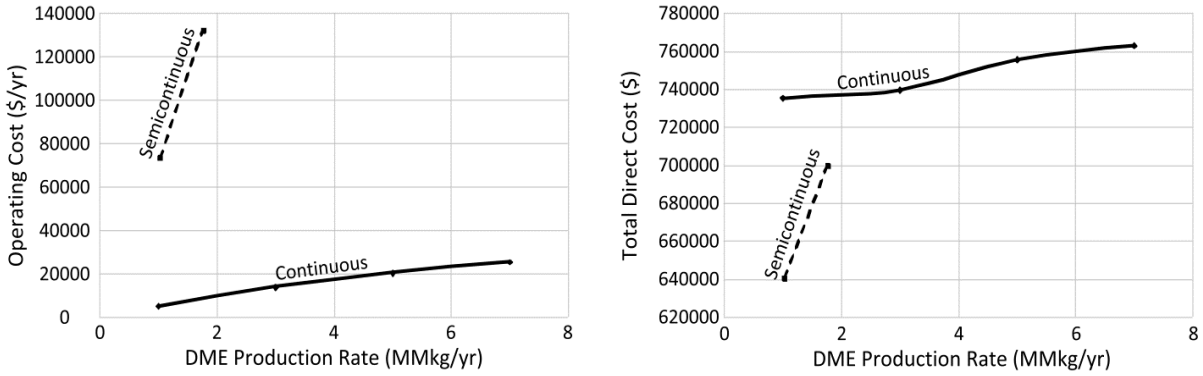

Figure 4.27: Annual operating and total direct costs of continuous and semicontinuous systems at various production rates

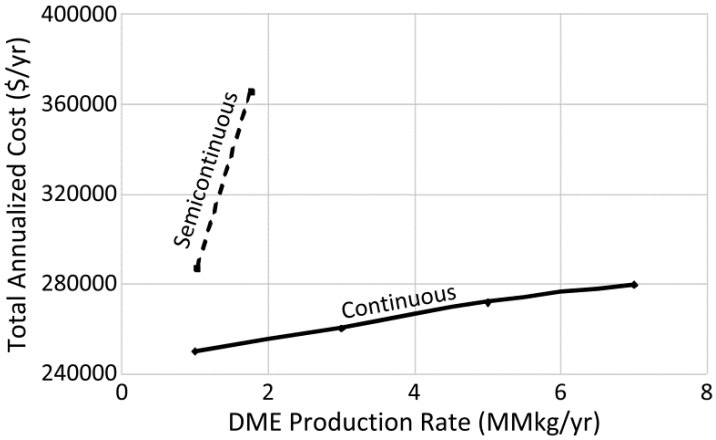

Figure 4.28: Total annualized cost of continuous and semicontinuous systems at various production rates

Examining the cumulative operating cost over one cycle, we see that the DME purity specification has a large influence on operating cost. As the cycle progresses and the

DME purity increases from 98 to 99.95 mol%, this results in a 100% increase in operating cost.

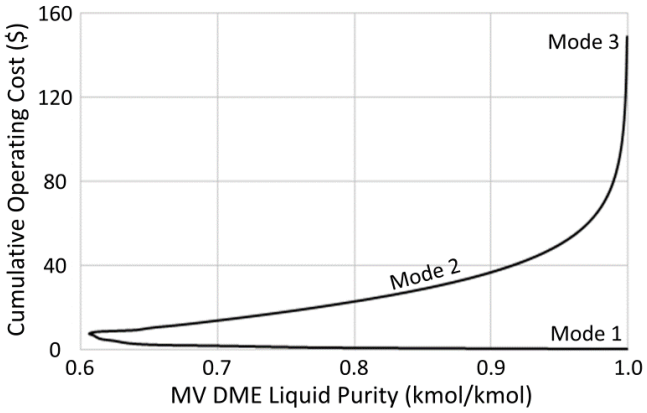

Figure 4.29: Cumulative operating cost versus MV liquid composition

To further examine the impact of final MV product purity on operating cost, we consider three DME product purity cases of 99, 98 and 96 mol%. The results for the various DME target purities (Table 4.9) illustrate that the operating cost per DME produced increases significantly as the purity specification is increased.

Table 4.9: Operating cost per DME for various target DME purities

MV DME Purity (kmol/kmol)	Operating cost per DME ($/kg)	
	1.5 ft	2.0 ft
99.95	0.071	0.075
99.00	0.041	0.044
98.00	0.035	0.038
96.00	0.028	0.031

4.5. Conclusion

This section presented a design and control strategy for separation of a multi-component CO_2, DME, MeOH, H_2O mixture in a single partial condenser distillation column integrated with a middle vessel. This is the first such system to utilize a partial condenser which created unique challenges, particularly due to the strong interaction between pressure, temperature and reflux drum level controllers. Despite this a control configuration which handles these interactions together with effective tuning parameters was identified. The simulation results indicate the efficacy of inferential-temperature control configuration 1a (a distillate-bottoms configuration consisting of two temperature differential control loops in which distillate flow rate is manipulated to maintain the differential temperature in the top section, bottoms flow rate manipulated to maintain the differential temperature in the bottom section with the side stream controlled at a fixed rate) in product purity control over the range of feed flow rate and composition changes. This temperature control configuration in is also shown to handle disturbances in fresh feed composition and temperature.

An economic evaluation of the semicontinuous and continuous system shows that the continuous system is more cost effective for the range of production rates studied. It has been illustrated that the operating cost of the semicontinuous system overshadows the capital cost savings, resulting in higher TAC. The very high purity requirements of the MV product purity results in a rapid increase in the cumulative operating cost towards the end of the cycle. Further evaluation has shown that the operating cost of the partially optimized semicontinuous system is highly dependent on the purity specification of the middle vessel as seen by the 61% decrease in operating cost per DME produced in shifting the purity specification from 99.95 to 96 mol%. The finding shows that although the economic results for this case were less favorable, it is not an indication that this strategy will be less economic in other situations, especially those with less rigid purity specifications. This is evident by the many previous studies discussed earlier in which the semicontinuous system is more economical compared to traditional continuous and batch processes.

Based on an overall evaluation of the two possible semicontinuous distillation systems which can be integrated in the DME separation train, the semicontinuous distillation system used to effect the separation of the DME and Methanol columns is the most economical. As such this semicontinuous system represents the best semicontinuous configuration for the distillation section of the biomass-to-DME facility with an annual production less than 5.7 MMkg/yr.

Chapter 5

CONCLUSION AND RECOMMENDATIONS

5.1. Conclusion

The objective of this research was to design a semicontinuous system for the separation of bio-DME and evaluate its economic competitiveness compared to the traditional continuous systems at various production rates.

In Chapter 2, a semicontinuous system to facilitate the separation objectives of the second and third distillation columns in the separation train was simulated using a rigorous pressure-driven dynamic model in Aspen Dynamics. Initially, the *"DB"* material balance control strategy using a fixed flow rate, which was shown to be effective for separation of ternary equimolar hydrocarbons feeds, rendered the system inoperable. As the control strategy is integral to the operation of this forced cycle system, this motived an examination of the *"DB"* configuration under varying feed flow rate and material balance control configurations (*"LB*" and "*DV"*) not previously considered.

Temperature control was utilized for maintaining stream purities, as in industrial practice, instead of composition control as used in previous studies. Controlling temperature as oppose to composition significantly improves the performance of the semicontinuous system. Simulation results indicated that configuration 5a (*"DB"* control using two temperature inferential controllers with feed rate manipulated and side stream operated at a fixed rate) provided effective control over the range of operating conditions while avoiding hydrodynamic problems such as weeping and

flooding. Additionally, disturbances in the form of ±10% changes in the DME mole fraction in the fresh feed are rejected effectively by this control configuration.

In Chapter 3, the continuous system and the semicontinuous using control configuration 5a are optimized with total annualized cost taken as the objective function. The decision variables in the continuous system are the total number of trays, feed tray location and reflux and reboil ratios. In the semicontinuous system, however, due to the complexity of the system and computational requirements in optimizing decision variables: number of trays, feed and side stream location, middle vessel volume, reflux drum volume, sump volume, S/F ratio and control decision variables could not be optimized simultaneously. The structural variables were determined by examining the effect of one design variable at a time on the total annualized cost. Once the structural variables were fixed, the control decision variables were determined using particle swarm optimization. Even though the results obtained are locally optimal the economical assessment indicates that the semicontinuous system is more favourable for DME production rates less than 5.70 MMkg/yr compared to the continuous system.

The accuracy of the economic analyses is highly dependent on the data source and assumptions used in generating capital and operating costs. According to Seider et al., 2009 commonly used methods such as those available in Turton, Peters and Timmerhaus etc. have an accuracy greater than ±25% while more accurate estimates can be obtained from commercial simulators such as Aspen Icarus Process Evaluator. As the analyses performed for both semicontinuous and continuous system utilize the same capital cost estimator, Aspen In-Plant Cost Estimator, the final results will vary by the same extent. As such the production range in which the semicontinuous system is more economical would remain fairly constant.

A study by Wang, Li, Ma, & Wu, 2010 showed that the optimal bio-DME facility plant size was in the range 3-10 MMkg/yr for dispersed facilities in rural areas of China. Although the optimal bio-DME plant capacity is site specific, this comparison

shows that plant size for bio-DME facilities using the semicontinuous process is realistic.

In Chapter 4, a semicontinuous system to achieve the separation objectives of the first and second columns was presented. The aim was to determine whether potential economic improvement can be attained compared to the first semicontinuous system investigated. In contrast to the semicontinuous system in chapter 2 and previous semicontinuous systems examined, this is one of the first attempts to develop a semicontinuous system which utilizes a partial condenser and separates a vapour-liquid fresh feed. A differential temperature control strategy is proposed to account for the variations in the non-key component since tray temperature is not an accurate indicator of product composition for multi-component systems (three or more components). The *"DB"* control configuration 1a (two differential temperature PI controllers employed to maintain product purities with the side stream operated at a fixed feed rate) was shown to be effective in maintaining product purities over the range of operating conditions while avoiding weeping and flooding conditions. Additionally, simulations results show the efficacy of this differential temperature control configuration in handling disturbance in the DME composition in the fresh feed and feed temperature.

Although, this semicontinuous configuration was less economical than the continuous process, simulation results demonstrate that semicontinuous systems can be applied to partial condenser applications and for separation of biphasic multicomponent mixtures. Useful insight into the effect of the middle vessel purity on the operating cost of the semicontinuous system was obtained. It was shown that the operating cost increases significantly when high purity specifications are required. However, in other applications with lower purity targets it is worth revaluation.

Overall, this research shows that the semicontinuous process for the second and third distillation columns shows promise in reducing the overall cost associated with the separation section and consequently the economics of the bio-DME facility.

Additionally, this study contributes to the further development of theory for semicontinuous systems through a new methodology for developing semicontinuous distillation systems, using rigorous equipment and extensive physical property models of Aspen Dynamics, application of temperature control strategies and extension to partial condenser columns.

5.2. Recommendations for future work

Based on an assessment of this study the following recommendations are proposed:

1. **Control Strategy**

   In this work the classical PI control was shown to be effective in maintaining specification and operational objectives in spite of the non-linear and non-stationary behaviour of the process. This was achieved through tuning the controllers for the range of operation. However, the performance of PI controllers are limited as they do not account for multivariable interactions and optimality requirements. To address these limitations of PI controllers, the performance of non-linear model predictive control can be investigated for semicontinuous systems. The implementation of model-based control, however, requires an accurate process model that captures the non-linear behaviour of the system throughout each mode of operation while maintaining a manageable computational demand. Strategies such as data-based modelling or neural networks which have been utilized for batch systems can be extended to the semicontinuous system using data from the rigorous Aspen Dynamics model.

2. **Optimization**

   The high computational demand required for optimization of the control decisions variables led to a two-tier approach in which the design variables were fixed prior to optimization by determining the effect of each variable on the total annualized cost. As such there is a great need for the development of improved black-box optimization algorithms which can handle both discrete and continuous variables without the added computation expense. Additionally, one avenue that can be explored is the development of reduced models for this simultaneous approach to optimization of design and control variables to ascertain the full economic potential of the semicontinuous system.

3. **System Flexibility – Production Rate**

   In the semicontinuous system, the production rate is not a specification but a result of the design and control strategy which determines the yearly production rate based on the cycle time for processing a specified feed volume. However, in chemical processes, the production system must exhibit a degree of flexibility to handle changes in production volumes due to demand requirements or feedstock availability. In the semicontinuous system the number of manipulated variables exceeded the number of controlled variables indicating that a degree of freedom can possibly be used as a production handle. This was shown in chapter 2 where the reflux rate was used to operate the column near its peak capacity thus reducing the cycle time. Future work can evaluate the ability of the semicontinuous system to transition to different production rates for a given design while ensuring specification and operational objectives are met.

LIST OF REFERENCES

Adams, T. A., & Pascall, A. (2012). Semicontinuous Thermal Separation Systems. *Chemical Engineering & Technology*, *35*(7), 1153–1170. doi:10.1002/ceat.201200048

Adams, T. A., & Seider, W. D. (2006). Semicontinuous Distillation with Chemical Reaction in a Middle Vessel. *Industrial & Engineering Chemistry Research*, *45*(16), 5548–5560. doi:10.1021/ie051139r

Adams, T. A., & Seider, W. D. (2008a). Semicontinuous Distillation for Ethyl Lactate Production. *AIChE Journal*, *54*(10), 2539–2552. doi:10.1002/aic.11585

Adams, T. A., & Seider, W. D. (2008b). Practical optimization of complex chemical processes with tight constraints. *Computers & Chemical Engineering*, *32*(9), 2099–2112. doi:10.1016/j.compchemeng.2008.02.007

Adams, T. A., & Seider, W. D. (2009a). Design heuristics for semicontinuous separation processes with chemical reactions. *Chemical Engineering Research and Design*, *87*(3), 263–270. doi:10.1016/j.cherd.2008.09.008

Adams, T. A., & Seider, W. D. (2009b). Semicontinuous reactive extraction and reactive distillation. *Chemical Engineering Research and Design*, *87*(3), 245–262. doi:10.1016/j.cherd.2008.08.005

Al-Arfaj, M. A., & Luyben, W. (2002). Control Study of Ethyl tert -Butyl Ether Reactive Distillation. *Industrial & Engineering Chemistry Research*, *41*(16), 3784–3796. doi:10.1021/ie010432y

Arcoumanis, C., Bae, C., Crookes, R., & Kinoshita, E. (2008). The potential of di-methyl ether (DME) as an alternative fuel for compression-ignition engines: A review. *Fuel*, *87*(7), 1014–1030. doi:10.1016/j.fuel.2007.06.007

Aspen Technology Inc. (2011). Aspen Capital Cost Estimator V7 3.1: User Guide. Burlington, Massachusetts: Aspen Technology, Inc.

Bauer, M. ., & Stichlmair, J. (1998). Design and economic optimization of azeotropic distillation processes using mixed-integer nonlinear programming. *Computers & Chemical Engineering*, *22*(9), 1271 – 1286. doi:10.1016/S0098-1354(98)00011-8

Biegler, L. T., & Grossmann, I. E. (2004). Retrospective on optimization. *Computers & Chemical Engineering*, *28*(8), 1169–1192. doi:10.1016/j.compchemeng.2003.11.003

Birky, G. J., McAvoy, T. J., & Modarres, M. (1988). An expert system for distillation control design. *Computers & Chemical Engineering*, *12*(9/10), 1045–1063. doi:10.1016/0098-1354(88)87026-1

Cabrera-Ruiz, J., Miranda-Galindo, E., Segovia-Hernández, J., Hernández, S., & Bonilla-Petriciolet, A. (2011). Evaluation of Stochastic Global Optimization Methods in the Design of Complex Distillation Configurations. In I. Dritsas (Ed.), *Stochastic Optimization - Seeing the Optimal for the Uncertain* (p. 17). Croatia: InTech. doi:10.5772/623

Clerc, M., & Kennedy, J. (2002). The particle swarm - explosion, stability, and convergence in a multidimensional complex space. *IEEE Transactions on Evolutionary Computation*, *6*(1), 58–73. doi:10.1109/4235.985692

Cocco, D., Tola, V., & Cau, G. (2006). Performance evaluation of chemically recuperated gas turbine (CRGT) power plants fuelled by di-methyl-ether (DME). *Energy*, *31*(10-11), 1446–1458. doi:10.1016/j.energy.2005.05.015

Eberhart, R.C., & Shi, Y. (2000). Comparing inertia weights and constriction factors in particle swarm optimization. *Proceedings of the 2000 Congress on Evolutionary Computation. CEC00 (Cat. No.00TH8512)* (Vol. 1, pp. 84–88). IEEE. doi:10.1109/CEC.2000.870279

Eberhart, Russell C., & Yuhui, S. (2001). Particle swarm optimization: developments, applications and resources. *Proceedings of the 2001 Congress on Evolutionary Computation* (Vol. 1, pp. 81–86). Seoul: IEEE. doi:10.1109/CEC.2001.934374

Environment Canada. (2012). *Canada's Emissions Trends 2012* (p. 66).

Fair, J. R., Steinmeyer, D. E., Penney, W. R., & Crocker, B. B. (1997). Gas Absorption and Gas-Liquid System Design. In R. H. Perry & D. W. Green (Eds.), *Perry's Chemical Engineers' Handbook* (7th Ed.). McGraw-Hill.

Floudas, C. A., Elia, J. A., & Baliban, R. C. (2012). Hybrid and single feedstock energy processes for liquid transportation fuels: A critical review. *Computers & Chemical Engineering*, *41*(11), 24–51. doi:10.1016/j.compchemeng.2012.02.008

Gengembre, E., Ladevie, B., Fudym, O., & Thuillier, A. (2012). A Kriging constrained efficient global optimization approach applied to low-energy building design problems. *Inverse Problems in Science and Engineering*, *20*(7), 1101 – 1114. doi:10.1080/17415977.2012.727084

Grossmann, I. E., Aguirre, P. a., & Barttfeld, M. (2005). Optimal synthesis of complex distillation columns using rigorous models. *Computers & Chemical Engineering*, *29*(6), 1203–1215. doi:10.1016/j.compchemeng.2005.02.030

Hori, A. E. S., & Skogestad, B. S. (2007). Control structure selection of a deethanizer column with partial condenser. *European Congress of Chemical Engineering (ECCE-6)* (pp. 16–20). Copenhagen.

Independent Electricity System Operator (IESO). (2012). Independent Electricity System Operator (IESO). *Hourly Ontario Energy Price*. Retrieved February 10, 2012, from http://www.ieso.ca/default.asp

Jenkins, B. M. (1997). A comment on the optimal sizing of a biomass utilization facility under constant and variable cost scaling. *Biomass and Bioenergy*, *13*(1-2), 1–9. doi:10.1016/S0961-9534(97)00085-8

Ju, F., Chen, H., Ding, X., Yang, H., Wang, X., Zhang, S., & Dai, Z. (2009). Process simulation of single-step dimethyl ether production via biomass gasification. *Biotechnology Advances*, *27*(5), 599–605.

Larson, E. D., Jin, H., & Celik, F. E. (2009). Large-scale gasification-based coproduction of fuels and electricity from switchgrass. *Biofuels, Bioproducts and Biorefining*, *3*(2), 174–194. doi:10.1002/bbb.137

Lipták, B. G. (2005). *Instrument Engineers' Handbook:Process Control and Optimization*. (B. G. Lipták, Ed.) (4th Ed.). Boca Raton, Florida: CRC Press.

Liu, Z., Sun, C., Wang, G., Wang, Q., & Cai, G. (2000). New progress in R&D of lower olefin synthesis. *Fuel Processing Technology*, *62*(2-3), 161–172. doi:10.1016/S0378-3820(99)00117-4

Luyben, W. (2006a). Evaluation of criteria for selecting temperature control trays in distillation columns. *Journal of Process Control*, *16*(2), 115–134. doi:10.1016/j.jprocont.2005.05.004

Luyben, W. (2006b). *Distillation design and control using Aspen simulation*. Hoboken, N.J.: Wiley-Interscience.

Luyben, W. (2010). Heuristic Design of Reaction/Separation Processes. *Industrial & Engineering Chemistry Research*, *49*(22), 11564–11571. doi:10.1021/ie101509w

Luyben, W. (2012). Realistic Models for Distillation Columns with Partial Condensers Producing Both Liquid and Vapor Products. *Industrial & Engineering Chemistry Research*, *51*(24), 8334–8339. doi:10.1021/ie300818b

Luyben, W., Pszalgowski, K., Schaefer, M., & Siddons, C. (2004). Design and Control of Conventional and Reactive Distillation Processes for the Production of Butyl Acetate. *Industrial & Engineering Chemistry Research*, *43*(25), 8014–8025. doi:10.1021/ie040167r

Marlin, T. (2000). *Process control: designing processes and control systems for dynamic performance* (2nd Ed.). Boston, Massachusetts: McGraw-Hill.

Mersmann, A., Kind, M., & Stichlmair, J. (2011). *Thermal Separation Technology: Principles, Methods, Process Design* (1st ed., p. 694). Heidelberg: Springer.

Monroy-Loperena, R., & Alvarez-Ramirez, J. (2004). Some aspects of the operation of semi-continuous, middle-vessel distillation columns. *Chemical Engineering Communications*, *191*(11), 1437–1455. doi:10.1080/00986440490472607

Moradi, G. R., Ahmadpour, J., Yaripour, F., & Wang, J. (2011). Equilibrium calculations for direct synthesis of dimethyl ether from syngas. *The Canadian Journal of Chemical Engineering*, *89*(1), 108–115. doi:10.1002/cjce.20373

Ogawa, T., Inoue, N., Shikada, T., & Ohno, Y. (2003). Direct Dimethyl Ether Synthesis. *Journal of Natural Gas Chemistry*, *12*, 219–227.

Pascall, A., & Adams, T. A. (2013). Semicontinuous separation of dimethyl ether (DME) produced from biomass. *Can. J. Chem. Eng.* doi:10.1002/cjce.21813

Peng, X. D., Wang, A. W., Toseland, B. A., & Tijm, P. J. A. (1999). Single-Step Syngas-to-Dimethyl Ether Processes for Optimal Productivity, Minimal Emissions, and Natural Gas-Derived Syngas. *Industrial & Engineering Chemistry Research*, *38*(11), 4381–4388. doi:10.1021/ie9901269

Phimister, J. R., & Seider, W. D. (2000a). Semicontinuous , Middle-Vessel Distillation of Ternary Mixtures. *AIChE Journal*, *46*(8), 1508–1520. doi:10.1002/aic.690460804

Phimister, J. R., & Seider, W. D. (2000b). Semicontinuous, Pressure-Swing Distillation. *Industrial & Engineering Chemistry Research*, *39*(1), 122–130. doi:10.1021/ie9904302

Phimister, J. R., & Seider, W. D. (2000c). Semicontinuous, Middle-Vessel, Extractive Distillation. *Computers & Chemical Engineering*, *24*(2-7), 879–885. doi:10.1016/S0098-1354(00)00344-6

Poli, R., Kennedy, J., & Blackwell, T. (2007). Particle swarm optimization. *Swarm Intelligence*, *1*(1), 33–57. doi:10.1007/s11721-007-0002-0

Searcy, E., Flynn, P., Ghafoori, E., & Kumar, A. (2007). The relative cost of biomass energy transport. (J. Mielenz, K. Klasson, W. Adney, & J. McMillan, Eds.)*Applied Biochemistry And Biotechnology*, *137-140*(1-12), 639–652.

Seider, W., Seader, J., Lewin, D., & Widagdo, S. (2009). *Product and Process Design Principles: Synthesis, Analysis and Design* (3rd. ed., p. 736). USA: John Wiley & Sons.

Semelsberger, T. A., Borup, R. L., & Greene, H. L. (2006). Dimethyl ether (DME) as an alternative fuel. *Journal of Power Sources*, *156*(2), 497–511. doi:10.1016/j.jpowsour.2005.05.082

Shinskey, F. G. (1984). *Distillation control: for productivity and energy conservation* (2nd Ed.). New York: McGraw-Hill.

Shinskey, F. G., & Foxboro, M. (1977). Control for maximizing capacity and optimizing product cost of distillation column. U.S. Patent.

Skogestad, S. (1997). Dynamics and control of distillation columns - a critical survey. *Modeling Identification and Control A Norwegian Research Bulletin*, *18*(3), 177–217. doi:10.4173/mic.1997.3.1

Tock, L., Gassner, M., & Maréchal, F. (2010). Thermochemical production of liquid fuels from biomass: Thermo-economic modeling, process design and process integration analysis. *Biomass and Bioenergy*, *34*(12), 1838–1854. doi:10.1016/j.biombioe.2010.07.018

Towler, G., & Sinnott, R. (2012). *Chemical Engineering Design: Principles, Practice and Economics of Plant and Process Design* (2nd ed., pp. 107–113). Massachusetts, USA: Butterworth-Heinemann.

U.S Energy Information Administration (EIA - Official Energy Statistics from the US Government). (2012). Henry Hub Gulf Coast Natural Gas Spot Price. Retrieved February 10, 2012, from http://www.eia.gov/dnav/ng/hist/rngwhhdW.htm

Wang, T., Li, Y., Ma, L., & Wu, C. (2010). Biomass to dimethyl ether by gasification/synthesis technology-an alternative biofuel production route. *Frontiers of Energy and Power Engineering in China*, *5*(3), 330–339. doi:10.1007/s11708-010-0121-y

Wright, M., Brown, R. C., & August, R. (2007). Establishing the optimal sizes of different kinds of biorefineries. *Biofuels, Bioproducts and Biorefining*, *1*(3), 191–200. doi:10.1002/bbb

Ye, K., Freund, H., & Sundmacher, K. (2011). Modelling (vapour+liquid) and (vapour+liquid+liquid) equilibria of {water (H2O)+methanol (MeOH)+dimethyl ether (DME)+carbon dioxide (CO2)} quaternary system using the Peng–Robinson EoS with Wong–Sandler mixing rule. *The Journal of Chemical Thermodynamics*, *43*(12), 2002–2014. doi:10.1016/j.jct.2011.07.016

Yu, C. C., & Luyben, W. L. (1984). Use of multiple temperatures for the control of multicomponent distillation columns. *Industrial & Engineering Chemistry Process Design and Development*, *23*(3), 590–597. doi:10.1021/i200026a031